Carnegie Mellon University
MELLON COLLEGE OF SCIENCE

THESIS

SUBMITTED IN PARTIAL FULFILLMENT OF THE REQUIREMENTS
FOR THE DEGREE OF

DOCTOR OF PHILOSOPHY IN THE FIELD OF PHYSICS

TITLE: "Masses and Weak Decay Properties of Heavy-quark Baryons from QCD Sum Rules and Production of Heavy Mesons in High Energy Collisions."

PRESENTED BY: Bijit Singha

ACCEPTED BY THE DEPARTMENT OF PHYSICS

Leonard Kisslinger	8/22/19
LEONARD KISSLINGER, CHAIR PROFESSOR	DATE

Scott Dodelson	8/21/19
SCOTT DODELSON, DEPT HEAD	DATE

APPROVED BY THE COLLEGE COUNCIL

Rebecca Doerge	8/22/19
REBECCA DOERGE, DEAN	DATE

Masses and Weak Decay Properties of Heavy-quark Baryons from QCD Sum Rules and Production of Heavy Mesons in High Energy Collisions

Bijit Singha

Dissertation submitted to the Faculty of the

Carnegie Mellon University

in partial fulfillment of the requirements for the degree of

Doctor of Philosophy

in

Physics

Leonard S. Kisslinger, Chair

Eric S. Swanson

Ira Z. Rothstein

Scott Dodelson

August, 2019

Pittsburgh, Pennsylvania

Masses and Weak Decay Properties of Heavy-quark Baryons from QCD Sum Rules and Production of Heavy Mesons in High Energy Collisions

Bijit Singha

(ABSTRACT)

Quantum Chromodynamics Sum Rules (QCD Sum Rules) is a non-perturbative technique which uses Wilson's Operator Product Expansion of n-point functions and quark-hadron duality together to extract various physical properties of hadrons. In this dissertation, we use QCD Sum Rules to calculate the masses of charmed lambda (Λ_c^+), strange lambda (Λ^0), and bottom lambda (Λ_b^0) baryons. We extend this framework to consider charm to strange quark transition in the presence of an external pion field to estimate the coupling corresponding to the Cabibbo-favored weak decay process: $\Lambda_c^+ \to \Lambda^0 + \pi^+$. This framework can be used further to estimate the Cabibbo-favored and Cabibbo-suppressed decays of the heavy-quark baryons. In the second part of this dissertation, we calculate the production cross-section of B mesons in unpolarized proton-proton and and heavy-ion collisions at $\sqrt{s} = 200$ GeV with the main aspect being the fragmentation of a color-octet bottom-antibottom quark pair to create B mesons.

Dedication

This thesis is dedicated to my grandmother who taught me how to read and write, and to my parents for their love and endless support.

को अद्धा वेद क इह प्र वोचत्कुत आजाता कुत इयं विसृष्टिः |

अर्वाग्देवा अस्य विसर्जनेनाथा को वेद यत आबभूव ॥

Who knows it all and who can say
When this was born, and how this was created?
For after this creation came the gods
Who truly knows how the creation happened?

-Nasadiya Sukta, Rigveda (10:129)

Acknowledgments

First and foremost, I would like to express my deepest gratitude to my advisor Professor Leonard S. Kisslinger for his guidance, patience and encouragement. I am grateful to Professor George Klein and Professor Tina Kahniashvili for their encouraging words and valuable advices. I would like to thank all committee members Professor Eric S. Swanson, Professor Ira Z. Rothstein, Professor Scott Dodelson for their careful critiques of this work. I am grateful to my fellow graduate students Vikesh Siddhu, Michael Andrews, Mukund Bapna, Sayan Mandal for all the discussions on several topics in physics and for being around whenever I needed help. I am also thankful to my roommates Sushil Lathwal, Priyank Lathwal, Saigopalakrishna Yerneni for providing me strength throughout my graduate years.

All my accomplishments so far have been initiated with the simple intention of making my family proud of me. I am eternally indebted to my parents, brother, and sister-in-law for all their love, support, and sacrifices.

Contents

List of Figures

Chapter 1

Introduction

In order to categorize the huge number of strongly interacting particles already discovered by the end of 1960's, Murray Gell-Mann [1] and George Zweig [2] independently proposed the existence of quarks. The categorization scheme, famously called 'the eightfold way', led Gell-Mann and Ne'eman to predict the existence of yet another hadron (Ω^-) and its mass, and its decay products. Ω^- was discovered in 1964 [3] in accord with these predictions. Shortly after the quark model was proposed, Oscar W. Greenberg introduced the idea of color charge in order to allow the quarks in baryons to be in symmetric configuration in the space, spin and flavor degrees of freedom [4]. Following this work, in two separate papers by Nambu [5], and Han and Nambu [6], an octet of gluons as the mediator of strong interaction between the three-valued color charges of the quarks were introduced, leading to the present form of Quantum Chromodynamics(QCD) as a $SU(3)$ gauge theory.

1.1 Quantum Chromodynamics

Quantum Chromodynamics (QCD) is now widely accepted to be the theory of strong interactions, where the hadrons are assumed to be bound states of more fundamental, constituent particles called quarks interacting with each other through the exchange of force-carriers called gluons. Quarks come in six flavors: up, down, charm, strange, top and bottom. Mathematically, QCD is formalized as a non-Abelian gauge theory with a local (gauge)

symmetry group $SU(3)$. Much like quantum electrodynamics (QED), where the subset of global symmetries among the $U(1)$ gauge symmetry led to conservation of electric charge, $SU(3)$ symmetry group in QCD leads to another kind of conservation law called conservation of *color* charge. The constituent particles of QCD are three-colored quarks (red, blue and green), that lives in the fundamental representation of $SU(3)$ of color and they interact with each other, in the simplest case, through exchanging a massless gauge boson (called gluon) that lives in the adjoint representation of $SU(3)$. Unlike QED where photons are uncharged and locally don't interact with each other, gluon fields are, in general, color-charged and self-interacting. The strength of interaction of quark fields with the gluon field as well as self-interactions of the gluon field, are parametrized by a coupling constant g. The dynamics of QCD is dictated by the lagrangian [7]

$$\mathcal{L}_q = \sum_f \bar{\psi}_f \left[i\gamma^\mu (\partial_\mu + igA_\mu) - m_f \right] \psi^f - \frac{1}{4} F^a_{\mu\nu} F^{a\mu\nu} \ , \tag{1.1}$$

where $\psi_f(x)$ is the quark field of flavor f and mass m_f, A_μ is the gluon field which can be expanded in the basis of Gell-Mann matrices (generators of $SU(3)$ color group)

$$A_\mu(x) = \sum_a \lambda^a A^a_\mu(x), \tag{1.2}$$

where a is color index, and $F^{\mu\nu}(x)$ is the gluon field strength tensor:

$$F_{\mu\nu}(x) = \sum_a \lambda^a F^a_{\mu\nu}(x) \tag{1.3}$$

and is related to the gluon field through the following relation:

$$F^a_{\mu\nu} = \partial_\mu A^a_\nu - \partial_\nu A^a_\mu + g f_{abc} A^b_\mu A^c_\nu \ . \tag{1.4}$$

Like any renormalizable theories, the mass and the coupling parameters in QCD get a scale dependence after the renormalization procedure in such a way that the lagrangian is unchanged. The invariance of a theory under such a continuous transformation is referred to as Renormalization Group (RG) transformation. This scale dependence of the parameters in the theory can be expressed by a differential equation, called RG equation. The physical processes in QCD are described by the dependence of the coupling g on energy scale. If we define $\alpha_s = \frac{g^2}{4\pi}$, then, for QCD with N_c colors and N_f flavors the *running* of α_s assumes the form

$$\alpha_s(P^2) = \frac{g^2(P^2)}{4\pi} = \frac{4\pi}{b \ln P^2/\Lambda^2_{QCD}}, \qquad \text{where } b = \frac{11N_c - 2N_f}{3}. \tag{1.5}$$

Λ_{QCD} is a parameter in QCD that breaks the scale invariance of QCD even in the limit of vanishing quark masses. Due to this fall-off of the effective coupling with the increase in momenta P^2 as shown in Eq. (1.5), the coupling vanishes at sufficiently high energy scale. This phenomenon is famously called *asymptotic freedom*. So, at very high energy or short-distance scale, α_s becomes very small, allowing us to treat the theory of QCD as quark-gluon interaction perturbatively.

But $\alpha_s(P^2)$ becomes very large at a distance scale $\sim$ 1 fm and larger, or an energy scale $\sim$ 1 GeV and smaller and non-perturbative effects of the interactions start to dominate in this regime. Thus, although we start with a fairly simple QCD lagrangian, the complex infrared structure arising from asymptotic freedom poses significant challenge to extract any information about the low-lying energy spectrum assumed by the theory.

A few more things about QCD are: color symmetry, as we know so far, is an exact symmetry, and we can observe only the color-singlet bound states of QCD. We call them hadrons. These hadrons, although they are comprised of *color*-ed quarks, are always color-singlet. Note that

an isolated color charge will require an infinite amount of energy due to the non-Abelian nature of the interaction which is why a physical meson or baryon must be a color-singlet.

1.2 Charm in the Standard Model

The charm quark (charge $+\frac{2}{3}$, spin $\frac{1}{2}$, running mass $1.275^{+0.025}_{-0.035}$ GeV in the $\overline{MS}$ scheme) is a up-type quark of the second of the three generations and is the third most massive quark in the standard model (SM) of particles and can decay through strong, electromagnetic and weak interactions. Charm quantum number is conserved in strong and electromagnetic interactions while it is violated in weak interactions. Strong and electromagnetic decays can occur for a charmed hadron if its mass is not the lowest in the corresponding symmetry channel, otherwise the same hadron can decay via weak interactions through emission, exchange or absorption of weak gauge bosons. Thus, for example, charmed lambda (Λ_c^+) can decay only through weak interactions. Charmness is violated in weak decays, where a charm quark (c) decays to either a strange (s) or a down quark (d). The strength of these flavor-changing weak interactions is modelled through the Cabibbo-Kobayashi-Maskawa (CKM) matrix [8]. The CKM matrix element V_{cs} that parametrizes the charm to strange transition is close to 1, thus this transition is called *Cabibbo-favored*. The element V_{cd} is much smaller compared to V_{cs}, thus charm to down transition is called *Cabiboo-suppressed* [9].

In order to explain the non-existence of flavor-changing neutral currents in decay such as $K^0 \to \mu^+\mu^-$ [10, 11], the observation of the mixing of neutral kaons [12, 13, 14], and to properly order the divergences appearing in the weak interaction, Glashow, Iliopoulos and Maiani proposed the existence of charm quark [15]. Charm was subsequently interpreted to be hidden in the J/ψ state discovered in SLAC and Brookhaven [16, 17]. These observations followed the first possible detection of open charm decay in cosmic ray [18]. Open charmed

baryons (Λ_c^+) and mesons (D^0, D^+, D_s^-) were discovered soon with the observation of various decay modes of these particles.

Charm physics garnered attention again after the discovery of open charmed mesons [19, 20] that the conventional QCD could not explain [21, 22]. This opened up a whole new area of excited charmonia states which are still being explored. The resurgence of charm physics happened for the third time when BaBar and Belle reported the mixing of neutral charm mesons [23, 24]. Since this discovery, a lot of effort has been put into searching for CP violation in the charm sector as well as precision calculations and experiments. These recent developments in charm spectroscopy, decay constants and new physics with charmed mesons compelled Ikaros Bigi to wonder [25]: "Could Charm's 'Third Time' Be the Real Charm?" in hope for the 'intervention of New Physics'.

Study of charm physics is so important mainly because it plays the unique role of opening up the door to heavy quark physics. Almost all the theoretical models and speculations of heavy quark physics have been first implemented to the charm sector. Furthermore, the *beauty* or *bottom* quark (b quark) decays predominantly to charm quark, making charm an indispensable part of b-physics as well.

1.3 Scope of the Thesis

In the first part of this thesis, we focus on estimating the mass and nonleptonic decay properties of $\Lambda_c^+(udc)$, the lightest charmed baryon. For this purpose, we use a non-perturbative method called Quantum Chromodynamics Sum Rules (QCD Sum Rules) (for a detailed discussion, see Chapter 3). Although Λ_c^+ was the first charmed baryon ever to be discovered [26], the knowledge of Λ_c^+ physics is much limited, primarily because it has many available modes of decay. Studies of charmed baryon decays provide important information about

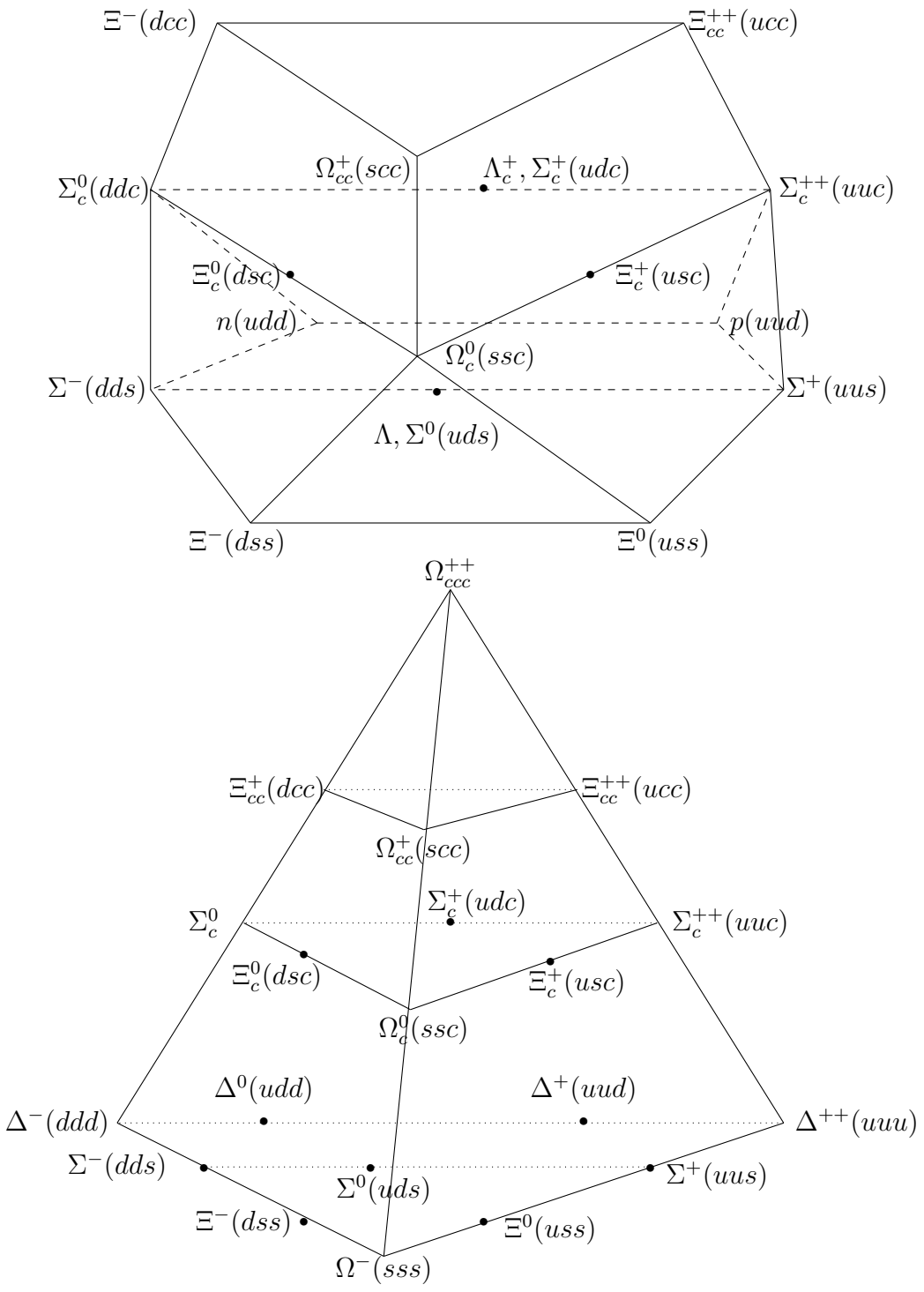

Figure 1.1: Baryon family predicted by the Standard Model for $J^P = 1/2^+$ (top) and $J^P = 3/2^+$ (bottom) with different charmness. Baryons in the same plane have broken $SU(3)$ flavor symmetry in light quark (u, d, s) sector while particles in different horizontal planes have different charmness.

both strong and weak interactions. As discussed above, measurements of Λ_c^+ decay can provide us input on Λ_b^0 hadronic decays because the dominant branching fraction of Λ_b^0 involves decaying to Λ_c^+ [27]. Furthermore, they can help us to constrain the fragmentation function of c and b quarks in heavy-quark baryons [28].

Significant progress of technologies in particle tracking, identification and luminosity recently has enabled us to detect a number of missing modes [29]-[35]. However, we know only about 68% of the total branching ratio [36], mostly measured against the Cabibbo-favored channel $\Lambda_c^+ \to pK^-\pi^+$. The first model-independent measurements of the absolute branching fraction of this *golden* channel, $\Lambda_c^+ \to pK^-\pi^+$, have been made by Belle [37] and BESIII [38] only recently. Studying these decays of Λ_c^+ is important because it provides us important insights on subjects such as the internal dynamics between heavy and light quarks within hadrons. Additionally, all other charmed baryons eventually decay to Λ_c^+ because it is the lightest charmed baryon, thus studying the decay modes of this particle makes it possible to study the decay properties of heavier charmed baryons as well.

Using QCD Sum Rules discussed in Chapter 3, we estimate the charmed lambda (Λ_c^+) baryon mass in Chapter 4 using a two-point correlation function of Λ_c^+ current operator. The same calculations also help us to estimate the baryonic mass of Λ^0 and Λ_b^0 by replacing charm quark mass with strange and bottom quark masses respectively. In Chapter 5, we extend this framework to consider a three-point function comprised of the Λ_c^+ and Λ_b^0 current operators (used in Chapter 4) and weak Hamiltonian in the presence of an external pion field to estimate the coupling constant corresponding to the decay process $\Lambda_c^+ \to \Lambda^0\pi^+$. The Sum Rule framework developed in Chapter 5 can be used further to estimate both the Cabibbo-favored and Cabibbo-suppressed decays of heavy-quark baryons even for the cases when the masses of the parent and product baryons are not close.

Publications:

- Leonard S. Kisslinger, Bijit Singha. *Charm, Bottom, Strange Baryon Masses Using QCD Sum Rules.* Int. J. Mod. Phys. A 33 (2018) 1850139: **discussed in Chapter 4**,

- Leonard S. Kisslinger, Bijit Singha. *Charmed Baryon Decay to a Strange Baryon Plus a Pion Using QCD Sum Rules.* Int. J. Mod. Phys. A 34 (2019) 1950015: **discussed in Chapter 5**.

In the second part of the thesis, we extend our previous work on the charmed mesons $D^+(c\bar{d})$ and $D^0(c\bar{u})$ production from proton-proton (p-p) and heavy-ion (A-A) collisions [39] to consider $B^0(b\bar{d})$ and $B^-(b\bar{u})$ production via unpolarized p-p and A-A collisions at 200 GeV in Chapter 6. Two main new aspects of this work are that a gluon can create a heavy quark-antiquark pair $b\bar{b}$ and then a fragmentation process converts a $b\bar{b}$ into a $b\bar{d} - d\bar{b}$. We also use the color octet model which assumes that the $b\bar{b}$ pairs created from the gluons are predominantly color-octet. At the proton-proton energies of the Fermilab, BNL-RHIC, or the Large Hadron Collider, the color-octet mechanism [40, 41, 42] dominates the color-singlet mechanism, as shown in studies of J/ψ production at $\sqrt{s} = 200$ GeV at BNL [43, 44]. Our estimates of the B-production cross-section are expected to be tested by heavy-ion collision experiments in the near future.

Publication:

- Leonard S. Kisslinger, Bijit Singha. *B Production In p-p and A-A Collisions.* Int. J. Theor. Phys. 56 (2017) 3648: **discussed in Chapter 6**.

Chapter 2

On the Origin of Hadronic Mass

Over a few centuries, our understanding about mass has changed gradually from a foundational extensive parameter of an object to an emergent property. In Newtonian mechanics, mass is defined as 'the quantity of matter'. It is the measure of the matter arising from its density and volume conjointly [46]. Newton assumed mass as a conserved quantity of any object that is not altered, created or destroyed during its motion through the absolute space and time. Newton, then, went on to define momentum as the 'quantity of motion' and expressed it as the product of the mass of any object times its velocity.

This notion of mass changed substantially during the early twentieth century with the advent of the special and general theory of relativity. In relativity, mass is essentially defined as the Minkowski norm of the four-momentum which is to say, two observers sitting in different reference frames will measure different energy (E) and momentum ($\vec{p}_R$) of any object but they will agree upon the fact that $E^2 - (\vec{p}_R c)^{\,2} = (mc^2)^2$ is an invariant quantity, where m is the particle's proper mass or rest mass and c is the speed of light. Consequently,

- Unlike Newtonian mechanics where the momentum of any object was defined through its mass: $\vec{p}_N = m\vec{v}$, relativity allows even a particle with zero rest mass to have a non-zero momentum through the relation $p_R = E/c \neq 0$ even if $m \to 0$. Also, it is the energy of a set of objects and not the mass that is conserved as assumed in Newtonian mechanics.

- In general relativity, the cause of curvature in spacetime is attributed to the energy-momentum tensor and not just the mass. Thus, the importance of mass as the central parameter to determine the inertia and thus the motion of any object through an absolute space-time in the classical Newtonian description is weakened in the relativistic formulation of physics.

However, both Newtonian and relativistic mechanics treat mass (or specifically, the rest mass) as a parameter and do not give us any information about the origin of it. Furthermore, both the theories fail to provide the reason behind identical particles and their identical mass. If we observe two electrons that were created in different galaxies at different time, they will have the same mass. Not only that, different subatomic particles (*e.g.* electron and positron) are found in nature that have different quantum numbers but same mass. Newtonian mechanics and Einstein's theory of relativity fail to provide any fundamental reason behind this universality. In order to address these issues we need quantum field theory, which assumes that any fundamental particle can be thought of as quanta of an underlying field prevalent in spacetime across the universe. Thus, the matter and energy content of the universe and their chemistries that we perceive around us are nothing but excitations of a few quantum fields spanning across the whole universe and their interactions consistent with a few basic symmetries!

From the following section onward, we are going to narrow down our focus to describe the emergence of mass in the specific area of nuclear and hadronic physics. We will start with the nuclear mass and its relationship to the mass of the nucleons. Then, we will discuss the origin of mass of nucleons and hadrons in general using QCD. We will also discuss different symmetries of QCD that exist in the limit where QCD contains no mass parameters and how they get broken by the introduction of mass in the theory. Discussion on Higgs physics, although it is an important topic in the context of the current section, is beyond the scope

of this thesis and we will not discuss it here. For more discussions on this topic, see [47, 48].

2.1 Origin of Mass within Nucleus and Low-lying Hadron Spectrum

A nucleus is the dense center of an atom, a few fermi in size and is comprised of protons and neutrons (together called nucleons). The mass of a nucleus is approximately the sum of the masses of its individual nucleons. Thus, if mass of proton and a neutron is M_p and M_n, then the mass of the ground state nucleon, M_N, is given by

$$M_N(Z, A) = ZM_p + (A - Z)M_n + \Delta(Z, A) \ , \tag{2.1}$$

where A is nucleon number and Z is atomic number. The quantity $\Delta(Z, A) \ll M_N$ is called the mass defect of a nucleon and is related to the interaction energy between nucleons inside a nucleus through the expression: $\Delta = -E_B/c^2$, where E_B is the binding energy and the negative sign signifies that the nuclear force is attractive inside a stable nucleus. $\Delta(Z, A)$ can be modelled by the semi-empirical Bethe-Weizsäcker formula [49]. One may also ask, from the perspective of QCD, why there exists a separation between nucleons in the nucleus if every nucleon is made of three light quarks and the inter-nucleon separation is of the same size as the size of the nucleons. This is because, although scalar (spin 0) meson exchange between two nucleons is the main source of attraction between two nucleons at around the equilibrium distance, vector (spin 1) meson exchange dominates at the nearer distances contributing to short-range repulsion. Also, the nucleons are fermions, thus there exists an effective repulsion arising from Fermi-Dirac statistics. These two reasons give us a qualitative explanation behind the fact that the nucleons inside a nucleus do not merge

together to form a *quark-commune*. An important development towards the understanding of this phenomenon has been through an effective field theory of the nuclear force, namely Quantum Hadrodynamics [50]. Attempts have been made to understand nuclear interactions in terms of quark degrees of freedom (*e.g.* [51, 52, 53, 54] where the authors have used QCD Sum Rules), however, a full quantitative description of nuclear medium from QCD is still missing in the literature.

In order to understand the origin of nucleon mass we try to calculate, using the theory of QCD, how the chromoelectric and chromomagnetic fields from gluons and quarks can have back-reactions resisting the acceleration of the quarks and gluons in a hadron. This is challenging especially because around 1 GeV the coupling parameter becomes of the order of unity making the QCD processes non-perturbative. One way to make quantitative predictions of these non-perturbative processes is lattice QCD which uses Markov Chain Monte Carlo methods to evaluate the path integrals formulated in a four-dimensional spacetime lattice. In fact, there has been significant progress in calculating the low-lying hadron spectrum through this procedure as shown in Fig. 2.1.

To calculate the same spectrum analytically, we must try to understand the nontrivial structure of the QCD vacuum. Due to the non-perturbative nature of QCD in the infrared regime, non-zero quantum fluctuations of quark and gluon fields persist in QCD vacuum and manifest themselves through different vacuum condensates. These condensates break a number of symmetries (*e.g.* chiral and dilatation symmetries) many of which are present in the QCD lagrangian. The true nature of these condensates is not well understood yet. In fact, even basic questions such as whether these condensates are properties of the QCD vacuum or just the property of the hadrons themselves are still being debated [56, 57, 58, 59].

From here onwards, we use natural units: $\hbar = c = 1$.

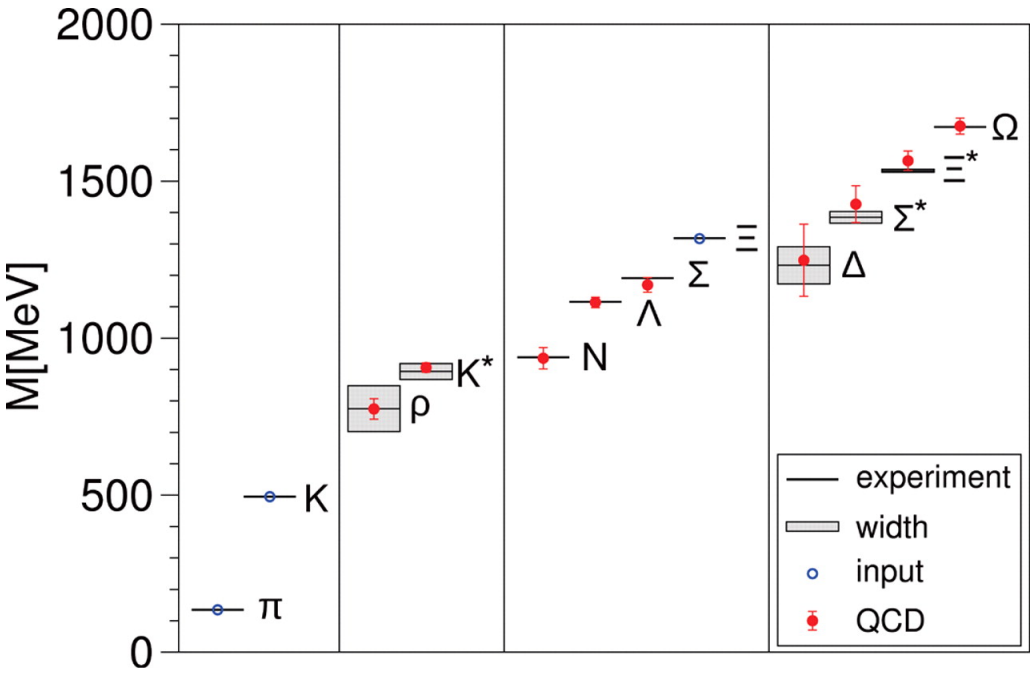

Figure 2.1: Low-lying hadron spectrum derived from ab initio calculations in lattice QCD [55]. π and K masses fix the masses of the light quarks (u, d, s) and Ξ sets the overall scale, thus these three hadrons do not have any error bar. Three lattice spacings were used for extrapolating the results to continuum.

2.2 Formation of Quark Condensates

The vacuum expectation value (VEV) of an antiquark-quark operator is called quark condensate. These condensates are formed in the ground state $|\Omega(U)\rangle$ and are given by

$$\langle\Omega(U)|\bar{q}_f q^{f'}|\Omega(U)\rangle = -\sigma U_f^{f'}, \tag{2.2}$$

where f and f' are flavor indices and $U \in SU(N_f)$. We get a ground state for any given choice of U and all these ground states are orthogonal and degenerate. The long-wavelength ripples generated due to the small variations of U over spacetime are the Nambu-Goldstone modes and can be parametrized as

$$U(x) = \exp\left[\frac{2i}{f_\pi}\pi^a(x)T^a\right], \qquad a = 1, 2, ..., N_f^2 - 1\ . \tag{2.3}$$

Here $\pi^a(x)$ are the corresponding fields, $\{T^a\}$ are the generators of $SU(N_f)$, and f_π is the pion decay constant. A full quantitative understanding of why these condensates form is still lacking but let me try to provide a heuristic picture here. The tree level gluon exchange processes that are dominating in the UV regime ($g_S^2 \ll 1$) are shown in Figure 2.2. The anti-symmetric diagram of the quark-antiquark pairs leads to attraction while the symmetric diagrams of color-adjoint quark pair lead to repulsion.

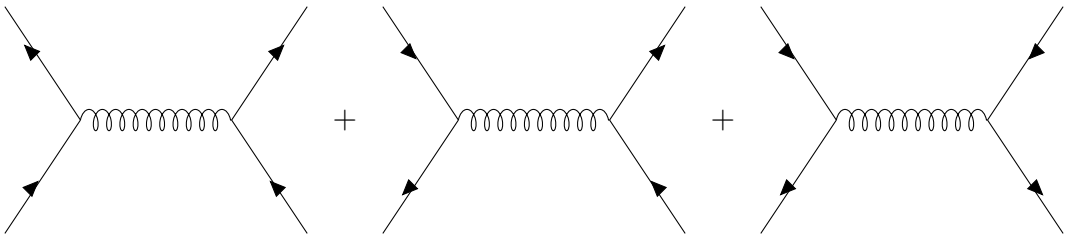

Figure 2.2: Tree-level gluon exchange diagrams dominant in the high energy limit, $g^2 \ll 1$.

But these diagrams do not give us non-zero matrix elements between the vacuum and the

quark-antiquark pairs. The ones that give such matrix elements is shown in Figure 2.3. In the infrared regime ($g_S^2 \sim 1$), these diagrams dominate and change the total number of quarks and antiquarks in the system. As a result, the QCD vacuum gets populated with such pairs leading to a non-zero VEV of $\bar{q} - q$. Also, the Lorentz invariance is still preserved in this process constraining the momentum and the angular momentum of the quark and antiquark to be opposite.

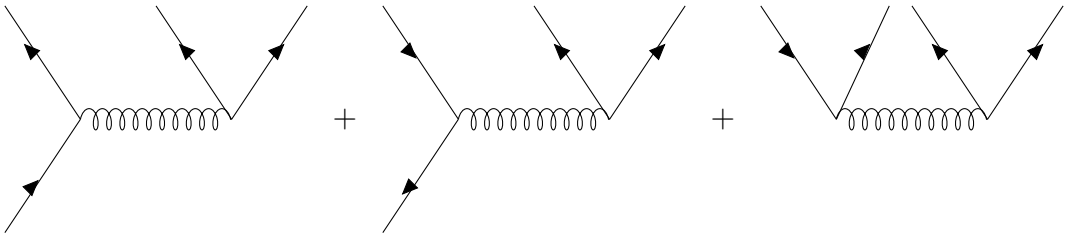

Figure 2.3: Tree-level gluon exchange diagrams dominant in the low energy limit, $g^2 \sim 1$.

2.3 Formation of Gluon Condensates

Another condensate that appears in QCD Sum Rules is of mass dimension four and is called the gluon condensate, $\langle \frac{\alpha_s}{\pi} G^a_{\mu\nu} G^{a\mu\nu} \rangle$, where $G^{a\mu\nu}$ denotes the gluon field. Unlike the quark condensates, this is not an order parameter of any spontaneous symmetry breaking and to understand the origin of this condensate, see Ref. [61].

Within hadrons exist unphysical quarks with spacelike momentum p where $-p^2 = P^2 \gg \Lambda^2_{QCD}$. The uncertainty principle tells us that such quarks can propagate only for a small amount of time $\delta t \sim (P^2)^{-1/2}$. Figure 2.4 shows such quark propagators created and absorbed by external currents within a hadron. These quarks can exchange gluons with soft momentum $k^2 \ll P^2$ (where k denotes momentum of the gluon). The soft gluons, due to their high uncertainty in spacetime, can propagate a very long distance before getting absorbed by other quarks. Furthermore, these gluons are mostly modified due to strong coupling in

the infrared regime and their behavior cannot be explained within the realm of perturbative QCD but can be characterized by the so-called gluon condensates. This phenomenon will also contribute to the vacuum energy density, ϵ, through the relation

$$\epsilon = \frac{\pi}{8\alpha_s^2}\beta(\alpha_s)\langle\frac{\alpha_s}{\pi}G^a_{\mu\nu}G^{a\mu\nu}\rangle \ , \tag{2.4}$$

where $\beta(\alpha_s)$ is the beta function.

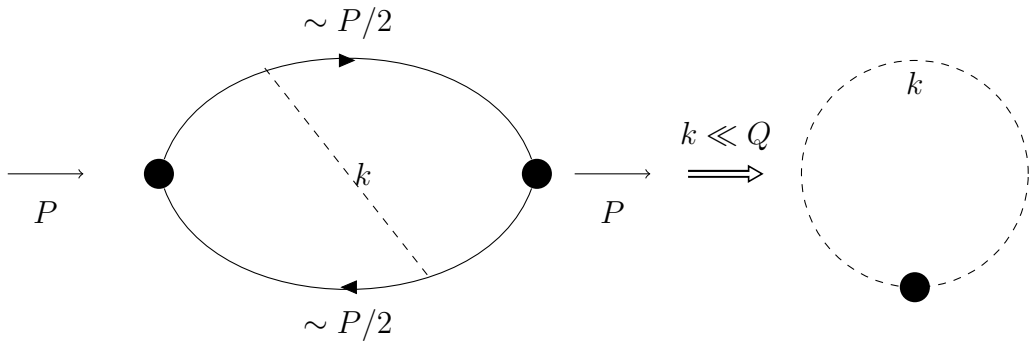

Figure 2.4: Feynman diagram of injected quark-antiquark current with one soft gluon exchange. If the momentum of the gluon is much smaller compared to that of the quark propagators, the gluon can travel far away and is modified strongly by confinement, giving rise to gluon condensate. This diagram is taken from [61].

Since a negative value of the energy density is expected from bag model and instanton gas model calculations and $\beta(\alpha_s)$ is negative, the gluon condensate has a positive value. We use Lorentz invariance and anti-symmetry of G to write

$$\langle\frac{\alpha_s}{\pi}G^a_{\mu\nu}G^b_{\kappa\lambda}\rangle = C\delta^{ab}(g_{\mu\kappa}g_{\nu\lambda} - g_{\mu\lambda}g_{\kappa\nu}) \ , \tag{2.5}$$

where we must determine the constant C. Contracting Eq. (2.5) gives

$$\begin{aligned} \delta^{ab}g^{\mu\kappa}g^{\nu\lambda}\langle\frac{\alpha_s}{\pi}G^a_{\mu\nu}G^b_{\kappa\lambda}\rangle &= C\delta^{ab}g^{\mu\kappa}g^{\nu\lambda}\left(g_{\mu\kappa}g_{\nu\lambda} - g_{\mu\lambda}g_{\kappa\nu}\right) = 96C, \\ C &= \frac{1}{96}\langle\frac{\alpha_s}{\pi}G^2\rangle \end{aligned} \tag{2.6}$$

allowing us to write

$$\langle \frac{\alpha_s}{\pi} G^a_{\mu\nu} G^{b\mu\nu} \rangle = \frac{\delta^{ab}}{96} \langle \frac{\alpha_s}{\pi} G^2 \rangle \ . \tag{2.7}$$

In the next section, we will discuss the different QCD condensates and recent progress in their evaluation through experiments, lattice simulations, and chiral perturbation theory.

2.4 Estimating the QCD Condensates

The chiral condensate or quark condensate $\langle \bar{q}q \rangle$ is defined as the average of up and down quark condensates:

$$\langle \bar{q}q \rangle = \frac{1}{2} \left(\langle \bar{u}u \rangle + \langle \bar{d}d \rangle \right) \tag{2.8}$$

and is estimated by using the Gell-Mann-Oakes-Renner relation [62]:

$$f_\pi^2 m_\pi^2 = -2 m_q \langle 0 | \bar{q}q | 0 \rangle \ . \tag{2.9}$$

Here, m_π is the pion mass, m_q is the averaged u and d quark mass. This can also be estimated in lattice QCD and its present averaged value is given by [63]

$$\langle \bar{q}q \rangle = - \left[272(5) \text{ MeV} \right]^3 \tag{2.10}$$

with $2+1$ flavors in $\overline{MS}$ scheme at a renormalization scale of 2 GeV. The strange quark condensate is found from QCD Sum Rule analysis of baryon energy level splitting and has a value $\langle 0 | \bar{s}s | 0 \rangle / \langle 0 | \bar{q}q | 0 \rangle = 0.8 \pm 0.1$ [64]. All the other vacuum condensates cannot be

estimated analytically from first principles calculations.

A recent estimate has been made for $\langle \frac{\alpha_s}{\pi} G^2 \rangle$ by using stochastic perturbation theory [65] where this quantity was calculated in perturbative series to order α_s^{35} and subsequently was subtracted from the lattice observable. The final values of the gluon condensate obtained by this procedure is given below:

$$\langle \frac{\alpha_s}{\pi} G^2 \rangle \;=\; 0.077 \text{ GeV}^4 \text{ (uncertainty } 0.087 \text{ GeV}^4\text{)} \qquad (\text{up to } \alpha_s^{35}), \tag{2.11}$$

where the uncertainty arose due to the truncation prescription in the perturbative series.

There exist condensates of higher dimensions such as $\langle \bar{q}\sigma.Gq \rangle$, $\langle \bar{q}q \rangle \langle \frac{\alpha_s}{\pi} G^2 \rangle$ *etc.*. In the discussion for QCD Sum Rules in Chapter 3, we will expand the n-point functions of the time-ordered product of hadron currents in terms of these condensates. The non-perturbative contributions to the n-point function will be captured in these condensates.

Chapter 3

Quantum Chromodynamics Sum Rules

If we can deal with the unsatisfaction of assuming only the phenomenon of color-confinement, we would be able to produce a large amount of predictions using Quantum Chromodynamics (QCD) Sum Rules [66]. The main idea is to attack the bound state problem from the short distance side and gradually move to larger distances where asymptotic freedom starts to break down, making the QCD vacuum non-trivial quantified by the emergence of power corrections.

The method of QCD Sum Rules developed in 1979 has become an important tool in hadron phenomenology in which hadrons are represented by their interpolating quark current considered at large virtualities instead of treating the hadrons in a model-independent way in terms of constituent quarks. We write a two-point correlator using the hadron operator and treat the correlator in the framework of Operator Product Expansion (OPE), where the short and large distance contributions are dealt separately. The former is represented by a vacuum condensate while the latter is called Wilson's coefficient and evaluated using perturbative QCD. The condensates carry information about the infrared behavior of the quark and gluon Green's functions. We further use quark-hadron duality to relate the spectral density obtained by treating quarks and gluons as the fundamental degrees of freedom with the phenomenological model of hadron spectrum. A review of this method is given in [64].

In order to illustrate QCD Sum Rules, let's consider a meson current of the general form $j_\Gamma(x) = \bar{q}_i \Gamma q_j$, where the subscript i and j denote the flavors and Γ encodes a tensor structure. This current is projected to definite J^{PC} quantum numbers. Additionally, we have to create the right combination of flavors to create a current of definite isospin. This current will polarize the vacuum and this phenomenon is quantified by the two-point function

$$i \int d^4x e^{ip.x} \langle 0|T\left\{j_\Gamma(x) j_\Gamma(0)\right\}|0\rangle = T_{\mu\nu\ldots}\ \Pi^j(p^2)\ , \tag{3.1}$$

where we have denoted the time-ordered product of the meson currents on the left hand side by T, $\Pi^j(p^2)$ is a scalar function (possibly) related to vacuum polarization, $T_{\mu\nu\ldots}$ is tensor arising from the tensor structure of the current.

Mentioned below is a list of meson currents corresponding to different J^{PC} channels [66, 67]

$$\begin{aligned}
j_{\text{scalar}} &= \bar{q}_i q_j\ , & J^{PC} &= 0^{++}, \\
j_{\text{pseudoscalar}} &= i\bar{q}_i \gamma_5 q_j\ , & J^{PC} &= 0^{-+}, \\
j_{\text{vector}} &= \bar{q}_i \gamma_\mu q_j\ , & J^{PC} &= 1^{--}, \\
j_{\text{axial}} &= \eta_{\mu\nu} \bar{q}_i \gamma_\mu \gamma_5 q_j\ , & J^{PC} &= 1^{++}, \\
j^{C=-1}_{\text{axial}} &= \bar{q}_i \partial_\mu \gamma_5 q_i\ , & J^{PC} &= 1^{+-}, \\
j_{\text{tensor}} &= i\bar{q}_i(\gamma_\mu \partial_\nu + \gamma_\nu \partial_\mu + \frac{2}{3}\eta_{\mu\nu}\not{\partial}) q_i\ , & J^{PC} &= 2^{++},
\end{aligned} \tag{3.2}$$

where $\eta_{\mu\nu} = p^\mu p^\nu / p^2 - g_{\mu\nu}$. We can construct baryon current operators in a similar way, for example

$$j^N(x) = \epsilon_{abc}\left[u^a(x)C\gamma^\mu u^b(x)\right]\gamma_5\gamma_\mu d^c(x), \tag{3.3}$$

$$j_\mu^{\Delta^{++}}(x) = \epsilon_{abc}\left[u^a(x)C\gamma_\mu u^b(x)\right]u^c(x), \tag{3.4}$$

where C denotes the charge conjugation matrix, N stands for nucleon, and Δ^{++} stands for delta baryon. We want to mention here that the choice of current for a given J^{PC} is not unique and a number of currents can couple to a physical state of a given channel.

Notice that we are including non-perturbative effects through the condensates which do not take into account the leading non-perturbative contributions coming from the instantons. However, it has been shown that the assumptions behind the OPE are valid in Eq. (3.6) and they break down only at higher orders in P^{-2} [66].

3.1 Operator Product Expansion

The theoretical basis of QCD Sum Rules relies on the OPE for n-point correlation function. We start at short distances, assuming that OPE is valid for the time-ordered product of hadron currents allowing one to write, in coordinate space

$$\langle T\left\{J(x)J(0)\right\}\rangle_{x\to 0} = \sum_n C_n(x;\mu)\langle\mathcal{O}_n(\mu)\rangle\ . \tag{3.5}$$

μ is an artificial momentum that sets the normalization scale, meaning all fluctuations higher than μ are assumed to be hard while fluctuations lower than μ are soft processes. Thus, the modes lower than μ that are responsible for the non-perturbative effects will

remain in the condensates while the higher modes will contribute to the Wilson coefficients. Because the physical processes of our consideration are μ-independent, the μ-dependence of the condensates are cancelled by the μ-dependence of the Wilson coefficients.

Taking the Fourier transform of Eq. (3.5) will give us

$$i\int d^4x e^{ip.x}T\left\{j_\Gamma(x)j_\Gamma(0)\right\} = C_I^\Gamma(p;\mu)I + \sum_n C_n^\Gamma(p;\mu)\langle\hat{O}_n(\mu)\rangle\ . \tag{3.6}$$

Here I is the identity operator, $\langle\hat{O}\rangle = \langle 0|\hat{O}_n|0\rangle$ with $\hat{O}_n$'s gauge invariant operators comprised of quark and gluon fields. These operators are arranged in the order of increasing mass dimension, so the mass dimension of the Wilson coefficients C_n's decrease in power of p^2. So, at high virtualities, the operator with the low dimensions will dominate and subsequently give power corrections to the perturbative contribution coming from the unit operator. Since, we are dealing with only the Vacuum Expectation Value(VEV) of the operators, we consider only the spin-0 operators. Mentioned below is a list of all such operators of mass dimensions less than equal to 6:

$$\begin{aligned}
I, &\quad d = 0,\\
m\bar{q}q, &\quad d = 4,\\
G^a_{\mu\nu}G^a_{\mu\nu}, &\quad d = 4,\\
\bar{q}\Gamma_1 q\ \bar{q}\Gamma_2 q, &\quad d = 6,\\
m\bar{q}\sigma_{\mu\nu}\frac{\lambda^a}{2}qG^a_{\mu\nu}, &\quad d = 6,\\
f_{abc}G^a_{\mu\nu}G^b_{\nu\gamma}G^c_{\gamma\mu}, &\quad d = 6,
\end{aligned}$$

where λ^a are Gell-Mann matrices, $\sigma_{\mu\nu} = \frac{1}{2}i\left[\gamma_\mu,\gamma_\nu\right]$. Thus, in Eq. (3.6), we consider VEV of the operators O_n which are zero in perturbation theory. This is due to the nature of the QCD

vacuum that it has non-perturbative fluctuations of the quark and gluon fields. But non-zero values of these VEVs are a well-known phenomenon in QCD, for example, chiral symmetry breaking is attributed to the VEV $\langle 0|\bar{q}q|0\rangle \neq 0$ and we had an extensive discussion about this in the last chapter. As we will see next, all the soft, non-perturbative contributions to the correlation function will be manifested through these VEV elements.

The most important expression in this section is Eq. (3.6) and it has a very clear interpretation. In order to calculate the correlator, we start at short distances (with the perturbative term corresponding to the identity operator) and approach to large distance dynamics step by step by introducing the vacuum condensates of increasingly higher orders.

To understand this parametrization of the non-perturbative effects caused by the vacuum, let's start with a heuristic picture of injecting a quark-antiquark pair through external (vector or axial vector) current in the vacuum and analyzing its evolution. As a matter of fact, this kind of currents exist in nature and the effect of this current on the vacuum is not substantial if it can propagate only a small distance. In the realm of OPE, it just means that we have to deal with only a few vacuum condensates in order to explain the physics arising from these currents. Also, the momentum scale associated with the fluctuations of the valence quarks and gluons inside a hadron must be much larger than the fictitious scale, μ, that we have introduced in OPE.

The lowest-order gauge- and Lorentz-invariant condensate that we encounter in our formalism is the quark condensate $\langle \bar{q}q \rangle$, which can be thought of as the *order parameter* of spontaneous breaking of chiral symmetry responsible for generating massles pions. Thus, we can interprete the contributions coming from the condensate terms as deviations from perturbation theory. The most evident reason behind this statement is the gluon condensate, $\frac{\alpha_s}{\pi} G^a_{\mu\nu} G^a_{\mu\nu}$.

The gluon field can fluctuate with all possible frequencies ranging from very high (UV or hard) to very low (IR or soft) modes. The normalization scale μ seperates out these two regions. The hard modes contributes in a perturbative manner to the correlator, while the soft modes saturates the gluon condensate. So, for example, the power divergence of the energy density that we talked about in the last paragraph goes to the perturbative term of the expansion allowing us to construct the condensates only with soft modes.

3.2 Dispersion Relations

In this subsection, we derive a dispersion relation that relate the resonances to the analytic property of a two-point function. For this, we use Lehmann-Kallen spectral representation to write the propagator of an interacting field as

$$\Delta(p^2) = \frac{1}{\pi}\int_0^\infty ds^2 \frac{\rho(s^2)}{p^2 - s^2 + i\epsilon} \ , \tag{3.7}$$

which is basically showing that the full propagator in momentum space is a superposition of free single-particle propagators, each with different mass, weighted with a positive definite function $\rho(s^2)$ which is the spectral density of the theory. If we assume that the lowest single particle state in the theory is massive with $s^2 = m^2$, then the spectral density assumes the following form:

$$\rho(s^2) = \pi Z \delta(s^2 - m^2) + \rho(s^2)\Theta(s^2 - m^2_{\lambda\neq 1}) \ . \tag{3.8}$$

where Z is normalization factor. Using this spectral density in Eq. (3.7), we get

$$\Delta(p^2) = \frac{Z}{p^2 - m^2 + i\epsilon} + \frac{1}{\pi}\int_{m^2_{\lambda\neq 1}}^\infty ds^2 \frac{\rho(s^2)}{p^2 - s^2 + i\epsilon} \ . \tag{3.9}$$

Now we use Sokhotski-Plemelj theorem to write

$$\lim_{\epsilon\to 0^+} \frac{1}{p^2 - s^2 \pm i\epsilon} = \mathcal{P}\frac{1}{p^2 - s^2} \mp i\pi\delta(p^2 - s^2) \ . \tag{3.10}$$

This allows to write the full propagator as

$$\begin{aligned} \Delta(p^2) &= \frac{Z}{p^2 - m^2 + i\epsilon} + \frac{1}{\pi}\mathcal{P}\int_{m^2_{\lambda\neq 1}}^{\infty} \frac{\rho(s^2)}{p^2 - s^2} - i\int_{m^2_{\lambda\neq 1}}^{\infty} ds^2\delta(p^2 - s^2)\rho(s^2) & (3.11)\\ &= \frac{Z}{p^2 - m^2 + i\epsilon} + \frac{1}{\pi}\mathcal{P}\int_{m^2_{\lambda\neq 1}}^{\infty} \frac{\rho(s^2)}{p^2 - s^2} - i\rho(p^2)\Theta(p^2 - m^2_{\lambda\neq 1}) \ . & (3.12) \end{aligned}$$

Using the property of Lorentzian function,

$$\lim_{\epsilon\to 0} F_\epsilon(x) = \lim_{\epsilon\to 0} \frac{1}{\pi}\frac{\epsilon}{x^2 + \epsilon^2} = \delta(x). \tag{3.13}$$

the imaginary part of this full propagator can be written as

$$\begin{aligned} i \text{ Im } \Delta(p^2) &= -i\epsilon\frac{Z}{(p^2 - m^2)^2 + \epsilon^2} - i\rho_{a.t.}(p^2) & (3.14)\\ \Rightarrow \text{Im } \Delta(p^2) &= -\left[Z\pi\delta(p^2 - m^2) + \rho_{a.t}(p^2)\right], & (3.15) \end{aligned}$$

where $\rho_{a.t}(p^2) = \rho(p^2)\Theta(p^2 - m^2_{\lambda\neq 1})$ is the spectral density above the two-particle threshold. Comparing Eq. (3.14) with Eq. (3.9), we can write

$$\text{Im } \Delta(p^2) = -\rho(p^2) \ . \tag{3.16}$$

Also, from Eq. (3.12) we get

$$\begin{aligned}
\text{Re } \Delta(p^2) &= \frac{Z(p^2-m^2)}{(p^2-m^2)^2+\epsilon^2} + \frac{1}{\pi}\mathcal{P}\int_{m^2_{\lambda\neq 1}}^{\infty} ds^2 \frac{\rho(s^2)}{p^2-s^2} \\
&= \frac{Z}{p^2-m^2} + \frac{1}{\pi}\mathcal{P}\int_{m^2_{\lambda\neq 1}}^{\infty} ds^2 \frac{\rho(s^2)}{p^2-s^2} \\
&= \frac{1}{\pi}\mathcal{P}\int_0^{\infty} ds^2 \frac{Z\pi\delta(s^2-m^2)+\rho(s^2)\Theta(s^2-m^2_{\lambda\neq 1})}{p^2-s^2} \\
&= \frac{1}{\pi}\mathcal{P}\int_0^{\infty} ds^2 \frac{\rho(s^2)}{p^2-s^2} \ . \qquad (3.17)
\end{aligned}$$

Now using Eq. (3.16) in the above equation, we get the Kramers-Kronig dispersion relation

$$\text{Re } \Delta(p^2) = \frac{1}{\pi}\mathcal{P}\int_0^{\infty} ds^2 \frac{\text{Im } \Delta(s^2)}{s^2-p^2} \ . \qquad (3.18)$$

We will use this dispersion relation in QCD Sum Rules to compare Wilson's OPE of the n-point function to the phenomenological model.

Chapter 4

Charmed, Bottom, Strange Lambda Baryon Masses Using QCD Sum Rules

The application of QCD Sum Rules to calculate the hadronic mass spectrum started with B. L. Ioffe [68] who observed that the dominant power correction to the two-point function comes from the chiral symmetry breaking in the absence of any perturbative term. In this work, Ioffe found the masses of the Δ and nucleon and also considering the first order current mass of the strange quark to be 150 MeV, he calculated the mass splitting in the decouplet $\Sigma^*(\frac{3}{2}^+)$ and $\Delta(\frac{3}{2}^+)$ to be 125 MeV. In another work [69], Belyaev and Ioffe extended the framework to calculate the mass splitting in different hyperon multiplets expressed in terms of the current strange quark mass and the quark condensate $\langle\bar{s}s\rangle$. QCD Sum Rules were used in heavy-quark mesons to calculate the $S-$ and P-wave charmonium masses and $\Upsilon - \eta_b$ splitting [67]. In [72], Sum Rules were used in the heavy quark limit $m_Q \to \infty$ to calculate the mass gap between the resonances (Σ, Σ_b) and their heavy quarks. In [73], the neutron-proton mass differences were estimated up to the operators of mass dimension 9.

QCD Sum Rules have been used to calculate the quark masses as well. Recently using the Pseudoscalar Sum Rule, the strange quark mass $\bar{m}_s$ was calculated (in $\overline{MS}$ scheme) to $\mathcal{O}(\alpha_s^4)$ [74] $\bar{m}_s(2\text{ GeV}) = (105\pm6|_{\text{parameter}}\pm7|_{\text{hadron}})$ MeV, where the subscript *parameter* denotes the

Sum Rule parameters and *hadron* denotes hadronic inputs. In [75], the relativistic and non-relativistic ratios of Laplace transform QCD Moment Sum Rules for charmonia were used to calculate the on-shell charm quark mass $m_c(P^2 = m_c^2) = 1.46 \pm 0.07$ GeV. Narison studied the effect of continuum phenomenological model on the spectral density to conclude that the effect would be minimum for high enough moment of the n-point function and from this feature, he extracted the value of the gluon condensate $\langle \alpha_s G^2 \rangle = (7.0 \pm 1.3) \times 10^{-2}$ GeV^4 and on-shell masses of charm quark, $\bar{m}_c(\bar{m}_c) = 1261(16)$ MeV and of bottom quark, $\bar{m}_b(\bar{m}_b) = 4173(10)$ MeV.

QCD Sum Rules have also found wide applications in providing essential information on the exotic hadron spectroscopy. BaBar and Belle collaborations have detected a number of controversial XYZ resonances such as $X(3872), X(3940), Y(3930), Y(4008), Z(3930), Z^+(4430)$ etc. recently which can decay into final hadronic states that contain heavy quarks such as charm and anticharm. These discoveries has opened up the possibilities that some of these resonances are the exotics lying in the same region of the spectrum of heavy quarkonia. For earlier works on this topic, see [77, 78, 79, 80] and for a recent review, see [81].

In this chapter, we present one of our research works where we use QCD Sum Rules to estimate the lambda (Λ^0), charmed lambda (Λ_c^+), bottom lambda (Λ_b^0) baryon masses. We use a lambda baryon current consistent with all the symmetries of the corresponding particle and then use the two-point correlator of the lambda current operator. The terms containing the light quark condensates will be exponentially suppressed in the Borel-transformed two-point function, so the dominant contribution to the two-point function comes from the perturbative diagram. Furthermore, we ignore all the terms that later give rise to power divergences because those terms vanishes with Borel transformation. Eventually, as we found in the last chapter, the hadronic mass of the baryon is found from the minima of the graph of Borel-transformed two-point function. In this calculation, we have not used any

free parameter in our calculations other than the current quark masses. Also, we have not used any mass expansion of either the heavy- or the light-quark field propagator, thus the expression we use for the perturbative term of the Borel-transformed two-point function is exact.

4.1 Article

The following section (Section 4.2) has been adapted from:
Leonard S. Kisslinger, Bijit Singha. *Charm, Bottom, Strange Baryon Masses Using QCD Sum Rules.* Int. J. Mod. Phys. A 33 no.23 (2018) 1850139

4.2 Estimating Masses of Λ^0, Λ_c^+ and Λ_b^0 Using QCD Sum Rules

The two-point correlator in momentum space is used to estimate the mass of the Λ_c^+, a charmed baryon. The two-point correlator is

$$\Pi_2(p) = i \int d^4x \; e^{ip.x} \langle 0|T\left[\eta_{\Lambda_c^+}(x)\bar{\eta}_{\Lambda_c^+}(0)\right]|0\rangle \; . \tag{4.1}$$

where $\eta_{\Lambda_c^+}$ is the current for Λ_c^+:

$$\eta_{\Lambda_c^+}(x) = \epsilon^{efg}\left[u^{e^T}(x)C\gamma^\mu d^f(x)\right]\gamma^5\gamma_\mu c^g(x) \; . \tag{4.2}$$

with e, f, g color indices, u, d are up and down quarks and c is a charm quark, C is the charge conjugation matrix ($C^2 = -1$), and ϵ^{efg} is the totally antisymmetric tensor that makes $\eta_{\Lambda_c^+}$ a

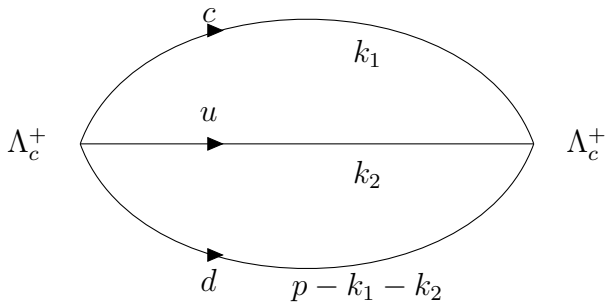

Figure 4.1: Perturbative diagram for the two-point correlator of Λ_c^+

color-singlet. The current operator in Eq. (4.2) is constructed with the appropriate quantum number corresponding to the hadronic system (Λ_c^+ here). The choice of the current operator is not unique but as we will see, the charmed lambda resonance couples most strongly to this current. The perturbative diagram that contributes to the two-point correlator is illustrated in Figure (4.1).

Using the method of QCD Sum Rules[64], the time-ordered product in Eq. (4.1) is replaced by a trace to give us

$$\Pi_2(p) = i \int \frac{d^4k_1}{(2\pi)^4} \frac{d^4k_1}{(2\pi)^4} \text{tr}\left[S_c(k_1)\gamma^5\gamma^\mu S_u(k_2)\gamma^5\gamma^\mu S_d(p-k_1-k_2)\right] \ , \tag{4.3}$$

where S_c, S_u, S_d are the charm, up, and down quark propagators. Using the Dirac slash notation $\not{p} = p_\mu\gamma^\mu$, we write

$$S_c(p) = i\frac{\not{p} + M_c}{p^2 - M_c^2} \ , \tag{4.4}$$

where $M_c = 1.27$ GeV is the on shell current charm quark mass. S_u, S_d have similar

expressions with $m_u \approx m_d \equiv m \ll M_c$. Using Eqs. (4.3, 4.4) in Eq. (4.1), we get

$$\Pi_2(p) = \int \frac{d^4k_1}{(2\pi)^4}\frac{d^4k_2}{(2\pi)^4}\frac{\mathrm{tr}\left[(\not{k}_1 + M_c)\gamma^5\gamma^\mu(\not{k}_2 + m)\gamma^5\gamma^\mu\left(\not{p} - \not{k}_1 - \not{k}_2 + m\right)\right]}{(k_1^2 - M_c^2)(k_2^2 - m^2)\left[(p - k_1 - k_2^2)^2 - m^2\right]} \ . \tag{4.5}$$

We use the trace identities of gamma matrices to evaluate the trace in the above equation. We use the fact that the trace of odd number of gamma matrices is zero and

$$\mathrm{tr}(\gamma^\mu\gamma^\nu) = 4g^{\mu\nu}, \tag{4.6}$$

$$\mathrm{tr}(\gamma^\mu\gamma^\nu\gamma^\kappa\gamma^\omega) = 4\left(g^{\mu\nu}g^{\kappa\omega} - g^{\mu\kappa}g^{\nu\omega} + g^{\mu\omega}g^{\kappa\nu}\right) \ . \tag{4.7}$$

Using the above identities in Eq. (4.5), we get

$$\begin{aligned}\Pi_2(p) &= 8\int \frac{d^4k_1}{(2\pi)^4}\frac{d^4k_2}{(2\pi)^4}\frac{2M_cm^2 + M_ck_2.(p - k_1 - k_2) + 2mk_1.(p - k_1 - k_2) + mk_1.k_2}{(k_1^2 - M_c^2)(k_2^2 - m^2)\left[(p - k_1 - k_2^2)^2 - m^2\right]} \\ &\equiv 8\int \frac{d^4k_1}{(2\pi)^4(k_1^2 - M_c^2)}\Pi_{k_1}(p) \ . \end{aligned} \tag{4.8}$$

To evaluate this integral, we define $\bar{p} = p - k_1$ and $k = k_2$. This gives us

$$\Pi_{k_1}(p) = \int \frac{d^4k}{(2\pi)^4}\frac{2M_cm^2 + M_ck.(\bar{p} - k) + 2mk_1.(\bar{p} - k) + mk_1.k}{(k^2 - m^2)\left[(\bar{p} - k)^2 - m^2\right]} \ . \tag{4.9}$$

We define

$$\Pi_1(p) = \int \frac{d^4k}{(2\pi)^4}\frac{1}{(k^2 - m^2)\left[(\bar{p} - k)^2 - m^2\right]} \ . \tag{4.10}$$

In Eq. (4.10), there is a four-dimensional integral which is UV-divergent. We parametrize all momentum-space propagators as

$$\frac{1}{k^2 - m^2} = \int_0^\infty d\alpha \ e^{-\alpha(k^2 - m^2)}, \qquad m^2 \neq 0 \ . \tag{4.11}$$

We then write all vector products over a complex $D = 4 - \epsilon$ dimensional space. Eq. (4.10) then reduces to generalized Gaussian integral which can easily be evaluated in the momentum space:

$$\int \frac{d^D\bar{k}}{(2\pi)^D} e^{-(\alpha+\beta)\bar{k}^2} = 1/(4\pi(\alpha+\beta))^{D/2} \; . \tag{4.12}$$

We use this dimensional regularization technique [82, 83] with the substitution

$$\bar{k} = k - \beta\bar{p}/(\alpha+\beta), \tag{4.13}$$

to evaluate the integral in Eq. (4.10):

$$\Pi_1(p) = \int_0^\infty d\rho \int_0^1 d\alpha \int_0^1 d\beta \frac{1}{(4\pi)^{D/2}} \rho^{1-D/2} \delta\left(1-\alpha-\beta\right) \rho^{1-D/2} e^{-\rho\left[-m^2+\alpha(1-\alpha)\bar{p}^2\right]} \; . \tag{4.14}$$

Integrating Eq. (4.14) by parts we obtain

$$\Pi_1(p) = \frac{1}{(4\pi)^2}(2m^2 - \bar{p}^2/2) I_0(\bar{p}) \tag{4.15}$$

$$\text{with} \quad I_0(p) = \int_0^1 d\alpha \frac{1}{\alpha(1-\alpha)p^2 - m^2} \; . \tag{4.16}$$

We use the same technique to evaluate the integral

$$\Pi_1^\mu(p) = \int \frac{d^4k}{(2\pi)^4} \frac{k^\mu}{(k^2-m^2)\left[(\bar{p}-k)^2-m^2\right]} = \frac{\bar{p}^\mu}{(4\pi)^2}\left[(m^2 - \bar{p}^2/4) I_0(\bar{p}) - \frac{7}{4}\right] \; . \tag{4.17}$$

We use Eq. (4.15) and Eq. (4.17) in Eq. (4.9) to get

$$\begin{aligned} \Pi_{k_1}(p) = \frac{1}{(4\pi)^2}\Big[& (2mk_1.\bar{p} + m^2 M_c)(2m^2 - \bar{p}^2/2) I_0(\bar{p}) \\ & + (M_c\bar{p}^2 - mk_1.\bar{p})\left((m^2 - \bar{p}^2/4) I_0(\bar{p}) - \frac{7}{4}\right)\Big] \; . \end{aligned} \tag{4.18}$$

From here we ignore the term $\frac{7}{4}$ because it vanishes with Borel transform. Thus, we have got the two-point function in terms of $I_n(p)$ as:

$$\Pi_2(p) = \frac{8}{(4\pi)^4}\int_0^1 d\alpha \left[2m^4 M_c I_1(p) + 3m^3 I_2(p) + \frac{3}{2}m^2 M_c I_3(p) - \frac{3m}{4}I_4(p) - \frac{M_c}{4}I_5(p)\right] . \tag{4.19}$$

where, for $k = k_1$:

$$I_1(p) = \int \frac{d^4k}{(2\pi)^4}\frac{1}{(k^2 - M_c^2)\left[-m^2 + \alpha(1-\alpha)(p-k)^2\right]}, \tag{4.20}$$

$$I_2(p) = \int \frac{d^4k}{(2\pi)^4}\frac{k.(p-k)}{(k^2 - M_c^2)\left[-m^2 + \alpha(1-\alpha)(p-k)^2\right]}, \tag{4.21}$$

$$I_3(p) = \int \frac{d^4k}{(2\pi)^4}\frac{(p-k)^2}{(k^2 - M_c^2)\left[-m^2 + \alpha(1-\alpha)(p-k)^2\right]}, \tag{4.22}$$

$$I_4(p) = \int \frac{d^4k}{(2\pi)^4}\frac{k.(p-k).(p-k)^2}{(k^2 - M_c^2)\left[-m^2 + \alpha(1-\alpha)(p-k)^2\right]}, \tag{4.23}$$

$$I_5(p) = \int \frac{d^4k}{(2\pi)^4}\frac{(p-k)^2(p-k)^2}{(k^2 - M_c^2)\left[-m^2 + \alpha(1-\alpha)(p-k)^2\right]}. \tag{4.24}$$

If we neglect the power divergences that appear in any of the above integrals, we can write

$$I_3(p) = \bar{m}^2 I_1(p), \tag{4.25}$$

$$I_4(p) = \bar{m}^2 I_2(p), \tag{4.26}$$

$$I_5(p) = \bar{m}^4 I_1(p), \tag{4.27}$$

where $\bar{m}^2 = m^2/\alpha(1-\alpha)$. Let's evaluate $I_1(p)$ and $I_2(p)$ now. For the first one,

$$I_1(p) = \int \frac{d^4k}{(2\pi)^4}\frac{1}{(k^2 - M_c^2)\left[-m^2 + \alpha(1-\alpha)(p-k)^2\right]} , \tag{4.28}$$

We use here the same regularization technique mentioned in this section before to write

$$I_1(p) = \int \frac{d^4k}{(2\pi)^4} \int_0^\infty d\kappa d\lambda \; e^{-\kappa(k^2-M_c^2)-\lambda[-m^2+\alpha(1-\alpha)(p-k)^2]} \; . \tag{4.29}$$

Now, we can evaluate the Gaussian integral over four-momenta to get

$$\begin{aligned} I_1(p) &= \frac{1}{(4\pi)^2} \int_0^\infty d\kappa d\lambda \; \left[\frac{1}{4\pi(\kappa+\lambda\alpha(1-\alpha))}\right]^{D/2} \\ &\times \exp\left[-\lambda\alpha(1-\alpha)p^2 + \kappa M_c^2 + \lambda m^2 + \frac{[\lambda\alpha(1-\alpha)p]^2}{\kappa+\lambda\alpha(1-\alpha)}\right]. \end{aligned} \tag{4.30}$$

Here we evaluate the one dimensional integral over λ to get

$$\begin{aligned} I_1(p) &= \frac{1}{(4\pi)^2} \int_0^\infty d\rho \int_0^1 d\kappa \; \rho^{(1-D/2)} \frac{1}{[\kappa+\alpha(1-\alpha)(1-\kappa)]^{D/2}} \\ &\times \exp\left[-\rho\left\{\frac{\kappa(1-\kappa)\alpha(1-\alpha)p^2}{\kappa+\alpha(1-\alpha)(1-\kappa)} - \kappa M_c^2 - (1-\kappa)m^2\right\}\right]. \end{aligned} \tag{4.31}$$

Let's define the quantity

$$a = \frac{\kappa(1-\kappa)\alpha(1-\alpha)p^2}{\kappa+\alpha(1-\alpha)(1-\kappa)} - \kappa M_c^2 - (1-\kappa)m^2 \tag{4.32}$$

to write

$$I_1(p) = \frac{1}{(4\pi)^2} \int_0^\infty d\rho \int_0^1 d\kappa \; \rho^{(1-D/2)} \frac{1}{[\kappa+\alpha(1-\alpha)(1-\kappa)]^{D/2}} \; e^{-\rho a}. \tag{4.33}$$

To evaluate the integral over ρ, we use the following expression of gamma function as an improper integral:

$$\Gamma(z) = \int_0^\infty x^{z-1} e^{-x} dx \; . \tag{4.34}$$

With this, we get

$$I_1(p) = \frac{1}{(4\pi)^2}\Gamma\left(\frac{\epsilon}{2}\right)\int_0^1 a^{-\frac{\epsilon}{2}}\frac{1}{[\kappa+\alpha(1-\alpha)(1-\kappa)]^2}. \tag{4.35}$$

With an infinitesimal ϵ, we can Taylor-expand $a^{-\frac{\epsilon}{2}} = e^{-(\epsilon/2)\ln a} = 1-(\epsilon/2)\ln a$ to get

$$I_1(p) = \frac{1}{(4\pi)^2}\int_0^1 d\kappa\frac{1}{[\kappa+\alpha(1-\alpha)(1-\kappa)]^2}\times(-\ln a). \tag{4.36}$$

We evaluate $I_2(p)$ in a similar way:

$$\begin{aligned} I_2(p) &= \int\frac{d^4k}{(2\pi)^4}\frac{k.(p-k)}{(k^2-M_c^2)\left[-m^2+\alpha(1-\alpha)(p-k)^2\right]} && (4.37)\\ &= p_\mu\int\frac{d^4k}{(2\pi)^4}\frac{k^\mu}{(k^2-M_c^2)\left[-m^2+\alpha(1-\alpha)(p-k)^2\right]} \\ &\quad -\int\frac{d^4k}{(2\pi)^4}\frac{M_c^2}{(k^2-M_c^2)\left[-m^2+\alpha(1-\alpha)(p-k)^2\right]} && (4.38)\\ &= p_\mu\bar{\Pi}_1^\mu(p) - M_c^2 I_1(p). && (4.39)\end{aligned}$$

Here $\bar{\Pi}_1^\mu$ is given by

$$\begin{aligned}\bar{\Pi}_1^\mu(p) &= \int\frac{d^4k}{(2\pi)^4}\,k^\mu\int_0^\infty d\kappa d\lambda\; e^{-\kappa(k^2-M_c^2)-\lambda[-m^2+\alpha(1-\alpha)(p-k)^2]} \\ &= \int_0^\infty d\kappa d\lambda\int\frac{d^4k}{(2\pi)^4}\,k^\mu\,\exp\Big[-\big(\kappa+\lambda\alpha(1-\alpha)\big)\left(k-\frac{\lambda\alpha(1-\alpha)p}{\kappa+\lambda\alpha(1-\alpha)}\right)^2 \\ &\qquad -\lambda\alpha(1-\alpha)p^2+\frac{(\lambda\alpha(1-\alpha)p)^2}{\kappa+\lambda\alpha(1-\alpha)}+(\kappa M_c^2+\lambda m^2)\Big]. \end{aligned}\tag{4.40}$$

Writing $k^\mu \to k^\mu + \frac{\lambda\alpha(1-\alpha)p^\mu}{\kappa+\lambda\alpha(1-\alpha)}$, we get

$$\begin{aligned}\bar{\Pi}_1^\mu(p) &= \int_0^\infty d\kappa d\lambda\int\frac{d^4k}{(2\pi)^4}\,\left[k+\frac{\lambda\alpha(1-\alpha)p}{\kappa+\lambda\alpha(1-\alpha)}\right]^\mu\times\exp\Big[-(\kappa+\lambda\alpha(1-\alpha))\,k^2 \\ &\qquad -\lambda\alpha(1-\alpha)p^2+\frac{(\lambda\alpha(1-\alpha)p)^2}{\kappa+\lambda\alpha(1-\alpha)}+(\kappa M_c^2+\lambda m^2)\Big]. \end{aligned}\tag{4.41}$$

We integrate over the four-momenta to get

$$\bar{\Pi}_1^{\mu}(p) = \frac{p^{\mu}}{(4\pi)^2}\int_0^1 d\kappa \frac{\alpha(1-\alpha)(1-\kappa)}{[\kappa+\alpha(1-\alpha)(1-\kappa)]^3} \times (-\ln a) \ . \tag{4.42}$$

This gives us

$$I_2(p) = p^2\bar{\Pi}(p) - M_c^2 I_1(p) \ , \tag{4.43}$$

where

$$\bar{\Pi}(p) = \frac{1}{(4\pi)^2}\int_0^1 d\kappa \frac{\alpha(1-\alpha)(1-\kappa)}{[\kappa+\alpha(1-\alpha)(1-\kappa)]^3} \times (-\ln a) \ . \tag{4.44}$$

We use the expressions in Eq. [4.36] and Eq. [4.42] to write the two-point function (Eq. [4.19]) as:

$$\begin{aligned}
\Pi_2(p) &= \frac{8}{(4\pi)^4}\int_0^1 d\alpha \left[2m^4 M_c I_1(p) + 3m^3 I_2(p) + \frac{3}{2}m^2 M_c I_3(p) - \frac{3m}{4}I_4(p) - \frac{M_c}{4}I_5(p)\right] \\
&= \frac{8}{(4\pi)^4}\int_0^1 d\alpha \ [2m^4 M_c I_1(p) + 3m^3\left\{p^2\bar{\Pi}(p) - M_c^2 I_1(p)\right\} + \frac{3m^4 M_c}{2\alpha(1-\alpha)}I_1(p) \\
&\quad -\frac{3m^3}{4\alpha(1-\alpha)}\left\{p^2\bar{\Pi}(p) - M_c^2 I_1(p)\right\} - \frac{M_c m^4}{4\alpha^2(1-\alpha)^2}I_1(p)] \\
&= \frac{8}{(4\pi)^4}\int_0^1 d\alpha \ \Big[\left\{2m^4 M_c - 3m^3 M_c^2 + \frac{3M_c m^4}{2\alpha(1-\alpha)} + \frac{3m^3 M_c^2}{4\alpha(1-\alpha)} - \frac{M_c m^4}{4\alpha^2(1-\alpha)^2}\right\} I_1(p) \\
&\quad + \left\{3m^3 - \frac{3m^3}{4\alpha(1-\alpha)}\right\} p^2\bar{\Pi}(p)\Big] \ .
\end{aligned} \tag{4.45}$$

The above expression contains physical and unphysical divergences. To achieve convergence, we make a Borel transformation of the form

$$\tilde{\Pi}_2(P_0^2) = \frac{1}{(n-1)!}\left(-\frac{d}{dP^2}\right)^{n-1} \Pi_2(P^2)|_{P^2=P_0^2} \ , \qquad P^2 = -p^2 \ . \tag{4.46}$$

that considers sufficiently high moment of the correlator and a high P^2, where only the contribution from the lowest resonance predominates all other resonances in the channel. Applying Borel transform to Eq. (4.45) gives us

$$\begin{aligned}\tilde{\Pi}_2(M_B) &= \frac{8}{(4\pi)^4}\int_0^1 d\alpha\,\Bigg[\left\{2m^4M_c - 3m^3M_c^2 + \frac{3M_cm^4}{2\alpha(1-\alpha)} + \frac{3m^3M_c^2}{4\alpha(1-\alpha)} - \frac{M_cm^4}{4\alpha^2(1-\alpha)^2}\right\}\mathcal{B}_{M_B}[I_1(p)] \\ &\quad + \left\{3m^3 - \frac{3m^3}{4\alpha(1-\alpha)}\right\}\mathcal{B}_{M_B}[p^2\bar{\Pi}(p)]\Bigg]\,, \end{aligned} \tag{4.47}$$

where M_B is the Borel mass. We use the following Borel-transformed functions:

$$\mathcal{B}_{M_B^2}[\ln(p^2-b^2)] = -M_B^2\; e^{-b^2/M_B^2}, \tag{4.48}$$

$$\mathcal{B}_{M_B^2}[p^2\;\ln(p^2-b^2)] = -M_B^2(b^2-M_B^2)\; e^{-b^2/M_B^2}\;. \tag{4.49}$$

The above two expressions allows us to write

$$\begin{aligned}\tilde{\Pi}_2(M_B) &= -\frac{8}{(4\pi)^6}\int_0^1 d\alpha\int_0^1 d\kappa\left(2m^4M_c - 3m^3M_c^2 + \frac{3M_cm^4}{2\alpha(1-\alpha)} + \frac{3m^3M_c^2}{4\alpha(1-\alpha)} - \frac{M_cm^4}{4\alpha^2(1-\alpha)^2}\right) \\ &\quad\times\left(\frac{-M_B^2\; e^{-b^2/M_B^2}}{[\kappa+\alpha(1-\alpha)(1-\kappa)]^2}\right) \\ &\quad -\frac{8}{(4\pi)^6}\int_0^1 d\alpha\int_0^1 d\kappa\left(3m^3 - \frac{3m^3}{4\alpha(1-\alpha)}\right)\left(\frac{-M_B^2(b^2-M_B^2)\;\alpha(1-\alpha)(1-\kappa)e^{-b^2/M_B^2}}{[\kappa+\alpha(1-\alpha)(1-\kappa)]^3}\right)\,. \end{aligned} \tag{4.50}$$

So, finally we get the expression that gives us the charmed Lambda mass:

$$\boxed{\tilde{\Pi}_2(M_B) = \frac{8M_B^2}{(4\pi)^6}\int_0^1 d\alpha\; d\kappa\;\frac{g(\alpha,\kappa)M_5(\alpha) + 3m^3M_2(\alpha,\kappa)}{g(\alpha,\kappa)^3}\;e^{-b(\alpha,\kappa)^2/M_B^2}\;.} \tag{4.51}$$

where

$$g(\alpha,\kappa) = \kappa+\alpha(1-\alpha)(1-\kappa), \tag{4.52}$$

$$b(\alpha,\kappa)^2 = g(\alpha,\kappa)\Big[\frac{M_c^2}{\alpha(1-\alpha)(1-\kappa)}+\frac{m^2}{\kappa\alpha(1-\alpha)}\Big], \tag{4.53}$$

$$M_2(\alpha,\kappa) = \Big(1-\frac{1}{4\alpha(1-\alpha)}\Big)\Big[b(\alpha,\kappa)^2-M^2\Big], \tag{4.54}$$

$$M_5(\alpha) = 2m^4M_c-3m^3M_c^2+\frac{3M_cm^4}{2\alpha(1-\alpha)}+\frac{3m^3M_c^2}{4\alpha(1-\alpha)}-\frac{M_cm^4}{4\alpha^2(1-\alpha)^2}. \tag{4.55}$$

We estimate The mass of Λ_c^+ from the minimum of the plot $\tilde{\Pi}_2(M_B)$ vs. M_B. Assuming $m = 0.004$ GeV, $M_c = 1.3$ GeV, we get a plot as shown in Figure 4.2.

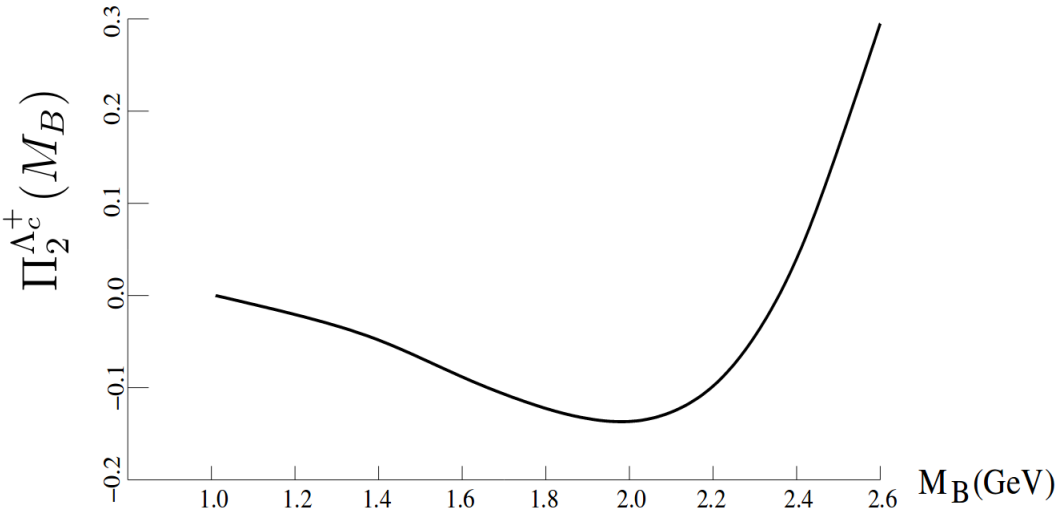

Figure 4.2: The Borel-transformed two-point correlator of charmed lambda current vs. Borel Mass (in GeV).

From the plot, we can conclude that the charmed Lambda mass,

$$M_{\Lambda_c^+} = (2.01 \pm 0.30)\ \text{GeV}, \tag{4.56}$$

assuming an error of 15% that appears typically in QCD Sum Rules due to the uncertainty

in the non-perturbative terms.

Obtaining the two-point correlator for Λ_b^0 and Λ^0 is straightforward. We replace the charm quark with strange and bottom ($c \to b, c \to s$) in Eqs. (4.1, 4.2) and using $M_c \to M_b, M_c \to M_s$ in Eqs. (4.53, 4.55). We have used $M_c \approx 1.27$ GeV and $M_b \approx 4.18$ GeV, and $M_s \approx 96$ MeV. We plot the Borel-transformed two-point function of Λ^0 and Λ_b^0 in Figure 4.3 and Figure 4.4 respectively.

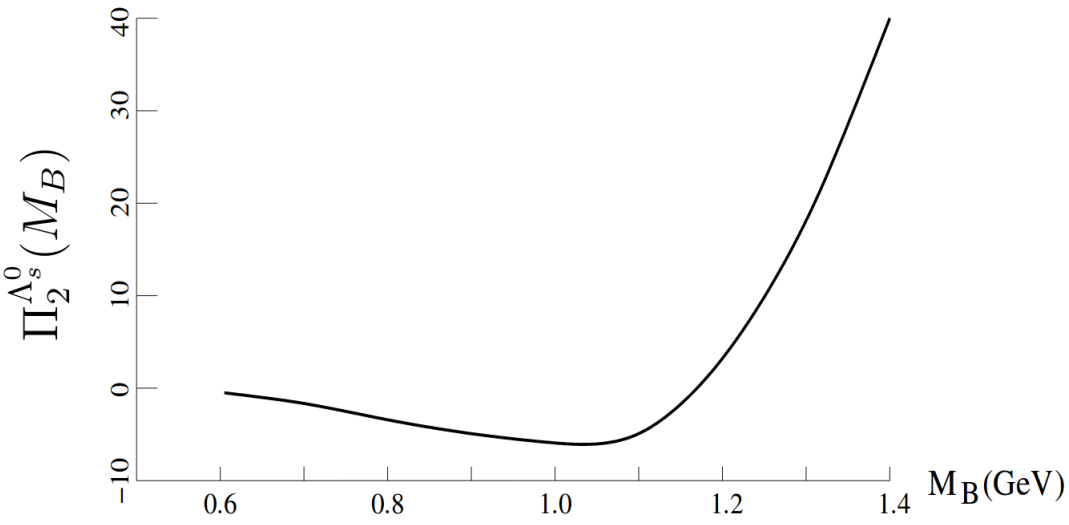

Figure 4.3: The Borel-transformed two-point correlator of strange lambda current vs. Borel Mass (in GeV).

The masses of charmed, bottom and strange lambda baryons are found to be:

$$M_{\Lambda_c^+} = 2.01 \pm 0.30 \text{ GeV}, \tag{4.57}$$

$$M_{\Lambda_b^0} = 5.34 \pm 0.25 \text{ GeV}, \tag{4.58}$$

$$M_{\Lambda^0} = 1.05 \pm 0.10 \text{ GeV}, \tag{4.59}$$

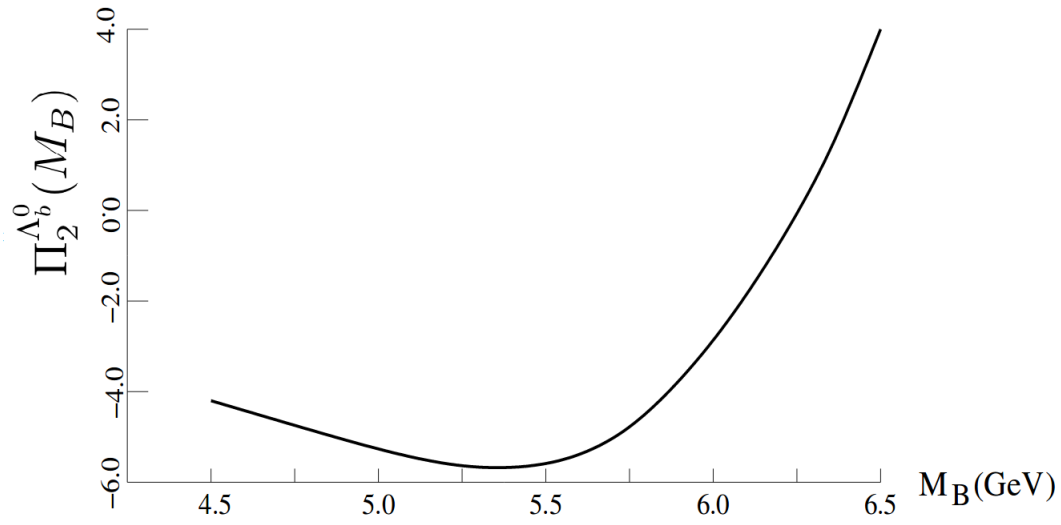

Figure 4.4: The Borel-transformed two-point correlator of bottom lambda current vs. Borel Mass (in GeV).

as compared to their experimentally found values

$$M_{\Lambda_c^+}^{\text{Exp}} = 2.28646 \pm 0.00014 \text{ GeV}, \tag{4.60}$$

$$M_{\Lambda_b^0}^{\text{Exp}} = 5.61958 \pm 0.00017 \text{ GeV}, \tag{4.61}$$

$$M_{\Lambda^0}^{\text{Exp}} = 1.115683 \pm 0.000006 \text{ GeV} . \tag{4.62}$$

A few more comments here. Following the calculation, we see that the quark condensate terms that contribute to the two-point function Eq. (4.51) will be proportional to a factor $\langle \bar{q}q \rangle \exp(-M_c^2/M_B^2)$ and thus will have a much suppressed contribution compared to the perturbative term. In the following chapter, we will use a three-point function in order to extract the decay properties of charmed lambda.

Chapter 5

Charmed Baryon to Strange Baryon Decay plus a Pion using QCD Sum Rules

In the previous chapter, we have used QCD Sum Rules for a two-point function where we extracted the mass of the lowest lying state of a channel from a two-point correlator made of hadron currents with the quantum numbers specific for the channel (isospin, angular momentum, parity, charge conjugation *etc.*). In this section, we describe how to extract information about the dynamic properties, e.g. the hadronic matrix elements corresponding to the electromagnetic and weak transitions, of hadrons by constructing a three-point function using the same hadronic local field operators used in the two-point formalism. The basic idea is simple: in the case where an external field is present, we have to include some new condensates in the OPE. These condensates describe the response of the vacuum to the correlation functions in the presence of an external field. For example, consider the VEV $\langle 0|\bar{q}\sigma_{\mu\nu}q|0\rangle$. In the absence of any external field, this will be identical to zero according to Lorentz invariance. But, in the presence of an external electromagnetic field, a quark propagating in vacuum will experience a VEV

$$\langle 0|\bar{q}\sigma_{\mu\nu}q|0\rangle_F = \sqrt{4\pi\alpha}\ \chi_q F_{\mu\nu}\langle 0|\bar{q}q|0\rangle \tag{5.1}$$

induced by the electromagentic field tensor $F_{\mu\nu}$ (the parameter χ_q having the interpretation of magnetic susceptibility of the quark condensate).

One more important distinction of the external field method is that the three point function is written in terms of the intermediate states (B with momentum p and B' with momentum p') with double poles:

$$\Pi_3(p,p') \sim \langle 0|\eta|B\rangle\langle B|j^{el}|B'\rangle\langle B'|\bar{\eta}|0\rangle \ (p^2-m^2)^{-1}(p'^2-m'^2)^{-1} \quad . \tag{5.2}$$

After the Borel transformation, both the single pole and the double pole acquire the same exponential factor, $\exp(-m^2/M^2)$ with M being the Borel mass parameter. Thus, we have to consider both the single pole and the double pole terms, giving us extra parameters on the phenomenological side of the Sum Rule. The first problem did not bother us in this work because we worked with only the Lorentz-invariant perturbative term of the three point function. To tackle the second issue with double pole, we have considered reduced Borel transformation of both the OPE and phenomenological sides as shown in Section 5.3.

In this chapter, we will estimate the coupling corresponding to a specific Cabibbo-favored weak mode in which the charmed lambda decays to a strange lambda and a pion:

$$\Lambda_c^+(udc) \to \Lambda^o(uds) + \pi^+ \ .$$

For this, we will consider a three-point correlation function of field operators corresponding to charmed lambda (Λ_c^+), strange lambda (Λ^0), and weak Hamiltonian (H_W) in the presence of an external pion field. A similar method was used in [84] to estimate the weak decays $\Sigma^- \to n + \pi^-, \Sigma^+ \to n + \pi^+$. The only difference here is that we consider a *charm* to *strange* transition rather than a *strange* to *up* transition. We have shown the perturbative diagram

for this process in Figure 5.1 in which the charm quark decays into the strange quark via a weak-charged current. All higher order diagrams will exponentially suppressed with a decaying exponent proportional to the heavy quark mass squared. We will use a dispersion relation for the correlator obtained from the OPE, and carry out a Borel transform to ensure rapid convergence. After comparing the decay rate for this process to the decay mode, $\Lambda_c^+ \to pK^-\pi^+$, we show that this weak decay mode has a comparatively small branching ratio.

The framework developed in this chapter will be useful to estimate other Cabibbo-favored and Cabibbo-suppressed decays of Λ_c^+ too. Charmed lambda was the first charmed baryon ever to be discovered, but it has many modes of decay. This makes the detection and estimation of the branching fraction of each mode considerably difficult. In this regard, our estimates should be useful for future experiments as well as it will help us to calculate the branching fraction of other modes as well. Also, this calculation can be extended in future to calculate the weak decays of other heavy-quark baryons.

5.1 Article

This chapter has been adapted from:

Leonard S. Kisslinger, Bijit Singha. *Charmed Baryon Decay to a Strange Baryon Plus a Pion Using QCD Sum Rules.* Int. J. Mod. Phys. A 34 (2019) 1950015

5.2 QCD Sum Rules with 3-pt Correlator for Weak Decay $\Lambda_c^+(udc) \to \Lambda^o(uds) + \pi^+$

For the 3-point correlator to estimate $\Lambda_c^+(udc) \to \Lambda^o(uds)\pi^+$ we need the currents for $\Lambda_c^+(udc)$ and $\Lambda^o(uds)$, and the weak Hamiltonian. We consider here the same currents that we used for $\Lambda_c^+(udc)$ and $\Lambda^o(uds)$ in [86] to estimate the lambda baryon masses:

$$\begin{aligned} \eta_{\Lambda_c^+}(x) &= \epsilon^{abc}[u^{aT}(x)C\gamma_\mu d^b(x)]\gamma^5\gamma^\mu c^c(x)\ , \\ \eta_{\Lambda^o}(x) &= \epsilon^{abc}[u^{aT}(x)C\gamma_\nu d^b(x)]\gamma^5\gamma^\nu s^c(x)\ . \end{aligned} \tag{5.3}$$

The weak Hamiltonian is

$$H_W = \frac{G_F}{\sqrt{2}} J^\mu J_\mu^\dagger\ , \tag{5.4}$$

$$J^\mu = V_{cs}\ \bar{s}\gamma^\mu(1-\gamma_5)c\ + V_{ud}\ \bar{d}\gamma^\mu(1-\gamma_5)u\ \ , \tag{5.5}$$

where G_F is the Fermi coupling constant and $V_{ud} = 0.97420 \pm 0.00021$ and $V_{cs} = 0.997 \pm 0.017$ are the elements of Cabibbo-Kobayashi-Maskawa matrix [9]. Notice that V_{cs} is close to 1, which makes this weak decay Cabibbo-favored.

The QCD diagram which is used for the 3-pt correlator to estimate $\Lambda_c^+(udc) \to \Lambda^0(uds) + \pi^+$ is shown in Figure 5.1. In this diagram, the charm-strange transition and the pion creation is mediated by a weak gauge boson represented by the wavy line. There are other higher order diagrams corresponding to the same process but their contribution is negligible compared to this leading order process, so we ignore them here. The 3-pt correlator is

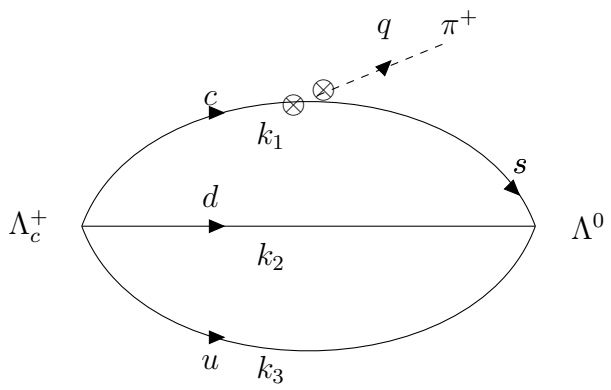

Figure 5.1: Perturbative diagram for the process: $\Lambda_c^+ \to \Lambda^0 + \pi^+$

$$\Pi_3(p,q) \;=\; i\int d^4x d^4y\; e^{ip\cdot x} e^{iq\cdot y} \Pi_3(x,y)\;, \tag{5.6}$$

where

$$\Pi_3(x,y) \;=\; <0|T[\eta_{\Lambda_c^+}(x) H_W(y) \bar{\eta}_{\Lambda^o}(0)]|0>_{\pi^+}\;. \tag{5.7}$$

where the subscript π^+ denotes that the constituent quarks of the lambda baryons propagate in an external pion field. We also write the weak matrix element

$$<\pi^+|J_\alpha|0> \;=\; \sqrt{2} F_\pi V_{ud}\; q_\alpha\;, \tag{5.8}$$

where F_π is the weak pion form factor and q is the momentum of the pion. We use the charmed and strange lambda baryon currents in Eqs. (5.3) and the weak Hamiltonian in Eq. (5.4) in the three-point function in Eq. (5.6) and evaluate in Appendix A to obtain the following expression for the three-point function:

$$\Pi_3(p,q) \;=\; -16 i m_c G_F F_\pi V_{ud} V_{cs}\; \Pi_{3Q}(p,q)\;, \tag{5.9}$$

where

$$\Pi_{3Q}(p,q) = q_\nu \left[\Pi^{\mu\mu\nu} + \Pi^{\mu\nu\mu} - \Pi^{\nu\mu\mu}\right], \tag{5.10}$$

$$\Pi^{\mu\nu\omega}(p,q) = \int \frac{d^4k}{(2\pi)^4}\frac{k_\mu}{k^2}\int \frac{d^4l}{(2\pi)^4}\frac{l^\nu (l-k-p-q)^\omega}{l^2\left[(l-k-p)^2-m_c^2\right]\left[(l-k-p-q)^2-m_s^2\right]} \tag{5.11}$$

We evaluate $\Pi^{\mu\mu\nu}$, $\Pi^{\mu\nu\mu}$ and $\Pi^{\nu\mu\mu}$ in Eq. (5.10) using a dimensional regularization technique that uses Schwinger's proper-time representation of the propagator, $1/(p^2-m^2) = \int_0^\infty d\alpha e^{-\alpha\left(p^2-m^2\right)}$, with the generalization of the gaussian integrals to $D = (4-2\epsilon)$-dimensions [82, 83]. We evaluate Eq. (5.11) in Appendix B to get

$$\Pi_{3Q}(p,q) = \frac{1}{2(4\pi)^4}\int_0^1 d\gamma d\rho 2\rho^3(1-\rho)^2\,(p.q)\int_0^1 d\kappa \frac{1}{g(\rho,\kappa,\gamma)^3}\Big[\kappa(p+\gamma q)^2\Gamma(\epsilon)a^{-\epsilon} + \rho\Gamma(-1+\epsilon)a^{1-\epsilon}\Big] + \frac{1}{2(4\pi)^4}\int_0^1 d\gamma d\rho\,\frac{2p.q}{(1-\rho)}\,\left[\Gamma(-1+\epsilon)(a')^{1-\epsilon}\right], \tag{5.12}$$

where

$$\mathcal{Z}^2(\gamma) = (1-\gamma)m_c^2 + \gamma m_s^2, \tag{5.13}$$

$$g(\rho,\kappa) = \kappa\rho(1-\rho) + (1-\kappa), \tag{5.14}$$

$$a(\rho,\kappa,\gamma) = -\kappa\rho\mathcal{Z}^2 + \kappa\rho(1-\rho)p.(p+\gamma q) - \left\{\frac{\kappa\rho(1-\rho)}{g}\right\}\kappa\rho(1-\rho)(p+\gamma q)^2, \tag{5.15}$$

$$a'(\rho,\kappa,\gamma) = -\rho\mathcal{Z}^2 + \rho(1-\rho)p.(p+\gamma q) - \left\{\frac{\kappa\rho(1-\rho)}{g}\right\}\rho(1-\rho)(p+\gamma q)^2\,. \tag{5.16}$$

Notice that, in Eq. (5.12), $\Pi_{3Q}(p,q)$ will have both power and logarithmic divergences. The former ones are insignificant for our purpose and we should only be interested in log-divergences only. We address this issue in the next section, where we apply Borel transform on Eq. (5.12) to extract the physical information relevant to the decay process.

5.3 Borel Transformation of $\Pi_{3Q}(p,q)$

In this section, we carry out a Borel transformation $\mathcal{B}$ on $\Pi_{3Q}(p,q)$ to ensure rapid convergence of the integrals:

$$\mathcal{B}_{M^2}\Pi_{3Q}(P^2) \;=\; \tilde{\Pi}_{3Q}(M^2)\;. \tag{5.17}$$

Here, we write $\Gamma(-1+\epsilon)a^{1-\epsilon} = a\ln a$ and $\Gamma(\epsilon)a^{-\epsilon} = -\ln a$, ignoring the power-divergent terms that vanish with the Borel transformation anyway. This finally gives us an expression

$$\begin{aligned}\Pi_{3Q}(p,q) \;=\; & \frac{1}{2(4\pi)^4}\int_0^1 d\gamma d\rho d\kappa \frac{2\rho^3(1-\rho)^2}{g(\rho,\kappa,\gamma)^3}(p.q)\left[\kappa(p+\gamma q)^2\,(-\ln a)+\rho\,(a\ln a)\right] \\ & +\frac{1}{2(4\pi)^4}\int_0^1 d\rho d\gamma \frac{2p.q}{(1-\rho)}\left[a'\ln a'\right]\;.\end{aligned} \tag{5.18}$$

Notice that, we have two parameters here in our expressions (p and q, or alternatively p^2 and $p'^2 = (p+q)^2$). This means Borel transformation should give us an expression for the three-point function in terms of two Borel masses, M_B^2 and ${M'_B}^2$. If the baryon masses were close, we could use $M_B^2 = {M'_B}^2$. But in this case, we are behooved to consider different values of the Borel masses. Following [89], we assume that they should obey a ratio

$$\frac{{M'_B}^2}{{M_B}^2} = \frac{M'^2}{M^2}\;, \tag{5.19}$$

where M and M' are respective Lambda baryon (Λ_c and Λ_s) masses in this case. This helps us to express the $\Pi_{3c}(p,q)$ in Eq. (5.18) in terms of one variable p^2. We define a quantity δ as

$$\delta \equiv \left(\frac{M'^2}{M^2}-1\right) \tag{5.20}$$

to write, in the limit of zero pion mass,

$$\begin{aligned} q.(p+\gamma q) &= q.p = \frac{1}{2}(p'^2 - p^2) = \frac{1}{2}\delta p^2, && (5.21)\\ (p+\gamma q)^2 &= (1+\gamma\delta)p^2, && (5.22)\\ (1-\gamma)p^2 + \gamma p'^2 &= (1+\gamma\delta)p^2, && (5.23)\\ p.(p+\gamma q) &= (1+\frac{\gamma\delta}{2})p^2, && (5.24) \end{aligned}$$

Also, we can express a and a' in a form that is convenient for Borel transform:

$$\begin{aligned} a(\rho,\kappa,\gamma) &= c_1(\rho,\kappa,\gamma)\Big[p^2 - b(\rho,\kappa,\gamma)^2\Big]\ , && (5.25)\\ a'(\rho,\kappa,\gamma) &= c_2(\rho,\gamma)\Big[p^2 - b'(\rho,\gamma)^2\Big]\ , && (5.26) \end{aligned}$$

where

$$\begin{aligned} c_1(\rho,\kappa,\gamma) &= \Big\{\frac{\kappa\rho(1-\rho)}{g(\rho,\kappa)}\Big\}\left[(1-\kappa)+\frac{1}{2}\gamma\delta g'(\rho,\kappa)\right], && (5.27)\\ b^2(\rho,\kappa,\gamma) &= \frac{g(\rho,\kappa)\mathcal{Z}^2}{(1-\rho)\left[(1-\kappa)+\frac{1}{2}\gamma\delta g'(\rho,\kappa)\right]}, && (5.28)\\ c_2(\rho,\gamma) &= \Big[-\frac{\delta\gamma\rho(1-\rho)}{2}\Big], && (5.29)\\ b'^2(\rho,\gamma) &= -\frac{2}{\gamma\delta(1-\rho)}\mathcal{Z}^2, && (5.30)\\ g'(\rho,\kappa) &= (1-\kappa)-\kappa\rho(1-\rho)\ . && (5.31) \end{aligned}$$

Using $P^2 = -p^2$ and applying the Borel transformation

$$\mathcal{B}_{M_B^2} = \lim_{P^2,n\to\infty;P^2/n=M_B^2} \frac{(P^2)^{n+1}}{n!}\left(-\frac{d}{dP^2}\right)^n, \qquad (5.32)$$

we find

$$\mathcal{B}_{M_B^2}\left[\ln(P^2+b^2)\right] = -M_B^2 e^{-b^2/M_B^2}, \tag{5.33}$$

$$\mathcal{B}_{M_B^2}\left[P^2\ln(P^2+b^2)\right] = M_B^2(b^2+M_B^2)e^{-b^2/M_B^2}, \tag{5.34}$$

$$\mathcal{B}_{M_B^2}\left[(P^2)^2\ln(P^2+b^2)\right] = -M_B^2(2M_B^4+2b^2M_B^2+b^4)e^{-b^2/M_B^2} \tag{5.35}$$

to write the Borel-transformed function $\tilde{\Pi}_{3c}(M_B)=\mathcal{B}_{M_B}\left[\Pi_{3c}(P;P^2=-p^2)\right]$ as

$$\begin{aligned}\tilde{\Pi}_{3Q}(M_B) &= \frac{1}{2(4\pi)^4}\int_0^1 d\gamma d\rho d\kappa \frac{\delta\rho^3(1-\rho)^2}{g^3}\Big[2\Big(\kappa(1+\gamma\delta)-c_1\rho\Big)M_B^6 \\ &\quad +\Big(2\kappa(1+\gamma\delta)-c_1\rho\Big)M_B^4b^2+\kappa(1+\gamma\delta)M_B^2b^4\Big]e^{-b^2/M_B^2} \\ &\quad +\frac{1}{2(4\pi)^4}\int_0^1 d\gamma d\rho\left(\frac{\delta}{1-\rho}\right)\left[-2c_2M_B^6-c_2b'^2M_B^4\right]e^{-b'^2/M_B^2}\ . \end{aligned} \tag{5.36}$$

What we have got finally in Eq. (5.36) is the Operator Product Expansion (OPE) of the three-point correlator. We will equate this expression to a phenomenological model for the decay process in order to calculate the coupling, $g_{\Lambda_c\to\Lambda_s\pi}$.

5.4 Phenomenological Side of the Decay

We obtain the phenomenological side for this process from the restrictions imposed by symmetry. To illustrate that, let's recall the three-point function here:

$$\Pi_3(p,q) = i\int d^4x d^4y\ e^{ip.x+iq.y}\ \langle 0|T\Big[\eta_{\Lambda_c}(x)H_W(y)\eta_{\Lambda_s}(0)\Big]|0\rangle\ . \tag{5.37}$$

We can express this function in terms of the physical intermediate states of our interest through the following matrix elements:

$$\langle 0|\eta_{\Lambda_c}|\Lambda_c(p)\rangle = \lambda_{\Lambda_c} u(p), \tag{5.38}$$

$$\langle \Lambda_s(p')|\eta_{\Lambda_s}|0\rangle = \lambda_{\Lambda_s} \bar{u}(p'), \tag{5.39}$$

$$\langle \Lambda_c(p)|j^\mu|\Lambda_s(p')\rangle = g(p,p')\left[\bar{u}(p) i\gamma^\mu u(p')\right], \tag{5.40}$$

where λ_{Λ_c} and λ_{Λ_s} are the couplings of the charmed and the strange lambda baryon currents to their hadronic states $u(p)$ is a spinor obeying the normalization $u(p)\bar{u}(p) = 2m_B$ with m_B being the mass of the the baryon B, and $g(p,p')$ is the coupling of the pion current to the baryons and is related to the dimensionless coupling constant, $g_{\Lambda_c\to\Lambda_s\pi}$ that we seek to find out in this paper, through the following relation[87]:

$$g(p,p') = g_{\Lambda_c\to\Lambda_s\pi}\left[\frac{2m_\pi^2 f_\pi}{(m_u+m_d)\,(q^2-m_\pi^2)}\right], \tag{5.41}$$

where m_π, m_u and m_d are the mass of pion, up and down quarks, f_π is the pion decay constant, and $q^2 = (p'-p)^2$. Using Eq. (5.39), (5.39), (5.40), (5.41) and (5.4), we get

$$\begin{aligned}\Pi_3^{\text{pheno}}(p,p') &= iG_F F_\pi V_{ud}\left[\frac{\langle 0|\eta_{\Lambda_c}|\Lambda_c(p)\rangle}{\not{p}-m_{\Lambda_c}}\right]\langle\Lambda_c(p)|j^\mu|\Lambda_s(p')\rangle\left[\frac{\langle\Lambda_s(p')|\eta_{\Lambda_s}|0\rangle}{\not{p}'-m_{\Lambda_s}}\right]\\ &= 4iG_F\; g_{\Lambda_c\to\Lambda_s\pi}\; V_{ud}\frac{2\lambda_{\Lambda_c}\lambda_{\Lambda_s}m_{\Lambda_c}m_{\Lambda_s}m_\pi^2F_\pi^2}{(m_u+m_d)\,(q^2-m_\pi^2)}\;\frac{(\not{p}+m_{\Lambda_c})\;\not{q}\,(\not{p}'+m_{\Lambda_s})}{(p^2-m_{\Lambda_c}^2)(p'^2-m_{\Lambda_s}^2)}\,.\end{aligned} \tag{5.42}$$

Note that

$$\begin{aligned}(\not{p}+m_{\Lambda_c})\;\not{q}(\not{p}'+M_{\Lambda_s}) &= (m_{\Lambda_c}+m_{\Lambda_s})\,p.q + (m_{\Lambda_c}m_{\Lambda_s}-p^2)\;\not{q} + 2q.p\;\not{p}\\ &\quad -i\left[q_\mu\sigma^{\mu\nu}p_\nu m_{\Lambda_c} + p_\mu\sigma^{\mu\nu}q_\nu m_{\Lambda_s}\right]\,.\end{aligned} \tag{5.43}$$

Out of all the terms present in Eq. (5.43), we can only concentrate on the first one and ignore the others because only the first term is consistent with the Lorentz structure of the OPE side of the three-point function. Inserting it back to Eq. (5.42), and considering $m_u \approx m_d = m_q$, we get

$$\Pi_3^{\rm pheno}(p,p') = -\frac{i\, g_{\Lambda_c\to\Lambda_s\pi}\, G_F V_{ud}\lambda_{\Lambda_c}\lambda_{\Lambda_s} m_{\Lambda_c} m_{\Lambda_s} F_\pi^2}{m_q}\left[\frac{\delta p^2\,(m_{\Lambda_c}+m_{\Lambda_s})}{(p^2-m_{\Lambda_c}^2)(p'^2-m_{\Lambda_s}^2)}\right]. \tag{5.44}$$

In the above expression, we have considered $q^2 = 0$ and δ is defined in Eq. (5.20). Using Eq. (5.19), we get eventually

$$\Pi_3^{\rm pheno}(p) = -\frac{i g_{\Lambda_c\to\Lambda_s\pi}\, G_F V_{ud}\lambda_{\Lambda_c}\lambda_{\Lambda_s} m_{\Lambda_c} m_{\Lambda_s} F_\pi^2}{m_q} \times \frac{\delta\,(m_{\Lambda_c}+m_{\Lambda_s})\, m_{\Lambda_c}^2}{m_{\Lambda_s}^2}\left[\frac{1}{p^2-m_{\Lambda_c}^2}+\frac{m_{\Lambda_c}^2}{(p^2-m_{\Lambda_c}^2)^2}\right]. \tag{5.45}$$

Now, we apply the Borel transformation [Eq. (5.32)] on $\Pi_3^{\rm pheno}(p)$ to get

$$\mathcal{B}_{M_B^2}\left[\Pi_3^{\rm pheno}(p)\right] = i g_{\Lambda_c\to\Lambda_s\pi} G_F V_{ud}\lambda_{\Lambda_c}\lambda_{\Lambda_s}\frac{\delta\,(m_{\Lambda_c}+m_{\Lambda_s})\,F_\pi^2}{m_q}\,\frac{m_{\Lambda_c}^2}{m_{\Lambda_s}^2}\left(1-\frac{m_{\Lambda_c}^2}{M_B^2}\right)e^{-\frac{m_{\Lambda_c}^2}{M_B^2}}, \tag{5.46}$$

where we consider $m_{\Lambda_s} = 1.115$ GeV, $m_{\Lambda_c} = 2.286$ GeV, $m_s = 0.095$ GeV, $m_c = 1.275$ GeV, $F_\pi = 0.092$ GeV, $m_q = 0.004$ GeV. For the couplings, λ_{Λ_c} and λ_{Λ_s}, we follow [90], where the values of these parameters were obtained from baryonic mass sum rules in heavy quark effective theory [91]:

$$2(4\pi)^4\,|\lambda_b|^2 e^{-M^2/M_B^2} = M_B^6 E_2^b + \frac{2}{3}am_Q(1-3\gamma)M_B^2E_0^b + \beta M_B^2 E_0^b + \frac{4}{9}a^2(3+4\gamma), \tag{5.47}$$

where b denotes the baryon Λ_c^+ or Λ^0, m_Q denotes the mass of the heavy quark (charm or strange). Also

$$a = -(2\pi)^2\langle\bar{q}q\rangle \approx 0.5 \text{ GeV}^3, \tag{5.48}$$

$$\beta = \pi^2\langle\alpha_s G^2/\pi\rangle \approx 0.12 \text{ GeV}^4, \tag{5.49}$$

$$\gamma = \langle\bar{q}q\rangle/\langle\bar{s}s\rangle - 1 \approx -0.2, \tag{5.50}$$

and E_n^b represents the continuum contribution,

$$E_n^b = 1 - \left(1 + x + \frac{x^2}{2} + \cdots + \frac{x^n}{n!}\right) e^{-x}, \tag{5.51}$$

with $x = s_b/M^2$, s_b being the continuum threshold. Notice that, we can only determine the absolute value of $g_{\Lambda_c\to\Lambda_s\pi}$ and not the sign, since Eq. (5.47) gives only the absolute value of λ_b.

5.5 Results

In this section, we compare the OPE side of the three-point function given in Eq. (5.36) to the phenomenological side in Eq. (5.46) to find out the coupling. The free parameters appearing in the latter expression are the continuum thresholds, s_b and $s_{b'}$, that determine the couplings, λ_b and $\lambda_{b'}$. From Eq. (5.47), we can write

$$|\lambda_b/\lambda_{b'}|^2\ e^{-(M^2-M'^2)/M_B^2} = \frac{E_2^b + \left(\frac{2am_c}{3M_B^4}\right)(1-3\gamma)E_0^b + \left(\frac{\beta}{M_B^4}\right)E_0^B + \left(\frac{4a^2}{9M^6}\right)(3+4\gamma)}{E_2^{b'} + \left(\frac{2am_s}{3M_B^4}\right)(1-3\gamma)E_0^{b'} + \left(\frac{\beta}{M_B^4}\right)E_0^{b'} + \left(\frac{4a^2}{9M^6}\right)(3+4\gamma)}\ . \tag{5.52}$$

For what follows from here, b denotes Λ_c, b' denotes Λ_s. To estimate s_b, $s_{b'}$, λ_b and $\lambda_{b'}$, we start with a residual

$$R(M^2) = (\text{rhs} - \text{lhs})^2/\text{lhs}^2, \tag{5.53}$$

where rhs and lhs denotes the right- and left-hand sides of Eq. (5.52) respectively. Then, we assume a prior range of values for the free parameters and minimize the residual in Eq. (5.53). Let's define

$$r = |\lambda_b/\lambda_{b'}|^2, \tag{5.54}$$

$$s_b = (M + \Delta)^2, \tag{5.55}$$

$$s_{b'} = (M' + \Delta)^2 \ . \tag{5.56}$$

The above definitions of s_b and $s_{b'}$ help us to constrain the continuum threshold with just one free parameter, Δ. Similar parametrization has been adopted in other works, *e.g.*, in [90] and [89]. Now, using this residual method, we attempt to find a Borel window over which (i) the residual will be close to zero, (ii) it will effectively become constant over this range (window) of M_B, because our result should be independent of the extra parameter M_B that we introduced just to regulate the divergences in the three-point function. We start with a prior range of the free parameters: $\Delta \in [0.5 \text{ GeV}, 0.9 \text{ GeV}]$, $r \in [1, 18]$ and attain a suitable Borel window for the following values of the free parameters:

$$r = 17.259, \ \Delta = 0.784 \text{ GeV} \ . \tag{5.57}$$

The residual is plotted in Figure 5.2 for the above-mentioned values of the free parameters. Using the values of Δ obtained in Eq. (5.57) in Eq. (5.46), and comparing Eq. (5.46) with

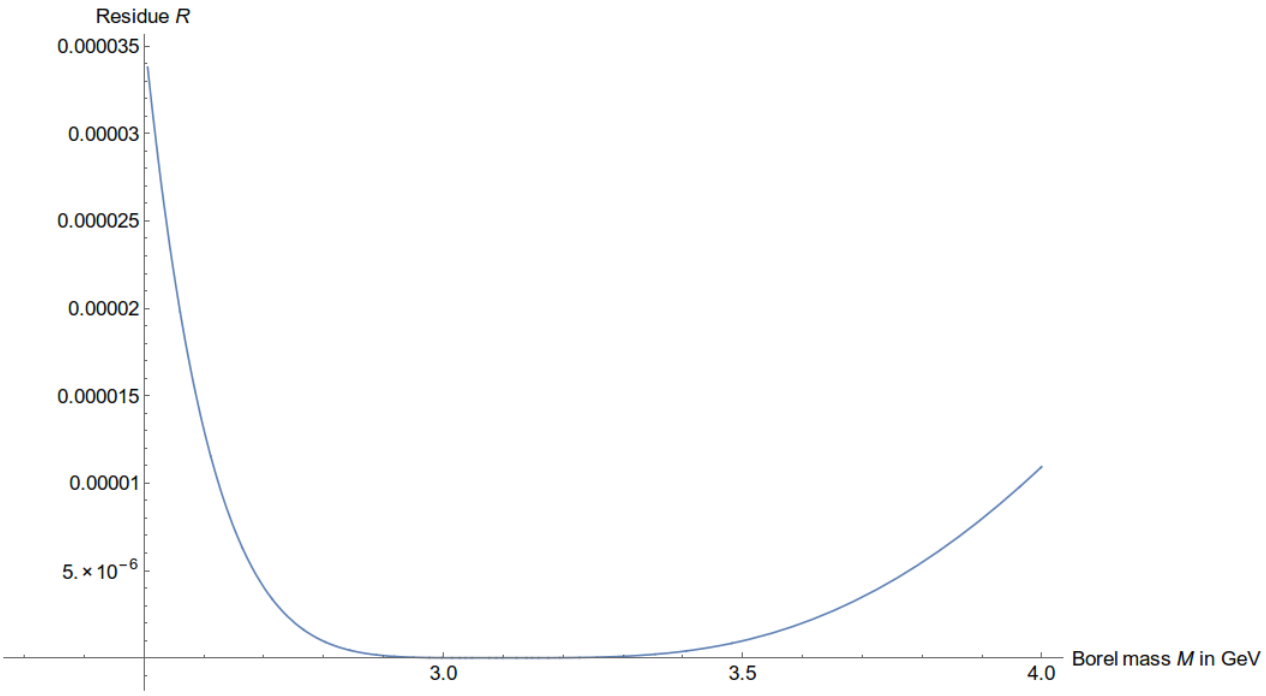

Figure 5.2: Residual of Eq. (5.53) as a function of Borel mass for $r = 17.259$, $\Delta = 0.784$ GeV.

Eq. (5.36), we get $g_{\Lambda_c \to \Lambda_s \pi}$ as a function of Borel mass, as shown in Figure 5.3. Figure 5.2 and Figure 5.3 allow us to choose a Borel window $M \in [2.7 \text{ GeV}, 3.2 \text{ GeV}]$ over which we estimate the value of the coupling constant, $g_{\Lambda_c \to \Lambda_s \pi}$.

$$g_{\Lambda_c \to \Lambda_s \pi} \quad = \quad 1.060 \pm 0.014 \ . \tag{5.58}$$

With the parametrization adopted in the last section, this value of the coupling close to unity indicates that the weak decay is Cabibbo-favored.

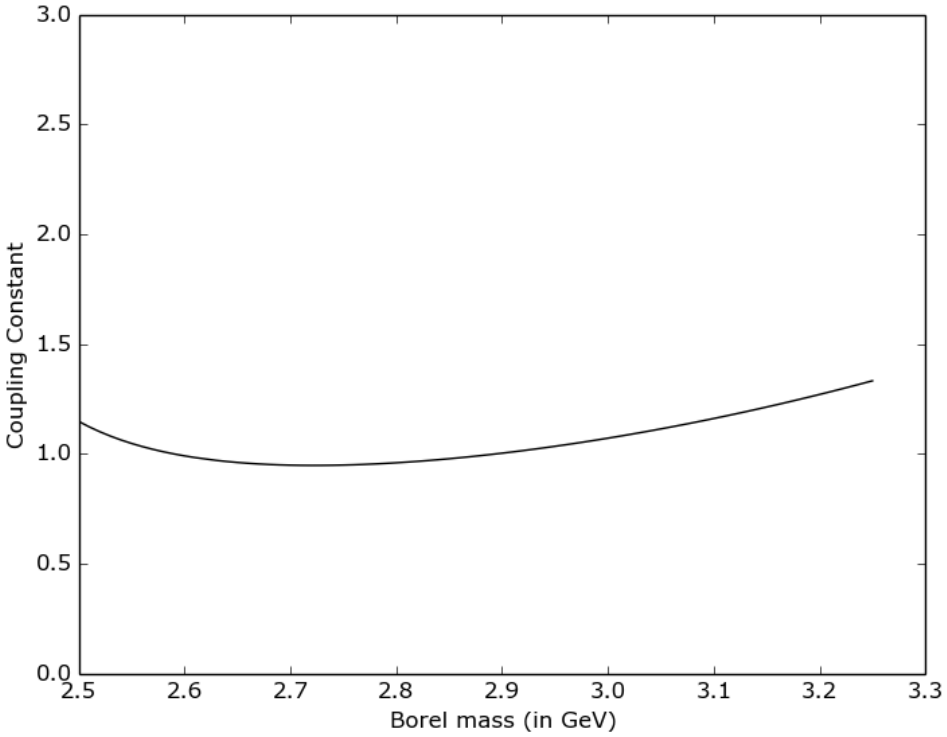

Figure 5.3: $g_{\Lambda_c \to \Lambda_s \pi}$ as a function of Borel mass.

5.6 Conclusions

In this work, we have calculated the coupling for the decay process $\Lambda_c^+ \to \Lambda^0 \pi^+$. We used a parametric representation of the propagators analytically continued to complex D-dimensions in order to solve the lowest order perturbative diagram corresponding to this process. We achieved convergence with a reduced Borel transformation. This method will be extended to estimate other Cabibbo-favored and Cabibbo-suppressed decays of heavy-quark baryons, and also to estimate decays for other weak modes of charmed lambda in future.

Chapter 6

Heavy-Quark State Production from p-p and A-A Collisions

Due to the abundance of the heavy-flavor quarks generated during the high-energy, inelastic proton-proton collisions, there has been considerable interest recently in the heavy-quark states production from such events. Measurements of the cross-sections of these events and matching them to the results derived from perturbative QCD provides us the opportunity to test QCD in the high energy limit. They could also serve as the background to explore new physics and the basis for the predictions on the quark-gluon plasma (QGP) formation in relativistic heavy-ion collisions (RHIC).

In this work, we estimate the production cross-section of $B^0(b\bar{d})$ and $B^-(b\bar{u})$ mesons in proton-proton (p-p) and heavy-ion (A-A) collisions. Due to flavor conservation, the heavy quarks are produced only in pairs during such collisions. We have incorporated this in our work to say that if a gluon produces a heavy-quark pair, $c\bar{c}$ or $b\bar{b}$, then a fragmentation process can convert the $b\bar{b}$ into two B mesons, $b\bar{d} - d\bar{b}$. We consider the fragmentation function from the works of Braaten *et al.* . Furthermore, we assume in this work that each gluon channel produces a color-octet S-wave state of the $b\bar{b}$ pair. The color octet mechanism [40, 41, 42] is found to dominate the color singlet mechanism in the experimental studies at $\sqrt{s} = 200$ GeV [43, 44]. The long-distance non-perturbative fragmentation function is expressed in terms of matrix elements corresponding to a color-octet state that basically encodes the probability

of a color-octet $b-\bar{b}$ state to form a B meson. These matrix elements can be found in [45].

The organization of this chapter is as follows. In Section 6.1 we give a brief introduction to the parton model. In Section 6.2.1, we discuss factorization theorem and parton fragmentation. In Section 6.2.2, we discuss the color-singlet and the color-octet mechanisms of the heavy-quark state production in high-energy collisions. We derive the fragmentation function $D_{b\to b\bar{q}}$ in Section 6.3. We assimilate all these ideas in Section 6.5 to estimate the B meson production cross-sections in p-p and A-A collisions.

6.1 The Parton Model

We start with an experimental fact that the pion production cross-section in high-energy ($\sim$ 10 GeV) $p-p$ collisions has an exponential fall-off in the value of its transverse momentum. This simple observation leads us to the following model [7]: a proton is composed of constituents that have their momenta almost collinear with the momentum of the protons. In a collision between two high-energy protons the final state (of hadrons) will have momenta parallel to the collision axis. The ejection of hadrons at large transverse momentum would need a large, spacelike q^2, prohibiting this process to happen. It is observed that the probability of hadron production with large transverse momentum is much suppressed, indicating that the strong interaction is much weaker at sufficiently high energy.

This 'jelly' model of a proton made of loosely bound pieces was put into rigorous test in the 1960's in SLAC-MIT deep inelastic scattering experiments. It was observed that the scattering rate at large deflection angles could be estimated from the momentum of the scattered electrons, indicating that the large momentum transfer happened through electromagnetic rather than strong interaction. However, the proton did not react to the scattering electrons as a fundamental particle with simple Coulomb charge. The largest part of the

scattering was contributed by the deep, inelastic region of phase space, in which the proton was broken apart.

This constitutes a puzzle. We are assuming a strong interaction at a much deeper length scale, *i.e.* at the scale of a proton but the same interaction is apparently absent in hard scattering processes. Bjorken and Feynman attempted to solve this puzzle by putting forward the 'parton' model [92, 93]. In this model, a proton is made of loosely bound, point-like constituents called 'partons'. Some of these partons are elementary fermions carrying some electric charge and some of them are electrically neutral particles binding these fermions loosely together. The electromagnetic interaction with the electron can knock a parton off a proton. This parton can have soft momentum tranfer with the remainder of the proton though, creating hadronic jets collinear with the original parton that was knocked out. In this way, the parton model imposes strict constraints on the deep inelastic scattering cross-section. It was later recognized that partons describe the same objects now more commonly referred to as quarks and gluons. A more profound explanation of this puzzle can be given by introducing asymptotic freedom in QCD.

6.2 Production of Heavy Quarkonium in High Energy Collisions

Tevatron data around 1993 suggested that the parton processes that create charmonium cannot be explained by the color-singlet model even in the lowest order of the strong coupling constant [94, 95]. This leads towards a revision of the idea that the $c\bar{c}$ pairs created from such processes are in a color-singlet state. This phenomenon leads to two important development in the understanding of charmonium physics:

- **Fragmentation:** Heavy quarkonium is produced predominantly from the partons of large transverse momentum (p_T).
- **Color-octet mechanism:** $c\bar{c}$ pair can be produced in a color-octet state at a sufficiently short distance scale.

In the following subsections, we discuss these two ideas in more detail.

6.2.1 Factorization Theorem and Parton Fragmentation

From the proton-proton or heavy-ion collision point emerges partons almost *collinearly* in a narrow cone of *jet*. In this process, a hadron can be created by the partons with sufficiently large transverse momentum. This phenomenon is called *fragmentation*. In the following paragraph, we discuss *factorization theorems* that will allow us to write the perturbative part of the B meson production cross-section in high-energy collisions separately from the part containing the non-perturbative effects of QCD by guaranteeing how hadron productions at very large momenta are dominated by fragmentation.

In order to explain factorization, let's start with the simplest scenario of a radiative QED process and assume that p_N denotes the probability of finding N number of soft photons with a frequency at most k_0. The scattering cross-section for the Bremsstrahlung process (Figure 6.1) in QED is given by

$$\frac{d\sigma}{d\Omega}(p \to p' + \gamma) \;=\; \left(\frac{d\sigma}{d\Omega}\right)_0 \left[+\frac{\alpha}{\pi} \ln\left(\frac{q^2}{m^2}\right) \ln\left(\frac{E_l^2}{\mu^2}\right) + \mathcal{O}(\alpha^2)\right] \;, \tag{6.1}$$

where α is the fine structure constant, q^2 is the virtual photon four momentum, m is electron mass term in the QED lagrangian, E_l is the detector resolution and μ is the photon mass. As we can see from the expression, the cross-section becomes infinite in the limit $\mu \to 0$.

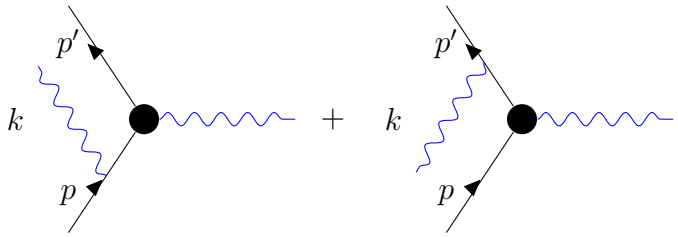

Figure 6.1: Bremsstrahlung process in QED. The divergence appearing in the Feynman diagram of this process cancels out the divergence appearing in the electron-photon vertex correction.

This divergence cancels with the infrared divergence arising from the quantum corrections in the electron-photon interaction vertex. The elastic cross-section found after quantum correction of vertex is given by

$$\frac{d\sigma}{d\Omega}(p \to p') = \left(\frac{d\sigma}{d\Omega}\right)_0 \left[1 - \frac{\alpha}{\pi} \ln\left(\frac{q^2}{m^2}\right) \ln\left(\frac{q^2}{\mu^2}\right) + \mathcal{O}(\alpha^2)\right] . \tag{6.2}$$

Summing Eq. (6.1) and (6.2) gives us the cross-section of a scattering event in which the detector detects no photon

$$\begin{aligned} \left(\frac{d\sigma}{d\Omega}\right)_{\text{Detected}} &= \left(\frac{d\sigma}{d\Omega}\right)_{\text{Elastic}} + \left(\frac{d\sigma}{d\Omega}\right)_{\text{Bremsstrahlung}} \\ &= \left(\frac{d\sigma}{d\Omega}\right)_0 \left[1 - \frac{\alpha}{\pi} \ln\left(\frac{q^2}{m^2}\right) \ln\left(\frac{q^2}{E_l^2}\right) + \mathcal{O}(\alpha^2)\right] . \end{aligned} \tag{6.3}$$

This result can be extended and generalized to the level of a theorem which says that, although the perturbative series expansion of transition amplitude often bugs us with divergences, they are cancelled if we consider the average over the whole ensemble of states. This is the famous 'Kinoshita-Lee-Nauenberg theorem' (KLN theorem) and is true of any quantum mechanical system (even the degenerate ones, irrespective of whether we perform Feynman diagram calculations explicitly or not). An equivalent statement of this theorem is that the standard model is free of mass singularities and infrared infinities.

Mass singularities appear when the massless limit of a theory is considered. In these cases, we are typically encountered with two kind of infinities [96]: one is IR infinity, which is the divergence associated with the zero limit for all the four components of momenta of the real or virtual particles. The other kind of infinity is called mass divergence or collinear divergence which appears with the vanishing electron mass in QED (in high energy limit, $p.p' = m^2$, where p and p' are momenta of the electron before and after the scattering) or in non-Abelian gauge theories such as QCD. In such cases, the massless particles lead to divergences if they are emitted parallel to the parent particle even if they carry large momentum. But the divergences associated with the soft momenta gives us a factored form for this contribution to inclusive cross-section. This idea was used in [97, 98] to define fragmentation function (FF). In general, FF tells us how a parton of a given momentum gets converted into a color-neutral hadron or a photon. Just like PDF tells us the probability density of a given parton inside a hadron, FF tells us the probability density of a parton to convert into a specific hadron.

Here are a few examplary processes and their schematic representations where the factorization theorem and the fragmentation functions have been used:

- single-inclusive hadron production in electron-positron annihilation, $e^+ + e^- \to h + X$.
- semi-inclusive deep-inelastic lepton-nucleon scattering, $l + N \to h + X$.
- single-inclusive hadron production in proton-proton collisions, $p + p \to h + X$.

The factorization theorem gives us for these processes [99].

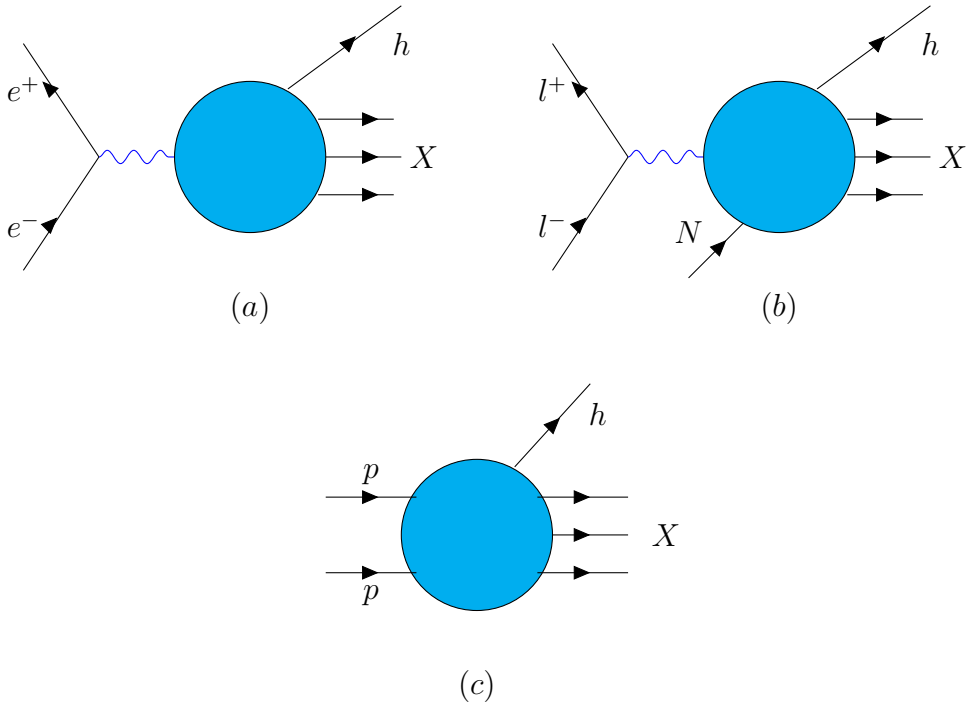

Figure 6.2: Diagrammatic representation of the processes: (a) semi-inclusive hadron production in $e^+ - e^-$ annihilation, (b) semi-inclusive deep inelastic lepton-nucleon scattering, (c) single-inclusive hadron production in $p - p$ collisions. To estimate B production in p-p collision, we use factorization of process (c).

$$\sigma^{e^+e^-\to hX} = \hat{\sigma} \otimes FF, \tag{6.4}$$

$$\sigma^{lN\to lhX} = \hat{\sigma} \otimes PDF \otimes FF, \tag{6.5}$$

$$\sigma^{pp\to hX} = \hat{\sigma} \otimes PDF \otimes PDF \otimes FF, \tag{6.6}$$

where $\hat{\sigma}$ denotes the perturbative field theory cross-section of the parton and FF denotes the fragmentation function. The corresponding processes are shown in Figure 6.2. We will use the factorization corresponding to the single-inclusive hadron production in $p - p$ collisions to estimate B production.

6.2.2 Color-octet Mechanism

Along with fragmentation, this mechanism gives us a quantitative understanding about modelling the formation of a bound state such as quarkonium. Before moving ahead to discuss the color-octet model of charmonia production, let's have a brief review of the color-singlet model first [100].

In the color-singlet model, the amplitude of $Q\bar{Q}$ production (Q denotes a heavy quark such as charm) is assumed to be zero if $Q\bar{Q}$ is not a color-singlet. Also, in order to form such a bound state, the relative momenta of Q and $\bar{Q}$ should be very small compared to the heavy-quark mass m_Q, otherwise Q and $\bar{Q}$ can escape easily to form heavy-light mesons (such as D and $\bar{D}$).

Now, if Q and $\bar{Q}$ are not present in the initial state, then they have to be produced from the virtual excitations with momenta $\sim m_Q$. This is called the short distance part of the amplitude in which $Q\bar{Q}$ is produced with a spatial separation $\sim m_Q^{-1}$. At this scale, the constituent quarks are less sensitive to their relative momentum that corresponds to a wavelength which is much larger than the length scale of the charmonium wavefunction. $Q\bar{Q}$ behaves like a pointlike pair while forming the bound state of quarkonium, H.

In the color-singlet model we denote, for example, a charmonium Fock-state $|c\bar{c}(\mathbf{1},^{2S+1}L_J)\rangle$, where $\mathbf{1}$ denotes that $c\bar{c}$ is in a color-singlet state with spin S, orbital angular momentum L and total angular momentum J. Factorization theorem tells us that the amplitude of a $c\bar{c}$ pair to form charmonium, $\hat{\mathcal{A}}(\psi + F)$ (F is some specific final state) are assumed to be factorized into two factors: one is the amplitude in the limit of vanishing relative momentum,

the other one being the L^{th} derivative of the radial wave-fucntion, $R(0)$:

$$\hat{\mathcal{A}}(\psi + F) = \hat{\mathcal{A}}\left(c\bar{c}(\mathbf{1},^3 S_1) + F\right) R_\psi(0), \tag{6.7}$$

$$\hat{\mathcal{A}}(\chi_{cJ} + F) = \hat{\mathcal{A}}\left(c\bar{c}(\mathbf{1},^3 P_J) + F\right) R'_{\chi_c}(0)\ . \tag{6.8}$$

The first term in the right hand side is the local amplitude and can be calculated using perturbation theory while the non-perturbative effects are absorbed in the radial wavefunction. These wavefunctions are specified from some physical processes, e.g. $R_\psi(0)$ is determined from the decay of ψ to electrons:

$$\Gamma(\psi \to e^+e^-) \approx \frac{4\alpha^2}{9m_c^2}|R_\psi(0)|^2. \tag{6.9}$$

Since, there cannot be any state other than color-singlet charm-anticharm pair that is contributing to the amplitude, the form of the inclusive cross-section for charmonia production is simply given by

$$d\sigma(\psi + X) = d\hat{\sigma}\left(c\bar{c}(\mathbf{1},^3 S_1) + X\right)\ |R_\psi(0)|^2, \tag{6.10}$$

$$d\sigma(\chi_{cJ} + X) = d\hat{\sigma}\left(c\bar{c}(\mathbf{1},^3 P_1) + X\right)\ |R'_{\chi_c}(0)|^2\ . \tag{6.11}$$

As we will see, this expression will change under the color-octet model as we will have to include the contribution from the color-octet $c\bar{c}$ pair as well.

This simple model gives rise to some problems. Other than the fact that this model is non-relativistic (as the relative momenta of the quark pair has been ignored throughout), in principle it is not guaranteed that the amplitude will obey the factorization assumed in Eq. (6.7) or (6.8) if we consider the higher order radiative processes too. Also, a color-octet $c\bar{c}$ can emit a soft gluon to become a color-singlet. But the color-singlet model does not allow

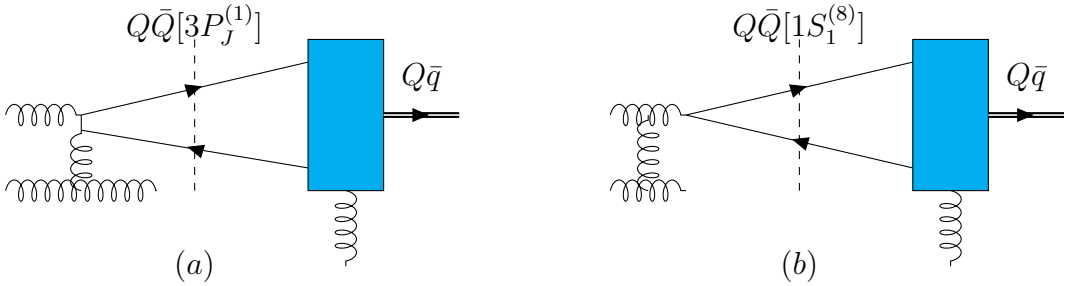

Figure 6.3: Feynman graph for heavy-light meson production at $\mathcal{O}(\alpha_s^3)$ through the (a)color singlet mechanism and (b) color octet mechanisms. Short distance collisions create the $Q\bar{Q}$ pairs that hadronize at long distances into $Q\bar{q}$ bound states.

this non-perturbative process to happen. Most evidently, there is no other process to cancel out the IR divergence appearing in the cross-section for the p-wave states. Our solution to these issues is that in our work, we have adopted this color-octet mechanism [101, 102, 103] in which the bottom-antibottom pair created from gluon fragmentation is predominantly color-octet and propagates before each of he two partons b and $\bar{b}$ fragmentizes to produce a B meson.

6.3 Fragmentation Function from First Principles

Brateen *et al* showed in 1993 that the parton fragmentation functions can be derived from the first principles calculations using perturbative QCD [104]. In order to calculate the fragmentation function, $D_{b\to b\bar{q}}$, corresponding to the process, $b \to b\bar{q}$, we consider an inclusive process, $b^* \to b\bar{q}+q$, as shown in Figure 6.4. It can be shown that the fragmentation function will be the ratio of the two scattering amplitudes:

1. $\mathcal{M}$ corresponding to the production of an off-shell b^* that subsequently fragmentize into a B meson ($B\bar{q}$) and a real q, where q denotes a light quark.

2. $\mathcal{M}_0$ corresponding to the process of producing on-shell b^* from Γ with the same three-

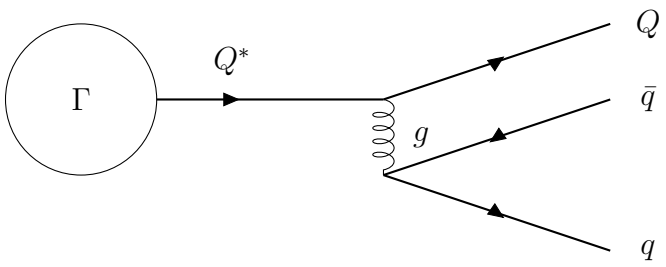

Figure 6.4: Feynman diagram for heavy quark fragmentation function calculation

momentum ($\vec{K}$) as (1) in the limit $K_0 \to \infty$.

Taking the ratio of these two processes, we get the following form of the fragmentation function:

$$D(z) = \frac{1}{16\pi^2} \int ds\ \theta\left(s - \frac{M^2}{z} - \frac{m_q^2}{1-z}\right) \times \lim_{K_0 \to \infty} \frac{\sum |\mathcal{M}|^2}{\sum |\mathcal{M}_0|^2}\ , \tag{6.12}$$

with $M = m_b + m_q$ is the mass of the meson in non-relativistic limit and z is longitudinal momentum fraction of the quarkonium state. The sums are over the spin and color of the light quarks. This function can be calculated in the axial gauge for which $K^\mu = (K_0, 0, 0, \sqrt{K_0^2 - s})$. As shown in the Feynman diagram, Γ denotes the part of the matrix element $\mathcal{M}$ that involves the production of a virtual b quark. Also, in the axial gauge we choose only the production of B meson from a virtual quark of momentum K^μ.

The spinor Γ appears also in the second amplitude, $\mathcal{M}_0 = \Gamma u(K)$. Next we project $b\bar{q}$ to ${}^1S_0$ state using heavy quark effective theory

$$b\bar{q} \to \frac{\delta^{ij}}{\sqrt{3}} \frac{R(0)\sqrt{M}}{\sqrt{4\pi}} \gamma^5 \left(\frac{1+\not{v}}{2}\right)\ , \tag{6.13}$$

where $R(0)$ is the radial wavefunction of the meson at the origin and v^μ is its four-velocity.

Then we use QCD Feynman rules for the light-quark spinor and $q\bar{q}g$ vertex and heavy-quark effective theory Feynman rules for heavy quark propagator and $b\bar{b}g$ vertex to derive the amplitude $i\mathcal{M}_1$ and perform the Dirac summation as given in Eq. (6.12) to write the fragmentation function in leading order in $r \equiv (m_H - m_b)/m_H$ (m_H = hadron mass, m_b = mass of the bottom quark):

$$D_{b\to b\bar{q}}(y) = N\frac{(y-1)^2}{ry^6}\left(3y^2+4y+8\right) - N\frac{(y-1)^3}{y^6}\left(3y^2+4y+8\right) + \mathcal{O}(r)\ , \tag{6.14}$$

where

$$y = \frac{1-(1-r)z}{rz}\ , \tag{6.15}$$

$$N = \frac{2\alpha_s^2|R(0)|^2}{81\pi m_q^3}\ . \tag{6.16}$$

We will use the frgamentation function in Eq. (6.14) in order to calculate the B meson production cross-section in the following section.

6.4 Article

The following sections of this chapter have been adapted from:

Leonard S. Kisslinger, Bijit Singha. *B Production In p-p and A-A Collisions.* Int. J. Theor. Phys. **56** (2017) 3648

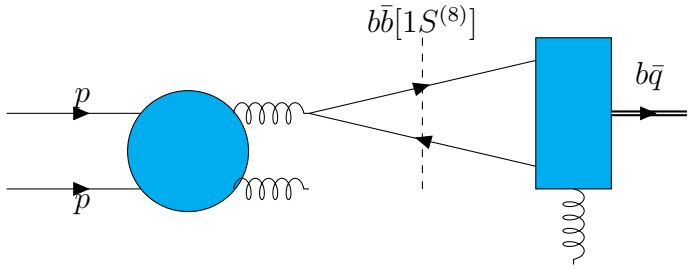

6.5 B Production in p-p and A-A Collisions

In this subsection we consider $B^0(b\bar{d})$ and $B^-(b\bar{u})$ production via unpolarized $p-p$ collisions at 200 GeV. This is an extension of the work on $D^+(c\bar{d})$ and $D^0(c\bar{u})$ production in high energy collisions [105] to the case of the heavy-light mesons containing a bottom quark. We have also made use of previous work on $J/\psi, \psi'(2S)$ and $\Upsilon(nS)$ productions in this work. In addition to providing quantitative evidence for QCD as the fundamental theory behind strong interactions, the estimate of B production via $A-A$ collisions could provide a test of Quark-Gluon Plasma (QGP) in relativistic heavy ion collisions. In Refs. [45], [106], the mixed hybrid theory was used for the cross-section calculations of $\psi'(2S)$ and $\Upsilon(3S)$ but is not used in this work. The main new aspects of the present work is that while a gluon can produce a $c\bar{c}$ or $b\bar{b}$ state, it cannot directly produce a $b\bar{d}$. A fragmentation process converts a $b\bar{b}$ into a $b\bar{d}-d\bar{b}$, for example. We use the fragmentation probability $D_{b\to b\bar{q}}$ of Braaten *et al.* [104] and derived in Section 6.3.

6.5.1 Differential $pp \to BX$ Cross-section

B production in high energy collisions can proceed through either the quark-antiquark or the gluon-gluon fusion channel [45]. But, the gluon distribution function evaluated at $Q = 2m_b$ (m_b = bottomonium mass) is much larger than the quark distribution function evaluated at

the same energy:

$$f_g(x, Q = 2m_b) \gg f_q(x, Q = 2m_b) \ . \tag{6.17}$$

Thus the gluon-gluon fusion channel will be the dominant channel in BX production cross-section (scenario 2 in [112]) and is given by

$$\sigma_{pp\to BX} \ = \ \int_a^1 \frac{dx}{x} f_g(x, 2m) f_g(a/x, 2m) \sigma_{gg\to BX} \ , \tag{6.18}$$

where we write using factorization theorem [111]

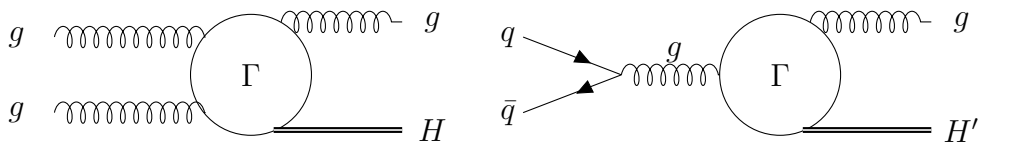

Figure 6.5: Gluon(dominant) and quark-antiquark(suppressed) fusion channels.

$$\sigma_{gg\to BX} = 2\hat{\sigma}_{gg\to b\bar{b}} D_{b\to b\bar{q}} \ , \tag{6.19}$$

where $\hat{\sigma}_{gg\to b\bar{b}}$ is the bottomonium production cross-section and can be evaluated using perturbative QCD [45] and $D_{b\to b\bar{q}}$ is the fragmentation function derived in section 6.3. For $E = \sqrt{s} = 200$ GeV, the gluon distribution function for the bottomonia quarks is [45]

$$f_g(y) = 275.14 - 6167.6 \ x(y) + 36871.3 \left[x(y)\right]^2 \ , \tag{6.20}$$

where y denotes rapidity:

$$y = \frac{1}{2} \ln \left(\frac{E + p_z}{E - p_z} \right) , \tag{6.21}$$

with E being the energy and p_z being the component of the momentum along the beam axis, and

$$x(y) = \frac{1}{2}\left[\frac{m}{E}\Big(\exp y - \exp(-y)\Big) + \sqrt{\Big(\frac{m}{E}(\exp y - \exp(-y))\Big)^2 + 4a}\right] . \quad (6.22)$$

From Ref. [111], using for the light quark mass=(up-mass+down-mass)/2= 3.5 MeV.

$$D_{b\to b\bar{q}} = 9.21\times 10^5 \alpha_s^2 |R(0)|^2/\pi \, , \quad (6.23)$$

in units of $(1/\mathrm{GeV}^3)$, with $\alpha_s = 0.26$. For a 1S state $|R(0)|^2 = 4/a_0^3$. For a $b\bar{q}$ state, $(1/a_o) = m_q \simeq 3.5$ MeV. Therefore,

$$\begin{aligned} |R(0)|^2 &\simeq 1.71\times 10^{-7} \ \mathrm{GeV}^3 \, , \\ D_{b\to b\bar{q}} &\simeq 3.39\times 10^{-3} \, , \end{aligned} \quad (6.24)$$

so $D_{b\to b\bar{q}} \simeq D_{c\to c\bar{q}}$ [105] as expected from heavy-quark symmetry. The calculation of the differential cross-section is similar to that in Ref. [45].

$$\frac{d\sigma_{pp\to BX}}{dy} = A_{bb}\times f_g(x(y),2m) f_g(a/x(y),2m)\frac{dx(y)}{dy}\frac{1}{x(y)} D_{b\to b\bar{q}} \, , \quad (6.25)$$

where A_{bb} is the matrix element for bottomonium production [45], $A_{bb} = \frac{5\pi^3\alpha_s^2}{288 m^3 s}\hat{O}\langle(^1S_0^{\mathbf{8}})\rangle$, and $a = 4m^2/s$ modified by an effective mass m: $A_{bb} = 7.9\times 10^{-4}(1.5/m)^3$ nb. For $m = 5.0$ GeV, $A_{bb} = 2.13\times 10^{-5}$ nb. From Eq. (6.25) we find the differential cross-section, $\frac{d\sigma_{pp\to BX}}{dy}$, shown in Figure 6.6, with m=5.0 GeV.

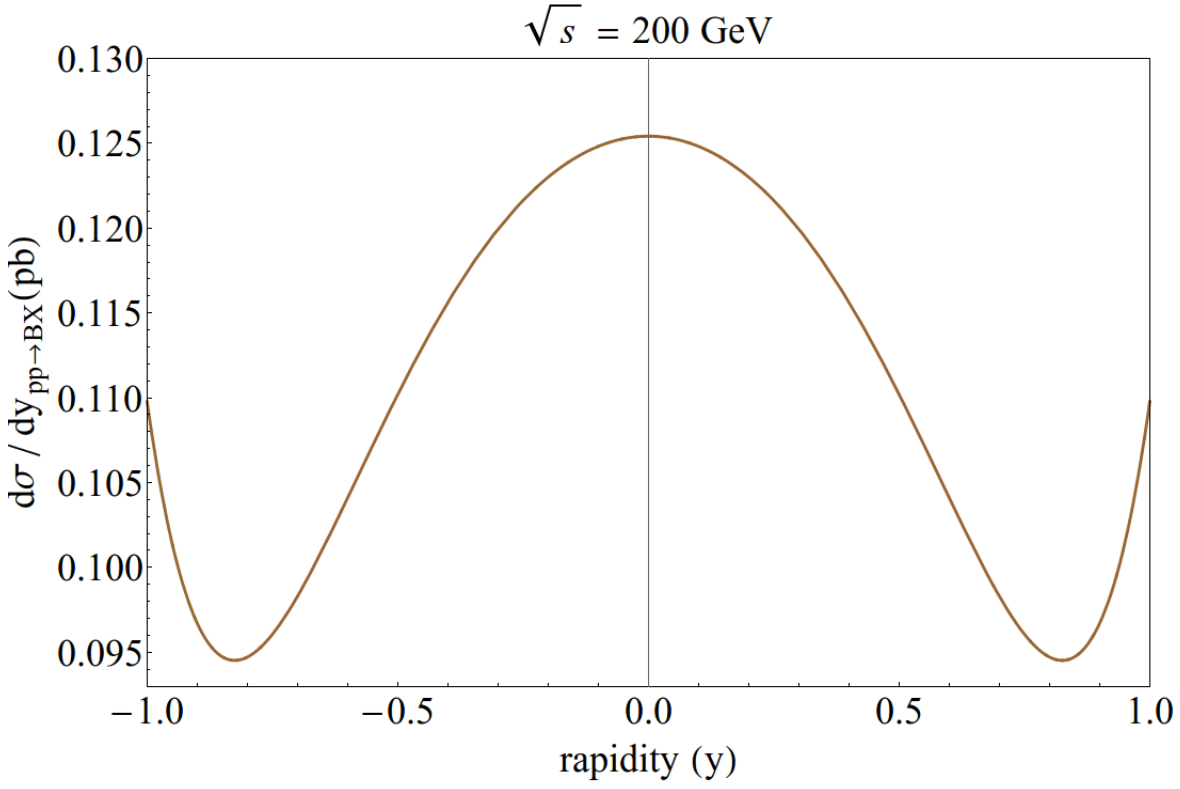

Figure 6.6: $d\sigma/dy$ for $\sqrt{s} = 200$ GeV unpolarized p-p collisions producing $B + X$.

6.5.2 Total $pp \to BX$ Cross-section

The total cross section for $pp \to BX$ is given by

$$\sigma_{pp\to BX} = \int_a^1 \frac{dx}{x} A_{bb} \times f_g(x(y), 2m) f_g(a/x(y), 2m) D_{b\to b\bar{q}} \; . \tag{6.26}$$

From Eqs. (6.17,6.24) and A_{bb} one obtains

$$\sigma_{pp\to BX} \;\; \simeq \;\; 0.4823 \text{ nb} \; . \tag{6.27}$$

Since $\sigma_{pp\to DX} \simeq 2680.0$ nb [105], the ratio of $\sigma_{pp\to BX}$ to $\sigma_{pp\to DX}$ is

$$RR \;\; \equiv \;\; \frac{\sigma_{pp\to BX}}{\sigma_{pp\to DX}} \simeq 1.8 \times 10^{-4} \; , \tag{6.28}$$

due to the difference in the quark mass and values of f_g for bottom vs charm quarks. A number of experiments have measured $\sigma_{c\bar{c}}$ cross sections at $\sqrt{s_{pp}}$=200 GeV [113, 116, 121, 122]. Experimental measurements of B production via p-p collisions are expected in the future.

6.5.3 Differential Cu-Cu, Au-$Au \to BX$ Cross-sections

Cold nuclear matter effects on heavy-quark production were estimated for a number of rapidities via PHENIX experiments [117]. We use the results of this experiment for the study of B production via Cu-Cu and Au-Au collisions.

In this section we estimate the production of B^0, B^- from Cu-Cu and Au-Au collisions, using the methods given in Ref. [106] for the estimate of production of Ψ and Υ states via

Cu-Cu and Au-Au collisions based on p-p collisions.

The differential rapidity cross section for $B + X$ production via A-A collisions is given by $\frac{d\sigma_{pp\to BX}}{dy}$ with modification described in Ref. [106] for Cu-Cu and Au-Au collisions:

$$\frac{d\sigma_{AA\to BX}}{dy} = R_{AA} N_{bin}^{AA} \left(\frac{d\sigma_{pp\to BX}}{dy} \right) , \tag{6.29}$$

R_{AA} is the nuclear-modification factor, N_{bin}^{AA} is the number of binary collisions in the AA collision, and $\left(\frac{d\sigma_{pp\to BX}}{dy}\right)$ is the differential rapidity cross section for BX production via nucleon-nucleon collisions in the nuclear medium.

$\left(\frac{d\sigma_{pp\to BX}}{dy}\right)$ is given by Eq. (6.25) with $x(y)$ replaced by the function $\bar{x}$, the effective parton x in the nucleus Au [118]:

$$\bar{x}(y) = x(y)(1 + \frac{\xi_g^2 (A^{1/3} - 1)}{Q^2}) , \tag{6.30}$$

which was evaluated in Ref. [106], where it was shown that $\bar{x}(y) \simeq x(y)$.

Experimental studies show that for $\sqrt{s_{pp}} = 200$ GeV, $R_{AA}^E \simeq 0.5$ both for Cu-Cu [119, 120] and Au-Au [121, 122, 123]. The number of binary collisions are N_{bin}^{AA}=51.5 for Cu-Cu [124] and 258 for Au-Au.

From Eqs. (6.25) and (6.29) one obtains the differential rapidity cross section for B+X production via Cu-Cu and Au-Au collisions

$$\begin{aligned} \frac{d\sigma_{Cu-Cu\to BX}}{dy} &= (51.5/2) \times A_{bb} \times f_g(x(y), 2m) f_g(a/x(y), 2m) \frac{dx(y)}{dy} \frac{1}{x(y)} D_{b\to b\bar{q}} , \\ \frac{d\sigma_{Au-Au\to BX}}{dy} &= (258/2) \times A_{bb} \times f_g(x(y), 2m) f_g(a/x(y), 2m) \frac{dx(y)}{dy} \frac{1}{x(y)} D_{b\to b\bar{q}} . \end{aligned} \tag{6.31}$$

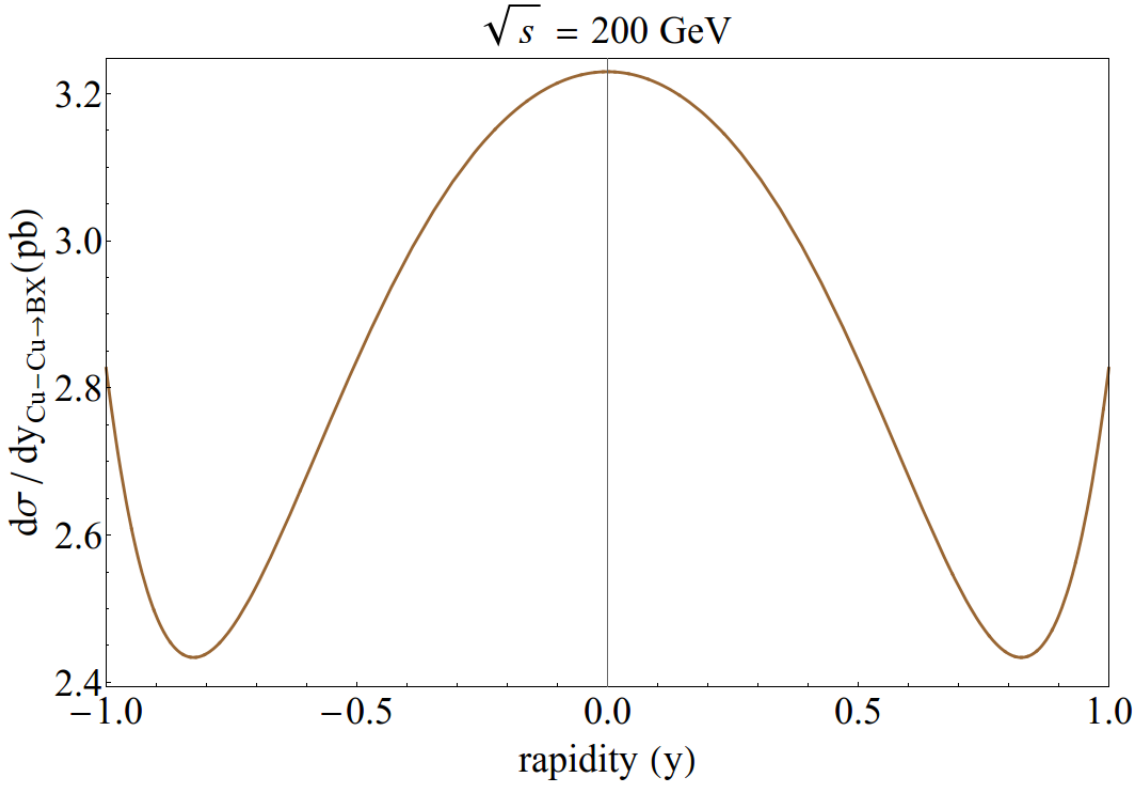

Figure 6.7: $d\sigma/dy$ for $\sqrt{s} = 200$ GeV unpolarized Cu-Cu collisions producing $B + X$.

$d\sigma_{Cu-Cu\to BX}/dy$ and $d\sigma_{Au-Au\to BX}/dy$ are shown in the Figure 6.7 and Figure 6.8.

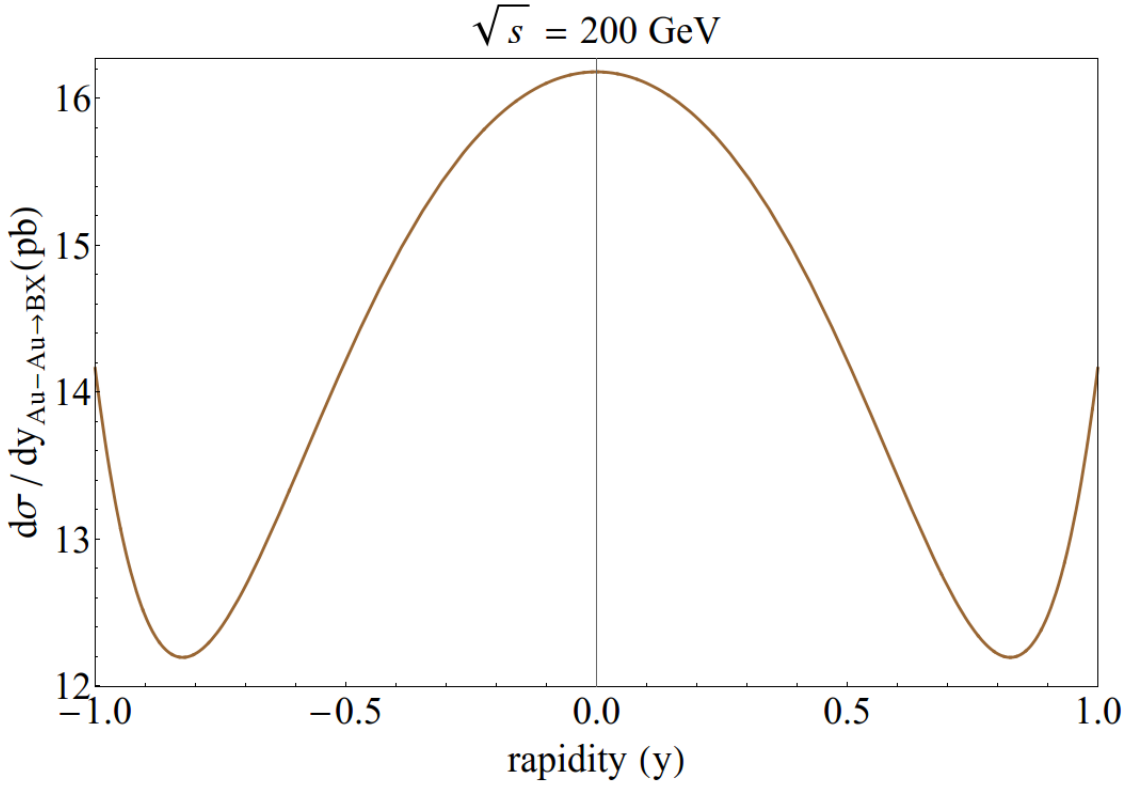

Figure 6.8: $d\sigma/dy$ for $\sqrt{s} = 200$ GeV unpolarized Au-Au collisions producing $B + X$.

6.5.4 Total Cu-$Cu \to BX$ and Au-$Au \to BX$ Cross-sections

Total $\sigma_{CuCu\to BX}$ and $\sigma_{AuAu\to BX}$ cross-sections are obtained from $\sigma_{pp\to BX}$ Eq. (6.27) by multiplying $\sigma_{pp\to BX}$ by $R_{AA}N_{\rm bin}^{AA}$. Therefore

$$\begin{aligned} \sigma_{CuCu\to BX} &\simeq (51.5/2)\times 0.4823 \text{ nb} = 12.42 \text{ nb}, \\ \sigma_{AuAu\to BX} &\simeq (258/2)\times 0.4823 \text{ nb} = 62.22 \text{ nb} . \end{aligned} \tag{6.32}$$

6.6 Conclusions

We have estimated the production of heavy-quark mesons $B^0(b\bar{d}), B^-(b\bar{u}) + X$ via p-p collisions using the color-octet model with an extension of our previous work on production of $\bar{c}c$ and $\bar{b}b$ states to $\bar{d}b$ or $\bar{u}b$ B-meson states using fragmentation. Our results are expected to be tested by p-p collision experiments in the future. We have also estimated the production of B-meson states via Cu-Cu and Au-Au collisions, using experimental results for the nuclear modification and number of binary collisions in recent A-A collisions experiments, which also might be measured in future experiments.

Chapter 7

Summary

In this dissertation, we calculated the baryonic masses of charmed lambda (Λ_c^+), strange lambda (Λ^0), bottom lambda (Λ_b^0) and have developed a framework to estimate the couplings corresponding to the Cabibbo-favored and Cabibbo-suppressed weak decay processes of heavy-quark baryons using the Quantum Chromodynamics Sum Rules (QCD Sum Rules). QCD Sum Rules are non-perturbative techniques that use Operator Product Expansion (OPE) of gauge-invariant QCD condensates of different mass dimensions to express the n-point functions of the hadronic current operators and then use quark-hadron duality to compare the OPE to a phenomenological model to extract various physical properties of the hadrons. We used a two-point correlator of a current operator that projects into the state of either Λ^0, Λ_c^+, or Λ_b^0 and evaluated exactly the perturbative term in the OPE. We achieved convergence through Borel transformation and extracted the mass from the minima of the Borel-transformed two-point correlators. We extended this work to consider a three-point correlator comprised of the Λ_c^+ and Λ^0 current operators, and the weak Hamiltonian responsible for charm to strange transition and an external pion creation. We compared the OPE to a phenomenological model of the three-point correlator to estimate the coupling corresponding to the process in which a charmed lambda decays to a strange lambda and a pion. Because the Λ_c^+ and Λ^0 masses are not close, we used reduced Borel transformation to achieve convergence.

In the second part of the thesis, we extended one of our recent works on the charmed meson

D production to calculate B meson production cross-section in unpolarized proton-proton and and heavy-ion (copper-copper and gold-gold) collisions at $\sqrt{s} = 200$ GeV. The dominant channel at this energy was the gluon-gluon fusion channel. While the gluons cannot directly produce B mesons, they can create bottom-antibottom pairs which can later get converted to B mesons($b\bar{d} - d\bar{b}$) through fragmentation process. The dominant mechanism behind the bottom-antibottom creation was color-octet mechanism. The total production cross-section of B meson at this energy was found to be much suppressed compared to that of D mesons and the experimental measurements of B production cross-section from such processes are expected in near future.

Appendices

Appendix A

OPE Side of the Three-point Function

Here we calculate the Operator Product Expansion side of the three-point function mentioned in Chapter 5. Using Eq. (5.3), (5.4) and (5.8) and keeping the essential terms, $\Pi_3(x,y)$ is

$$\begin{aligned}\Pi_3(x,y) &= iG_F F_\pi V_{ud}\, q_\alpha \langle 0|\, T\Big[\epsilon^{abc}\bar{u}(x)^a C\gamma_\mu d^b(x)\gamma_5\gamma^\mu c(x)^c s^j(y)\gamma^\alpha(1-\gamma_5)\bar{c}^j(y)V_{cs} \\ &\quad \epsilon^{def}u^d(0)C\gamma_\lambda\bar{d}^e(0)\gamma_5\gamma^\lambda\bar{s}^f(0)\Big]\,|0\rangle\ . \qquad \text{(A.1)}\end{aligned}$$

From Eq. (5.6), (A.1), and using $q(x) = \int \frac{d^4k}{(2\pi)^4} e^{-ik\cdot x} q(k)$,

$$\begin{aligned}\Pi_3(p,q) &= iG_F F_\pi V_{cs} V_{ud}\, q_\alpha \int d^4x d^4y e^{ip\cdot x} e^{iq\cdot y} \int \frac{d^4k_1}{(2\pi)^4}\frac{d^4k_2}{(2\pi)^4}\frac{d^4k_3}{(2\pi)^4}\frac{d^4k_4}{(2\pi)^4} \\ &\quad e^{ik_1\cdot x}e^{-ik_2\cdot x}e^{-ik_3\cdot(x-y)}e^{-ik_4\cdot y} Tr[S_u(k_1)C\gamma_\mu S_d(k_2)C^*\gamma_\lambda\gamma_5\gamma^\mu S_c(k_3)\gamma^\alpha(1-\gamma_5)S_s(k_4)\gamma^\lambda\gamma^5]\ , \qquad \text{(A.2)}\end{aligned}$$

where the quark propagator is $S_q(k) = (\not{k} + m_q)/(k^2 - m_q^2) = (k_\mu\gamma^\mu + m_q)/(k^2 - m_q^2)$.

Using $m_u, m_d \ll m_c$, the trace in Eq(A.2) is

$$\begin{aligned}Tr[S_u(k_1)C\gamma_\mu S_d(k_2)\gamma^\nu C\gamma_5\gamma^\mu S_c(k_3)S_s(k_4)\gamma_\nu\gamma_5] &= Tr[\not{k}_1 C\gamma_\mu\ \not{k}_2 C^*\gamma_\lambda\gamma_5\gamma^\mu(\not{k}_3 + m_c)\gamma^\alpha(1-\gamma_5) \\ &\quad (\not{k}_4 + m_s)\gamma_\lambda\gamma^5]\frac{1}{k_1^2 k_2^2(k_3^2 - m_c^2)(k_4^2 - m_s^2)}\ . \qquad \text{(A.3)}\end{aligned}$$

In carrying out the trace in Eq(A.3) note that $Tr[\gamma_5\gamma_\nu\gamma_\lambda] = 0$, and one obtains for the trace on the right hand side

$$\begin{aligned} TR &= Tr[\not{k}_1 C\gamma_\mu \not{k}_2 C^*\gamma_\lambda\gamma_5\gamma^\mu(\not{k}_3 + m_c)\gamma^\alpha(1-\gamma_5)(\not{k}_4 + m_s)\gamma_\lambda\gamma_5] \\ &= 16m_c(k_1\cdot k_2 k_4^\alpha + k_2\cdot k_4 k_1^\alpha - k_1\cdot k_4 k_2^\alpha) \\ &\quad -16m_s(-k_1\cdot k_2 k_3^\alpha + k_2\cdot k_3 k_1^\alpha - k_1\cdot k_3 k_2^\alpha)\ . \end{aligned} \tag{A.4}$$

Making use of $\int d^4x e^{ix\cdot(p-k)} = (2\pi)^4\delta^{(4)}(p-k)$ so $k_3 = p + k_1 - k_2$ and $k_4 = p + k_1 - k_2 + q$, one obtains

$$\begin{aligned} \Pi_3(p,q) &= 16iG_F F_\pi V_{cs}V_{ud}\int \frac{d^4k_1}{(2\pi)^4}\frac{d^4k_2}{(2\pi)^4}(m_c F_1 + m_s F_2) \\ &\quad \times \frac{1}{[k_1^2 k_2^2((p+k_1-k_2)^2 - m_c^2)((p+q+k_1-k_2)^2 - m_s^2)]}\ , \end{aligned} \tag{A.5}$$

where

$$F_1 = k_1.q\ k_2.(p+q+k_1-k_2) - k_2.q\ k_1.(p+q+k_1-k_2) + k_1.k_2\ q.(p+q+k_1-k_2), \tag{A.6}$$

$$F_2 = k_1.(p+k_1-k_2)\ k_2.q - k_2.(p+k_1-k_2)\ k_1.q + k_1.k_2\ q.(p+k_1-k_2)\ . \tag{A.7}$$

Using $(k_1 + p) \equiv l$ and $k_2 \equiv k$, $\Pi_3(p,q)$ in Eq(A.5) can be expressed as

$$\Pi_3(p,q) = 16iG_F F_\pi V_{ud}V_{cs}\left(m_c\Pi_{3c} + m_s\Pi_{3s}\right), \tag{A.8}$$

with

$$\Pi_{3c}(p,q) = \int \frac{d^4k}{(2\pi)^4}\frac{1}{k^2}\int \frac{d^4l}{(2\pi)^4}\frac{F_1}{(l+p)^2\left[(l-k)^2 - m_c^2\right]\left[(l-k-q)^2 - m_s^2\right]}\ . \tag{A.9}$$

$$\Pi_{3s}(p,q) \;=\; \int \frac{d^4k}{(2\pi)^4}\frac{1}{k^2}\int \frac{d^4l}{(2\pi)^4}\frac{F_2}{(l+p)^2\left[(l-k)^2-m_c^2\right]\left[(l-k-q)^2-m_s^2\right]}\;, \tag{A.10}$$

where

$$F_1 = k\cdot(l-p)q\cdot(l-k+q)+k\cdot(l-k+q)q\cdot(l-p)-(l-p)\cdot(l-k+q)q\cdot k \tag{A.11}$$

$$F_2 = k\cdot(l-p)\;q\cdot(l-k)-k\cdot(l-k)\;q\cdot(l-p)+(l-p)\cdot(l-k)\;q\cdot k\;. \tag{A.12}$$

Here we consider $m_s \ll m_c$ to write

$$\Pi_3(p,q) \;=\; 16im_cG_FF_\pi V_{ud}V_{cs}\;\Pi_{3c}(p,q)\;. \tag{A.13}$$

Defining

$$\begin{aligned}\tilde{\Pi}^{\mu\nu\omega}(p,q) \;&=\; \int \frac{d^4k}{(2\pi)^4}\frac{k_\mu}{k^2}\int \frac{d^4l}{(2\pi)^4}\frac{(l-p)^\nu(l-k+q)^\omega}{(l+p)^2\left[(l-k)^2-m_c^2\right]\left[(l-k+q)^2-m_s^2\right]}\\ &=\; \int \frac{d^4k}{(2\pi)^4}\frac{k_\mu}{k^2}\int \frac{d^4l}{(2\pi)^4}\frac{l^\nu(l-k+p+q)^\omega}{l^2\left[(l-k+p)^2-m_c^2\right]\left[(l-k+p+q)^2-m_s^2\right]}\end{aligned} \tag{A.14}$$

to write

$$\Pi_{3c}(p,q) \;=\; q_\nu\left[\tilde{\Pi}^{\mu\mu\nu}+\tilde{\Pi}^{\mu\nu\mu}-\tilde{\Pi}^{\nu\mu\mu}\right]\;. \tag{A.15}$$

Using $k\to -k$, $l\to -l$, we get

$$\Pi^{\mu\nu\omega}(p,q) = -\tilde{\Pi}^{\mu\nu\omega} \;=\; \int \frac{d^4k}{(2\pi)^4}\frac{k_\mu}{k^2}\int \frac{d^4l}{(2\pi)^4}\frac{l^\nu(l-k-p-q)^\omega}{l^2\left[(l-k-p)^2-m_c^2\right]\left[(l-k-p-q)^2-m_s^2\right]}\;. \tag{A.16}$$

Thus,

$$\Pi_3(p,q) \;=\; -16im_c G_F F_\pi V_{ud} V_{cs}\; \Pi_{3Q}(p,q), \tag{A.17}$$

where

$$\Pi_{3Q}(p,q) \;=\; q_\nu \left[\Pi^{\mu\mu\nu} + \Pi^{\mu\nu\mu} - \Pi^{\nu\mu\mu}\right] \;. \tag{A.18}$$

Appendix B

Evaluation of $\Pi^{\mu\nu\omega}(p,q)$

Here we evaluate the integral in Eq. (A.16). Let's define

$$\begin{aligned}
\Pi_{l0}(p,q) &= \int \frac{d^4l}{(2\pi)^4} \frac{1}{l^2\left[(l-k-p)^2-m_c^2\right]\left[(l-k-p-q)^2-m_s^2\right]}, \\
\Pi^{\mu}_{l1}(p,q) &= \int \frac{d^4l}{(2\pi)^4} \frac{l^{\mu}}{l^2\left[(l-k-p)^2-m_c^2\right]\left[(l-k-p-q)^2-m_s^2\right]}, \\
\Pi^{\mu\nu}_{l2}(p,q) &= \int \frac{d^4l}{(2\pi)^4} \frac{l^{\mu}l^{\nu}}{l^2\left[(l-k-p)^2-m_c^2\right]\left[(l-k-p-q)^2-m_s^2\right]} \ . \qquad \text{(B.1)}
\end{aligned}$$

These integrals are evaluated using the regularization technique adopted in [86] to give us

$$\Pi_{l0}(p,q) = \frac{1}{(4\pi)^2}\int_0^{\infty} d\alpha d\beta d\gamma \ \frac{e^{A(\alpha,\beta,\gamma)+\beta m_c^2+\gamma m_s^2}}{(\alpha+\beta+\gamma)^2}, \qquad \text{(B.2)}$$

$$\Pi^{\mu}_{l1}(p,q) = \frac{1}{(4\pi)^2}\int_0^{\infty} d\alpha d\beta d\gamma \ \frac{[(\beta+\gamma)k+s]^{\mu}}{(\alpha+\beta+\gamma)^3} \ e^{A(\alpha,\beta,\gamma)+\beta m_c^2+\gamma m_s^2}, \qquad \text{(B.3)}$$

$$\begin{aligned}
\Pi^{\mu\nu}_{l2}(p,q) &= \frac{1}{(4\pi)^2}\int_0^{\infty} d\alpha d\beta d\gamma \ e^{A(\alpha,\beta,\gamma)+\beta m_c^2+\gamma m_s^2}\Big[-\frac{1}{2(4\pi)^2}\frac{g^{\mu\nu}}{(\alpha+\beta+\gamma)^3} \\
&\quad + \frac{[(\beta+\gamma)k+s]^{\mu}\ [(\beta+\gamma)k+s]^{\nu}}{(\alpha+\beta+\gamma)^4}\Big] \ , \qquad \text{(B.4)}
\end{aligned}$$

where

$$s^{\mu} = (\beta+\gamma)p^{\mu}+\gamma q^{\nu} \ . \qquad \text{(B.5)}$$

Using $d^4k \to d^Dk$, $D \equiv 4-2\epsilon$, $\beta \to \rho\beta$, $\gamma \to \rho\gamma$, $\delta(\rho-\beta-\gamma) \to \delta(1-\beta-\gamma)/\rho$, and repeating for α as well, one obtains

$$\Pi_{l0}(p,q) = \frac{1}{(4\pi)^2}\int_0^1 d\gamma d\rho \int_0^\infty d\kappa\ \rho e^{A+\kappa\rho[(1-\gamma)m_c^2+\gamma m_s^2]}, \tag{B.6}$$

$$\Pi^{\mu}_{l1}(p,q) = \frac{1}{(4\pi)^2}\int_0^1 d\gamma d\rho \int_0^\infty d\kappa\ \rho^2[k+p+\gamma q]^\mu\ e^{A+\kappa\rho[(1-\gamma)m_c^2+\gamma m_s^2]}, \tag{B.7}$$

$$\Pi^{\mu\nu}_{l2}(p,q) = \frac{1}{(4\pi)^2}\int_0^1 d\gamma d\rho \int_0^\infty d\kappa\ \ \rho\left[-\frac{1}{2\kappa}g^{\mu\nu}+\rho^2(k+p+\gamma q)^\mu(k+p+\gamma q)^\nu\right] e^{A+\kappa\rho[(1-\gamma)m_c^2+\gamma m_s^2]}\ , \tag{B.8}$$

where we redefine

$$A = Dk^2 + F.k + f(p,q)\ , \tag{B.9}$$

where

$$D = -\kappa\rho(1-\rho), \tag{B.10}$$

$$F^\mu = -2\kappa\rho(1-\rho)(p+\gamma q)^\mu, \tag{B.11}$$

$$f(p,q) = -\kappa\rho(1-\rho)p.(p+\gamma q)\ . \tag{B.12}$$

Using Eq. (B.6), (B.7), (B.8) in Eq. (5.11), we get

$$\begin{aligned}
\Pi^{\mu\mu\nu}(p,q) &= \int \frac{d^4k}{(2\pi)^4}\,\frac{k_\mu}{k^2}\int \frac{d^4l}{(2\pi)^4}\,\frac{l^\mu(l-k-p-q)^\nu}{l^2\left[(l-k-p)^2-m_c^2\right]\left[(l-k-p-q)^2-m_s^2\right]} \\
&= \int \frac{d^4k}{(2\pi)^4}\,\frac{k_\mu}{k^2}\left[\Pi_{l2}^{\mu\nu}-(k+p+q)^\nu\,\Pi_{l1}^{\mu}\right] \\
&= \frac{1}{(4\pi)^2}\int_0^\infty d\alpha d\beta d\gamma\; e^{A+\beta m_c^2+\gamma m_s^2}\int \frac{d^4k}{(2\pi)^4}\,\frac{k_\mu}{k^2}\Big[-\frac{g^{\mu\nu}}{2(\alpha+\beta+\gamma)^3} \\
&\qquad +\frac{[(\beta+\gamma)k+s]^\mu\,[(\beta+\gamma)k+s]^\nu}{(\alpha+\beta+\gamma)^4}-\frac{(k+p+q)^\nu[(\beta+\gamma)k+s]^\mu}{(\alpha+\beta+\gamma)^3}\Big]\,.
\end{aligned} \tag{B.13}$$

Similarly, we can write

$$\begin{aligned}
\Pi^{\mu\nu\mu} &= \int \frac{d^4k}{(2\pi)^4}\,\frac{k_\mu}{k^2}\int \frac{d^4l}{(2\pi)^4}\,\frac{l^\nu(l-k-p-q)^\mu}{l^2\left[(l-k-p)^2-m_c^2\right]\left[(l-k-p-q)^2-m_s^2\right]} \\
&= \frac{1}{(4\pi)^2}\int_0^\infty d\alpha d\beta d\gamma\; e^{A+\beta m_c^2+\gamma m_s^2}\int \frac{d^4k}{(2\pi)^4}\,\frac{k_\mu}{k^2}\Big[-\frac{g^{\mu\nu}}{2(\alpha+\beta+\gamma)^3} \\
&\qquad +\frac{[(\beta+\gamma)k+s]^\mu\,[(\beta+\gamma)k+s]^\nu}{(\alpha+\beta+\gamma)^4}-\frac{(k+p+q)^\mu[(\beta+\gamma)k+s]^\nu}{(\alpha+\beta+\gamma)^3}\Big]\,,
\end{aligned} \tag{B.14}$$

$$\begin{aligned}
\Pi^{\nu\mu\mu} &= \int \frac{d^4k}{(2\pi)^4}\,\frac{k_\nu}{k^2}\int \frac{d^4l}{(2\pi)^4}\,\frac{l^\mu(l-k-p-q)^\mu}{l^2\left[(l-k-p)^2-m_c^2\right]\left[(l-k-p-q)^2-m_s^2\right]} \\
&= \frac{1}{(4\pi)^2}\int_0^\infty d\alpha d\beta d\gamma\; e^{A+\beta m_c^2+\gamma m_s^2}\int \frac{d^4k}{(2\pi)^4}\,\frac{k_\nu}{k^2}\Big[-\frac{g^{\nu\nu}}{2(\alpha+\beta+\gamma)^3} \\
&\qquad +\frac{[(\beta+\gamma)k+s]^\mu\,[(\beta+\gamma)k+s]^\mu}{(\alpha+\beta+\gamma)^4}-\frac{(k+p+q)^\mu[(\beta+\gamma)k+s]^\mu}{(\alpha+\beta+\gamma)^3}\Big]\,.
\end{aligned} \tag{B.15}$$

Multiplying Eq. (B.13), (B.14) and (B.15) with the pion four momentum, q_μ, we get

$$\begin{aligned}
q_\nu\Pi^{\mu\mu\nu} &= \frac{1}{(4\pi)^2}\int_0^1 d\gamma d\rho \int_0^\infty d\kappa\; e^{\kappa\rho\mathcal{Z}^2}\Big[-\frac{\rho}{2\kappa}\int\frac{d^4k}{(2\pi)^4}\,e^A\,\frac{q.k}{k^2} \\
&\quad +\rho^3\int\frac{d^4k}{(2\pi)^4}\,e^A\,\frac{k.(k+p+\gamma q)\;q.(k+p)}{k^2} \\
&\quad -\rho^2\int\frac{d^4k}{(2\pi)^4}\,e^A\,\frac{k.(k+p+\gamma q)\;q.(k+p)}{k^2}\Big], \qquad \text{(B.16)} \\
q_\nu\Pi^{\mu\nu\mu} &= \frac{1}{(4\pi)^2}\int_0^1 d\gamma d\rho \int_0^\infty d\kappa\; e^{\kappa\rho\mathcal{Z}^2}\Big[-\frac{\rho}{2\kappa}\int\frac{d^4k}{(2\pi)^4}\,e^A\,\frac{q.k}{k^2} \\
&\quad +\rho^3\int\frac{d^4k}{(2\pi)^4}\,e^A\,\frac{k.(k+p+\gamma q)\;q.(k+p)}{k^2} \\
&\quad -\rho^2\int\frac{d^4k}{(2\pi)^4}\,e^A\,\frac{k.(k+p+q)\;q.(k+p)}{k^2}\Big], \qquad \text{(B.17)} \\
q_\nu\Pi^{\nu\mu\mu} &= \frac{1}{(4\pi)^2}\int_0^1 d\gamma d\rho \int_0^\infty d\kappa\; e^{\kappa\rho\mathcal{Z}^2}\Big[-\frac{2\rho}{\kappa}\int\frac{d^4k}{(2\pi)^4}\,e^A\,\frac{q.k}{k^2} \\
&\quad +\rho^3\int\frac{d^4k}{(2\pi)^4}\,e^A\,\frac{k.q\;(k+p+\gamma q)^2}{k^2} \\
&\quad -\rho^2\int\frac{d^4k}{(2\pi)^4}\,e^A\,\frac{k.q\;(k+p+\gamma q).(k+p+q)}{k^2}\Big]\,. \qquad \text{(B.18)}
\end{aligned}$$

Eq. (B.16), (B.17) and (B.18) and (B.23) allows us to write

$$\begin{aligned}
\Pi_{3Q} &= \frac{1}{(4\pi)^2}\int d\gamma d\rho\int_0^\infty d\kappa\; e^{\kappa\rho\mathcal{Z}^2}\Big[\frac{\rho}{\kappa}\int\frac{d^4k}{(2\pi)^4}e^A\,\frac{k.q}{k^2} \\
&\quad +2\rho^3\int\frac{d^4k}{(2\pi)^4}e^A\,\frac{k.(k+p+q)\;q.(k+p)}{k^2} \\
&\quad -\rho^3\int\frac{d^4k}{(2\pi)^4}e^A\,\frac{(q.k)(k+p+\gamma q)^2}{k^2} \\
&\quad -\rho^2\int\frac{d^4k}{(2\pi)^4}e^A\,\frac{q.(k+p)}{k^2}\Big\{2k^2+(p+q).k+(p+\gamma q).k\Big\} \\
&\quad +\rho^2\int\frac{d^4k}{(2\pi)^4}e^A\,\frac{q.k}{k^2}\Big\{k^2+k.\big[(p+q)+(p+\gamma q)\big]+(p+q).(p+\gamma q)\Big\}\Big] \qquad \text{(B.19)}
\end{aligned}$$

After a little manipulation, we get

$$\begin{aligned}
\Pi_{3Q} &= \frac{1}{(4\pi)^2}\int_0^1 d\gamma d\rho \int d\kappa\ e^{\kappa\rho\mathcal{Z}^2}\Big[\frac{\rho}{\kappa}\int\frac{d^4k}{(2\pi)^4}e^A\ \frac{k.q}{k^2} \\
&\quad +2\rho^3\Big\{\int\frac{d^4k}{(2\pi)^4}e^A+(p+\gamma q)_\mu\int\frac{d^4k}{(2\pi)^4}e^A\frac{k^\mu}{k^2}\Big\}q.(k+p) \\
&\quad -\rho^3\int\frac{d^4k}{(2\pi)^4}e^A\ \frac{(k.q)\left[k^2+2k.(p+\gamma q)+(p+\gamma q)^2\right]}{k^2} \\
&\quad -2\rho^2\int\frac{d^4k}{(2\pi)^4}e^A\ q.(k+p)-\rho^2\int\frac{d^4k}{(2\pi)^4}e^A\ \frac{q.(k+p)\ k.\Big\{(p+q)+(p+\gamma q)\Big\}}{k^2} \\
&\quad +\rho^2\int\frac{d^4k}{(2\pi)^4}e^A\ q.k+\rho^2\int\frac{d^4k}{(2\pi)^4}e^A\ \frac{(q.k)\ k.\Big\{(p+q)+(p+\gamma q)\Big\}}{k^2} \\
&\qquad +\rho^2\int\frac{d^4k}{(2\pi)^4}e^A\ \frac{(q.k)(p+q).(p+\gamma q)}{k^2}\Big]\ ,
\end{aligned} \tag{B.20}$$

we get

$$\begin{aligned}
\Pi_{3Q} &= \frac{1}{(4\pi)^2}\int_0^1 d\gamma d\rho\int_0^\infty d\kappa\ e^{\kappa\rho\mathcal{Z}^2}\Big[\int\frac{d^4k}{(2\pi)^4}e^A\ \frac{k.q}{k^2}\Big\{\frac{\rho}{\kappa}-(\gamma+1)\rho^2q.p \\
&\quad +2\rho^3\gamma(p.q)-\rho^2(p+\gamma q).\left[\rho(p+\gamma q)-(p+q)\right]\Big\} \\
&\quad +2\rho^2(\rho-1)(p.q)\int\frac{d^4k}{(2\pi)^4}e^A\ \frac{k.p}{k^2}+2\rho^2(\rho-1)(p.q)\int\frac{d^4k}{(2\pi)^4}e^A+\rho^2(\rho-1)\int\frac{d^4k}{(2\pi)^4}e^A\ k.q\Big]\ ,
\end{aligned} \tag{B.21}$$

But

$$-(\gamma+1)\rho^2q.p+2\rho^3\gamma(p.q)-\rho^2(p+\gamma q).\left[\rho(p+\gamma q)-(p+q)\right] = -\rho^2(\rho-1)p^2\ . \tag{B.22}$$

This eventually gives us

$$\Pi_{3Q} = \frac{1}{(4\pi)^2}\int d\gamma d\rho\ \rho^2(\rho-1)\int_0^\infty d\kappa\ e^{\kappa\rho\mathcal{Z}^2}\Big[-p^2\int\frac{d^4k}{(2\pi)^4}e^A\ \frac{k.q}{k^2}+2p.q\int\frac{d^4k}{(2\pi)^4}e^A\ \frac{k.p}{k^2} +2p.q\int\frac{d^4k}{(2\pi)^4}e^A+\int\frac{d^4k}{(2\pi)^4}e^A\ (k.q)+\frac{\rho}{\kappa}\int\frac{d^4k}{(2\pi)^4}e^A\ \frac{k.q}{k^2}\Big]\ . \tag{B.23}$$

Using

$$\int\frac{d^4k}{(2\pi)^4}e^A = \frac{1}{2(4\pi)^2}\frac{e^{f-F^2/4D}}{D^3}\ (2D), \tag{B.24}$$

$$\int\frac{d^4k}{(2\pi)^4}\ k^\mu\ e^A = \frac{1}{2(4\pi)^2}\frac{e^{f-F^2/4D}}{D^3}\ (-F^\mu), \tag{B.25}$$

$$\int\frac{d^4k}{(2\pi)^4}\ \frac{k^\mu}{k^2}\ e^A = \int_0^\infty d\lambda\frac{e^{f-F^2/4(D-\lambda)}}{2(4\pi)^2(D-\lambda)^3}\,(-F^\mu)\,, \tag{B.26}$$

$$\int\frac{d^4k}{(2\pi)^4}\ \frac{k^\mu k^\nu}{k^2}\ e^A = \int_0^\infty d\lambda\frac{e^{f-F^2/4(D-\lambda)}}{2(4\pi)^2(D-\lambda)^3}\left[g^{\mu\nu}+\frac{F^\mu F^\nu}{2(D-\lambda)}\right], \tag{B.27}$$

we get

$$\Pi_{3Q} = \frac{1}{2(4\pi)^4}\int_0^1 d\gamma d\rho 2\rho^3(1-\rho)^2\ (p.q)\int_0^1 d\kappa\frac{1}{g(\rho,\kappa,\gamma)^3}\Big[\kappa(p+\gamma q)^2\Gamma(\epsilon)a^{-\epsilon} +\rho\Gamma(-1+\epsilon)a^{1-\epsilon}\Big]+\frac{1}{2(4\pi)^4}\int_0^1 d\gamma d\rho\ \frac{2p.q}{(1-\rho)}\ \left[\Gamma(-1+\epsilon)(a')^{1-\epsilon}\right]\ , \tag{B.28}$$

where

$$\mathcal{Z}^2(\gamma) = (1-\gamma)m_c^2+\gamma m_s^2, \tag{B.29}$$

$$g(\rho,\kappa) = \kappa\rho(1-\rho)+(1-\kappa), \tag{B.30}$$

$$a(\rho,\kappa,\gamma) = -\kappa\rho\mathcal{Z}^2+\kappa\rho(1-\rho)p.(p+\gamma q)-\left\{\frac{\kappa\rho(1-\rho)}{g}\right\}\kappa\rho(1-\rho)(p+\gamma q)^2, \tag{B.31}$$

$$a'(\rho,\kappa,\gamma) = -\rho\mathcal{Z}^2+\rho(1-\rho)p.(p+\gamma q)-\left\{\frac{\kappa\rho(1-\rho)}{g}\right\}\rho(1-\rho)(p+\gamma q)^2\ . \tag{B.32}$$

References

[1] M. Gell-Mann. *A schematic model of baryons and mesons.* Phys. Lett. **8** no. 3 (1964) 214

[2] G. Zweig. *An SU_3 Model for Strong Interaction Symmetry and its Breaking.* CERN Report 8419/TH.401 (Jan. 17, 1964)

[3] V. E. Barnes *et al.*. *Observation of a Hyperon with Strangeness Minus Three.* Phys. Rev. Lett. **12** no. 8 (1964) 204

[4] O. W. Greenberg. *Spin and Unitary Spin Independence in a Paraquark Model of Baryons and Mesons.* Phys. Rev. Lett. **13** (1964) 598

[5] Y. Nambu. *A Systematics of Hadrons in Subnuclear Physics. In Preludes in Theoretical Physics.* ed. A. de Shalit, H. Feshbach and L. Van Hove (North Holland, Amsterdam, 1966)

[6] M.Y. Han and Y. Nambu. *Three-Triplet Model with Double SU(3) Symmetry.* Phys. Rev. 139, (1965) B1006

[7] M. E. Peskin, D. V. Schroeder. *An Introduction To Quantum Field Theory.* CRC Press, 1st edition

[8] N. Cabibbo. *Unitary Symmetry and Leptonic Decays.* Phys. Rev. Lett. **10** (1963) 531

[9] M. Tanabashi *et al. Particle Data Group.* Phys. Rev. D **98** (2018) 030001

[10] M. Bott-Bodenhausen *et al.* . *Search for decay of neutral kaons into charged lepton pairs.* Phys. Lett. **B24** no. 4 (1967) 194

[11] H. Foeth *et al.* . *Search for $K_L^0 \to \mu^+\mu^-$ and $K_L^0 \to e^+e^-$ decays.* Phys. Lett. **B30** (1969) 282

[12] K. Lande, E. Booth, J. Impeduglia, L. Lederman, and W. Chinowsky. *Observation of long-lived neutral V particles.* Phys. Rev. **103** (1956) 1901

[13] K. Lande, L. Lederman, and W. Chinowsky. *Report on long-lived K^0 mesons.* Phys. Rev. **105** (1957) 1925

[14] F. Niebergall *et al.*. *Experimental study of the Δ-s/Δ-q rule in the time dependent rate of $K^0 \to \pi e \nu$.* Phys. Lett. **B49** (1974) 103

[15] S. L. Glashow, J. Iliopoulos and L. Maiani. *Weak Interactions with Lepton-Hadron Symmetry.* Phys. Rev. **D2** (1970) 1285

[16] J. Aubert *et al.*. *Experimental Observation of a Heavy Particle J.* Phys. Rev. Lett. **33** (1974) 1404

[17] J.-E. Augustin *et al.*. *Discovery of a Narrow Resonance in e^+e^- Annihilation.* Phys. Rev. Lett. **33** (1974) 1406

[18] K. Niu, E. Mikumo, Y. Maeda. *A possible decay in flight of a new type particle.* Prog. Theo. Phys. **46** (1971) 1644

[19] BaBar collaboration. B. Aubert *et al. Observation of a narrow meson decaying to $D_s^+\pi^0$ at a mass of* 2.32 GeV/c^2. Phys. Rev. Lett. **90** (2003) 242001

[20] Belle Collaboration, K. Abe *et al.* . *Measurements of the D_{sJ} resonance properties.* Phys. Rev. Lett. **92** (2004) 012002

[21] S. Godfrey and N. Isgur. *Mesons in a relativized quark model with chromodynamics.* Phys. Rev. D **32** (1985) 189

[22] N. Isgur and M. B. Wise. *Spectroscopy with heavy quark symmetry.* Phys. Rev. Lett. **66** (1991) 1130

[23] BaBar collaboration, B. Aubert *et al.* . *Evidence for $D^0 - \bar{D}^0$ mixing.* Phys. Rev. Lett. **98** (2007) 211802

[24] Belle collaboration, M. Staric *et al.* . *Evidence for $D^0 - \bar{D}^0$ mixing.* Phys. Rev. Lett. **98** (2007) 211803

[25] I. Bigi. *Could charm's 'third time' be the real charm? - A manifesto.* arXiv:0902.3048

[26] B. Knapp *et al.*, *Observation of a narrow antibaryon state at* $2.26 GeV/c^2$, Phys. Rev. Lett. **37** (1976) 882

[27] J. L. Rosner, *Prospects for improved Λ_c branching fractions*, Phys. Rev. **D86** (2012) 014017

[28] P. Abreu *et al.*, OPAL Collaboration, *Measurements of inclusive semileptonic branching fractions of b hadrons in Z0 decays,* Eur. Phys. J. **C12** (2000) 225; R. Barate *et al.*, *Study of charm production in Z decays*, Eur. Phys. J. **C16** (2000) 597

[29] M. Gronau and J. L. Rosner, "Ratios of heavy hadron semileptonic decay rates," Phys. Rev. **D83**, 034025 (2011)

[30] J. L. Rosner, *Prospects for improved Λ_c branching fractions*, Phys. Rev. **D86** (2012) 014017

[31] M. Ablikim et al. [BESIII Collaboration],*Measurements of the absolute branching fractions for $\Lambda_c^+ \to \Lambda e^+ \nu_e$*. Phys. Rev. Lett. **115** (2015) 221805

[32] M. Ablikim et al. [BESIII Collaboration], *Measurements of Absolute Branching Fractions for $\Lambda_c^+ \to \Xi^0 K^+$ and $\Xi(1530)^0 K^+$*. arXiv:1803.04299 [hep-ex]

[33] S. Meinel. $\Lambda_c \to N$ *form factors from lattice QCD and phenomenology of* $\Lambda_c \to nl^+\mu_l$ *and* $\Lambda_c \to p\mu^+\mu^-$ *decays.* Phys. Rev. **D97** (2018) 034511

[34] H. Y. Cheng, X. W. Kang and F. Xu, *Singly Cabibbo-suppressed hadronic decays of* Λ_c^+. arXiv:1801.08625 [hep-ph]

[35] M. Gronau, J. L. Rosner. *An overview of* Λ_c *decays.* arXiv:1803.02267

[36] G. Mezzadri (BESIII Collaboration), Λ_c Physics at BESIII, Int. J. Mod. Phys.: Conf. Series **46** (2018) 1860064

[37] A. Zupanc *et al.*, *Measurements of the branching fraction* $\mathcal{B}(\Lambda_c^+ \to pK^-\pi^+)$, Phys. Rev. Lett. **113** (2014) 042002

[38] M. Ablikim *et al.* (BESIII Collaboration), *Measurements of absolute hadronic branching fractions of the* Λ_c^+ *baryon*, Phys. Rev. Lett. **116** (2016) 052001

[39] L. S. Kisslinger, M. X. Liu, and P. McGaughey. *D Production In p-p and d-Au Collisions.* Int. J. Theor. phys. **55** (2016) 2026

[40] P. L. Cho and A. K. Leibovich. *Color-octet quarkonia production.* Phys. Rev. **D53** (1996) 150

[41] E. Braaten and S. Fleming. *Color-Octet Fragmentation and the* ψ' *Surplus at the Fermilab Tevatron.* Phys. Rev. Lett. **74** (1995) 3327

[42] E. Braaten and Y.-Q. Chen. *Helicity decomposition for inclusive* J/ψ *production.* Phys. Rev. **D54** (1996) 3216

[43] G.C. Nayak, M.X. Liu, and F. Cooper, Phys. Rev. **D68** (2003) 034003

[44] F. Cooper, M.X. Liu, and G.C. Nayak, Phys. Rev. Lett. **93** (2004) 171801

[45] L. S. Kisslinger, M. X. Liu, and P. McGaughey. *Heavy Quark State Production In p-p Collisions.* Phys. Rev. **D84** (2011) 114020

[46] I. Newton, Principia (1687)

[47] J. Iliopoulos, *The Origin of Mass: Elementary Particles and Fundamental Symmetries*, 1st ed., Oxford University Press (2017)

[48] F. Wilczek, *Origins of Mass*, arXiv:1206.7114

[49] C. F. Weizsäcker. *Zur Theorie der Kernmassen (The Theory of Nuclear Masses).* Zeitschrift für Physik **96** (1935) 431

[50] B. D. Serot, J. D. Walecka. *Recent Progress in Quantum Hadrodynamics.* Int. J. Mod. Phys. **E6** No. 04 (1997) 515

[51] R. J. Furnstahl, D. K. Griegel, T. D. Cohen. *QCD sum rules for nucleons in nuclear matter.* Phys. Rev. **C46** (1992) 1507

[52] X. Jin, T. D. Cohen, R. J. Furnstahl, and D. K. Griegel. *QCD sum rules for nucleons in nuclear matter II.* Phys. Rev. **C47** (1993) 2882

[53] X. Jin, T. D. Cohen, R. J. Furnstahl, and D. K. Griegel. *QCD sum rules for nucleons in nuclear matter III.* Phys. Rev. **C49** (1994) 464

[54] T. D. Cohen, R. J. Furnstahl, D. K. Griegel, X. Jin. *QCD Sum Rules and Applications to Nuclear Physics.* Prog. Part. Nucl. Phys. **35** (1995) 221

[55] S. Dürr, Z. Fodor, J. Frison *et al.*, *Ab Initio Determination of Light Hadron Masses*, Science **322** (2008) 1224

[56] S. J. Brodsky, C. D. Roberts, R. Shrock, P. C. Tandy. *Essence of the vacuum quark condensate.* Phys. Rev. **C82** (2010) 022201

[57] H. Reinhardt and H. Weigel. *The vacuum nature of the QCD condensates.* Phys. Rev. **D85** (2012) 074029

[58] S. J. Brodsky, C. D. Roberts, R. Shrock, P. C. Tandy. *Confinement contains condensates.* Phys. Rev. **C85** (2012) 065202

[59] T. Lee. *Vacuum quark condensate, chiral Lagrangian, and Bose-Einstein statistics.* Phys. Lett. **B713** (2012) 270

[60] H. Sazdjian. *Introduction to chiral symmetry in QCD.* EPJ Web. Conf. **137** (2017) 02001

[61] V. I. Zakharov. *Gluon Condensate and Beyond.* Int. J. Mod. Phys. **A14** (1999) 4865

[62] M. Gell-Mann, R. J. Oakes, B. Renner. *Behavior of Current Divergences under $SU_3 \times SU_3$.* Phys. Rev. **175** (1968) 2195

[63] S. Aoki *et al.*. *Review of lattice results concerning low-energy particle physics.* Eur. Phys. J. **C77** (2017) 112

[64] L.J. Reinders, H. Rubenstein, and S, Yazaki. *Hadron properties from QCD sum rules.* Phys. Reports **127** (1985) 1 Trottier. *Direct determination of the strange and light quark condensates from full lattice QCD.* Phys. Rev. **D87** (2013) 034503

[65] G. S. Bali, C. Bauer, and A. Pineda. *Model-independent determination of the gluon condensate in four-dimensional $SU(3)$ gauge theory.* Phys. Rev. Lett. **113** (2014) 092001

[66] M.A. Shifman, A.J. Vainshtein, and V.I. Zakharov. *QCD and resonance physics. theoretical foundations.* Nucl. Phys. **B147** (1979) 385

[67] L. J. Reinders, H. R. Rubinstein, S. Yazaki. *QCD Sum Rules for Heavy Quark Systems.* Nucl. Phys. **B186** (1981) 109

[68] B.L. Ioffe. *Calculation of baryon masses in quantum chromodynamics.* Nucl. Phys. **B188** (1981) 317

[69] V. M. Belyaev and B. L. Ioffe. *Determination of the baryon mass and baryon resonances from the quantum-chromodynamics sum rule. Strange baryons.* Zh. Eksp. Teor. Fiz. **84** (1983) 1236

[70] K. G. Chetyrkin, A. Khodjamirian. *Strange quark mass from pseudoscalar sum rule with $O(\alpha_s^4)$ accuracy.* Eur. Phys. J. **C46** (2006) 721

[71] B.L. Ioffe. *Spontaneous violation of chiral symmetry in QCD vacuum is the origin of baryon masses and determines baryon magnetic moments and their other static properties.* Phys. Atom. Nucl. **72** (2009) 1214

[72] E. Bagan, M. Chabab, H.G. Dosch and S.Narison. *Baryon sum rules in the heavy quark effective theory.* Phys. Lett. **B287** (1992) 176

[73] K.-C. Yang, W.-Y.P. Hwang, E. M. Henley, and L. S. Kisslinger. *QCD sum rules and neutron-proton mass difference.* Phys. Rev. **D47** (1993) 3001

[74] K.G. Chetyrkin and A. Khodjamirian. *Strange quark mass from pseudoscalar sum rule with $O(\alpha_s^4)$ accuracy.* Eur. Phys. J. **C46** (2006) 721

[75] C. A. Dominguez, G. R. Gluckman and N. Paver. *Mass of the charm-quark from QCD sum rules.* Phys. Lett. **B333** (1994) 184

[76] S. Narison. *A Fresh look into the heavy quark mass values.* Phys. Lett. **B341** (1994) 73

[77] J. Govaerts, L. J. Reinders, H. R. Rubinstein, and J. Weyers. *Hybrid quarkonia from QCD sum rules.* Nucl. Phys. **B258** (1985) 215

[78] J. Govaerts, L. J. Reinders, and J. Weyers. *Radial excitations and exotic mesons via QCD sum rules.* Nucl. Phys. B258 (1985) 575

[79] J. Govaerts, L. J. Reinders, P. Francken, X. Gonze, and J. Weyers. *Coupled QCD sum rules for hybrid mesons.* Nucl. Phys. **B284** (1987) 674

[80] L. S. Kisslinger. *Mixed Heavy Quark Hybrid Mesons, Decay Puzzles, and RHIC.* Phys. Rev. **D79** (2009) 114026

[81] M. Nielsen, F. S. Navarra, and S. H. Lee. *New charmonium states in QCD sum rules: A concise review.* Phys. Rept. **497** (2010) 41

[82] J. F. Ashmore. *On renormalization and complex space-time dimensions.* Commun. Math. Phys. **29** (1973) 177

[83] G. Leibbrandt. *Introduction to the technique of dimensional regularization.* Rev. Mod. Phys. **47** no 4 (1975) 849

[84] E. M. Henley, W-Y. P. Hwang, L. S. Kisslinger. *Nonleptonic Hyperon Decays with QCD Sum Rules.* Nucl. Phys. **A706** (2002) 163

[85] M. A. Shifman, A. J. Vainshtein, and V. I. Zakharov. *QCD and resonance physics. theoretical foundations.* Nucl. Phys. **B147** (1979) 385

[86] L. S. Kisslinger and B. Singha. *Charm, Bottom, Strange Baryon Masses Using QCD Sum Rules.* Int. J. Mod. Phys. **A33** (2018) 1850139

[87] L. J. Reinders, H. Rubenstein, and S. Yazaki. *Hadron properties from QCD sum rules.* Phys. Reports **127** (1985) 1

[88] J. F. Donoghue, E. Golowich, and B. R. Holstein. *Low-energy weak interactions of quarks.* Phys. Reports. **131** (1986) 319

[89] F. S. Navarra, M. Nielson, M. E. Bracco, M. Chiapparini, and C. L. Schat. *$D^*D\pi$ and $B^*B\pi$ form factors from QCD Sum Rules.* Phys. Lett. **B489** (2000) 319

[90] M. E. Bracco, F. S. Navarra, M. Nielson. *$g_{NK\Lambda}$ and $g_{NK\Sigma}$ from QCD sum rules in the $\gamma_5\sigma_{\mu\nu}$ structure.* Phys. Lett. **B454** (1999) 346

[91] E. Bagan, M. Chabab, H. G. Dosch, and S. Narison. *Baryon sum rules in the heavy quark effective theory.* Phys. Lett. **B301** (1993) 243

[92] R. P. Feynman. *Very High-Energy Collisions of Hadrons.* Phys. Rev. Lett. **23** (1969) 1415

[93] J. D. Bjorken and E. A. Paschos. *Inelastic Electron-Proton and gamma-Proton Scattering and the Structure of the Nucleon.* Phys. Rev. **185** (1969) 1975

[94] V. Papadimitriou, CDF Collaboration, presented at the "Rencontres de la Vallee d'Aoste", La Thuile, March 1994

[95] T. Daniels, CDF Collaboration, Fermilab-Conf-94/136-E

[96] Toichiro Kinoshita. *Mass Singularities of Feynman Amplitudes.* Journal of Mathematical Physics **3** (1962) 650

[97] G. Curki, W. Furmanski, R. Petronzio. *Evolution of parton densities beyond leading order: The non-singlet case.* Nucl. Phys. **B175** (1980) 27

[98] J. C. Collins, D. E. Soper. *Parton distribution and decay functions.* Nucl. Phys. **B194** (1982) 445

[99] A. Metz, A. Vossen. *Parton Fragmentation Functions.* Prog. Part. Nucl. Phys. (2016) 136

[100] E. Braaten, S. Fleming, T. C. Yuan. *Production of Heavy Quarkonium in High-Energy Colliders.* Annu. Rev. Nucl. Part. Sci. **46** (1996) 197

[101] R. Barbieri, M. Caffo, R. Gatto, E. Remiddi. *QCD Corrections to p-wave Quarkonium Decays.* Phys. Lett. **B192** (1976) 61.

[102] G. T. Bodwin, E. Braaten, G. P. Lepage. *P-wave charmonium production in B-meson decays.* Phys. Rev. **D46** (1992) R3703

[103] E. Braaten and Sean Fleming. *Color-Octet Fragmentation and the ψ' Surplus at the Fermilab Tevatron.* Phys. Rev. Lett. **74** (1995) 3327

[104] E. Braaten, T. C. Yuan. *Gluon Fragmentation into Heavy Quarkonium.* Phys. Rev. Lett. **71** (1993) 1673

[105] L. S. Kisslinger, M. X. Liu, P. McGaughey. *D Production in p-p and d-Au Collisions.* Int. J. Theor. Phys. **55** (2016) 2026

[106] L. S. Kisslinger, M. X. Liu, and P. McGaughey. *Heavy-quark state production in A-A collisions at $\sqrt{s} = 200$ GeV.* Phys. Rev. **C89** (2014) 024914

[107] P. L. Cho and A. K. Leibovich. *Color-octet quarkonia production.* Phys. Rev. **D53** (1996) 150

[108] E. Braaten and Y.-Q. Chen. Helicity decomposition for inclusive J/ψ production. Phys. Rev. **D54** (1996) 3216

[109] E. Braaten and S. Fleming. *Color-Octet Fragmentation and the ψ' Surplus at the Fermilab Tevatron.* Phys. Rev. Lett. **74** (1995) 3327

[110] E. Braaten, K. Cheng, T. C. Yuan. *QCD fragmentation functions for B_c and B_c^* production.* Phys. Rev. **D48** (1993) R5049

[111] E. Braaten, K. Cheng, S. Fleming, T. C. Yuan. *Perturbative QCD fragmentation functions as a model for heavy-quark fragmentation.* Phys. Rev. **D51** (1995) 4819

[112] G.C. Nayak and J. Smith. *J/ψ and ψ' polarizations in polarized proton-proton collisions at the BNL RHIC.* Phys. Rev. **D73** (2006) 014007

[113] A. Adare, *et al.*, PHENIX Collaboration. *Measurement of High-p_T Single Electrons from Heavy-Flavor Decays in $p+p$ Collisions at $\sqrt{s} = 200$ GeV.* Phys. Rev. Lett. **97** (2006) 252002

[114] S. S. Adler, *et al.*, PHENIX Collaboration. *J/ψ Production and Nuclear Effects for $d+Au$ and $p-p$ Collisions at $\sqrt{s_{NN}} = 200$ GeV.* Phys. Rev. Lett. **96** (2006) 012304

[115] B. I. Abelov, *et al.*, STAR Collaboration. *Transverse Momentum and Centrality Dependence of High-p_T Nonphotonic Electron Suppression in $Au-Au$ Collisions at $\sqrt{s_{NN}} = 200$ GeV.* Phys. Rev. Lett. **98** (2007) 192301

[116] A. Adare *et al.*, PHENIX Collaboration. *Dilepton mass spectra in $p+p$ collisions at s**(1/2) = 200-GeV and the contribution from open charm.* Phys. Lett. **B670** (2009) 313

[117] A. Adare, *et al.*, PHENIX Collaboration. *Cold-Nuclear-Matter Effects on Heavy-Quark Production at Forward and Backward Rapidity in $d+Au$ Collisions at $\sqrt{s_{NN}} = 200$ GeV.* Phys. Rev. Lett. **112** (2014) 252301

[118] I. Vitev, T. Goldman, M. B. Johnson, J. W. Qiu. *Open charm tomography of cold nuclear matter.* Phys. Rev. **D74** (2006) 054010

[119] B. I. Abelev *et al.*, STAR Collaboration. *J/ψ production at high transverse momenta in $p-p$ and $Cu-Cu$ collisions at $\sqrt{s_{NN}} = 200$ GeV.* Phys. Rev. **C80** (2009) 041902

[120] A. Adare *et al.*,PHENIX Collaboration. *J/ψ Production in $\sqrt{s_{NN}} = 200$ GeV $Cu-Cu$ Collisions.* Phys. Rev. Lett. **101** (2008) 122301

[121] A. Adare *et al.*, PHENIX Collaboration. *Energy Loss and Flow of Heavy Quarks in $Au-Au$ Collisions at $\sqrt{s}_{NN} = 200$ GeV.* Phys. Rev. Lett. **98** (2007) 172301

[122] B. I. Abelev *et al.*, STAR Collaboration. *Transverse Momentum and Centrality Dependence of High-p_T Nonphotonic Electron Suppression in $Au-Au$ Collisions at $\sqrt{s}_{NN} = 200$ GeV.* Phys. Rev. Lett. **98** (2007) 192301

[123] F. Karsch, D. Kharzeev and H. Satz. *Sequential charmonium dissociation.* Phys. Lett. **B637** (2006) 75

[124] S. Baumgart, STAR Collaboration. *Measurement of the Open Charm Cross-Section in $\sqrt{s_{NN}} = 200$ GeV Cu+Cu Collisions at STAR.* arXiv:0709.4223/nucl-ex